NTNU
Norwegian University of
Science and Technology

Integration of Renewable Production of Hydrogen in Current Biomass-to-Liquid Biofuels Production Systems

Eirik Samuelsen

Chemical Engineering and Biotechnology
Submission date: June 2017
Supervisor: Magne Hillestad, IKP
Co-supervisor: Erling Rytter, IKP

Norwegian University of Science and Technology
Department of Chemical Engineering

Abstract

This report focuses on the production of hydrocarbons in a biomass to liquid (BtL) process with integration of hydrogen production. The hydrogen will be produced from high temperature electrolysis of steam utilizing excess heat in the plant. This represents a novelty which will increase the carbon efficiency of the plant, and lower the production cost. The design and evaluation of the plant have been done by simulations in Aspen Hysys V9.

The conventional method of producing hydrocarbons in a BtL plant uses steam to adjust the syngas ratio by converting some of the CO into CO_2 and hydrogen. In this case, the CO_2 emissions from the plant are larger and the carbon efficiency is lower, typically 30-40%. However, the hydrogen enhanced BtL plant in this report has shown a carbon efficiency of 97%. This is because CO_2 is not removed from the syngas due to the low concentration obtained when using the produced hydrogen to convert CO_2 into CO and simultaneously adjusting the syngas ratio. The only carbon emission is the purge, which nonetheless is required to remove the inerts to avoid accumulation in the process. By heat integrating the whole process, the energy efficiency is found to be 70.4%.

The high temperature electrolysis for production of hydrogen and oxygen from steam currently have a high electrical energy consumption and investment cost. It is expected that the electricity consumption and equipment cost will be significantly reduced between 2020 and 2050 [45]. Currently, the HTE technology is only demonstrated in pilot scale for hydrogen production.

From the economic evaluation of the profitability of the project it is estimated that the production cost for one liter of products is 5.32 NOK. This is significantly lower than the 7.04 NOK/L estimated for the conventional steam BtL plants. The plant will also be able to tolerate the higher discounted cash-flow rate of return of 15% compared to 5% for the steam BtL plant. Compared to a conventional steam BtL plant, the hydrogen enhanced plant will have higher investment and operating costs, but this will be compensated by the increased production of hydrocarbons.

Sammendrag

Denne rapporten fokuserer på produksjon av hydrokarboner i et BtL anlegg med integrasjon av hydrogenproduksjon. Hydrogenet blir produsert fra høytemperatur elektrolyse av damp ved å utnytte overskuddsvarme fra prosessen. Dette er en forbedring av et standard BtL anlegg som vil øke karbon effektiviteten og redusere produksjonskostnadene til anlegget. Simuleringen av anlegget er foretatt i Aspen Hysys V9.

Den konvensjonelle metoden for å produsere hydrokarboner i et BtL anlegg er ved bruk av vanndamp til å justere forholdet mellom hydrogen og karbonmonoksid i syntesegassen, ved å konvertere noe av karbonmonoksidet til karbondioksid. Ved å gjøre dette vil utslippene av karbondioksid fra anlegget øke og karboneffektiviteten vil bli redusert til rundt 30-40%. BtL anlegget med hydrogentilsetning simulert i denne rapporten vil derimot ha en karboneffektivitet på 97%. Den høye effektiviteten skyldes at CO_2 konsentrasjonen i syntesegassen er mye lavere fordi det skjer en omvendt reaksjon når hydrogen blir tilsatt, og karbondioksid blir konvertert til karbonmonoksid samtidig som syntesegassforholdet blir justert. Da vil det heller ikke være nødvendig med rensing av syntesegassen ved å fjerne karbondioksid. Det eneste utslippet vil være fra purgen, som uansett er krevd for å unngå akkumulering av inerte gasser i prosessen. Ved å varmeintegrere hele anlegget er energieffektiviteten beregnet til å være 70,4%.

Høytemperatur elektrolysen brukt til å produsere oksygen og hydrogen fra vanndamp har foreløpig høyt energiforbruk samtidig som utstyrsprisen er høy. Det er derimot forventet at både prisen og energiforbruket vil bli betraktelig redusert mellom 2020 og 2050 [45]. Høytemperatur elektrolyse er foreløpig også bare demonstrert for pilotprosjekter med hydrogenproduksjon, og må bli videreutviklet for å bli kommersialisert for større anlegg.

Fra den økonomiske analysen av lønnsomheten til prosjektet er det funnet ut at den årlige produksjonskostnaden til anlegget for en liter produkt er 5,32 NOK/L. Sammenlignet med tall fra andre rapporter er dette betydelig lavere. Hydrogen BtL anlegget vil også kunne tolerere en høyere internrente på 15%, i motsetning til 5% for et konvensjonelt BtL anlegg. Den totale investeringen i et hydrogen BtL anlegg vil være større enn for et konvensjonelt anlegg, men dette vil bli kompensert for av den økte produksjonen av hydrokarboner.

Preface

This report was written in the spring 2017 as a master thesis for the M.Sc. degree in Chemical Engineering at the Norwegian University of Science and Technology (NTNU).

The report is a part of the REN-BTL project aiming to improve the carbon efficiency, economic profitability and environmental performance of a biomass to liquid process. This is done by integrating production and usage of hydrogen in the plant. The hydrogen is produced with high temperature electrolysis of steam, with utilization of excess heat in the process.

I would like to thank my supervisor Professor Magne Hillestad and co-supervisor Erling Rytter for giving me a very interesting project to work on and much appreciated help during the work with this thesis.

Contents

List of Figures

List of Tables

List of symbols

List of symbols.

Symbol	Unit	Description
A	m^2	Cross sectional area
C_e	$	Equipment cost
C_{eff}	%	Carbon efficiency
CF_0	$	Initial investment
CF_n	$	Cash flow in year n
C_p	kJ/kgK	Specific heat of steam
C_{2007}	$	Equipment cost in 2007
C_{2016}	$	Equipment cost in 2016
D_i	m	Internal diameter
E		Welded-joint efficiency
E_{eff}	%	Energy efficiency
H	m	Height
I_{2007}		Cost index in 2007
I_{2016}		Cost index in 2016
M		Total number of pieces of equipment
P_i	Pa	Design pressure
S		Size parameter
T	°C	Temperature
V_{CSTR}	m^3	Volume CSTR
W	J/s	Watt
a		Economic constant
b		Economic constant
f_c		Installation factor for civil engineering work
f_{el}		Installation factor for electrical work
f_{er}		Installation factor for equipment cost
f_i		Installation factor for instrumentation and process control
f_l		Installation factor for lagging, insulation or paint
f_m		Material cost factor
f_p		Installation factor for piping
f_s		Installation factor for structures and buildings
i		Interest rate
n		Scaling factor
n		Number of years of repayment
q_{in}	m^3/s	Volume flow

t		Lifetime in years
t	m	Thickness
u_s		Settling velocity
v	m/s	Velocity
ΔG	kJ/mole	Gibbs free energy
ΔH	kJ/mole	Enthalpy
ΔH_{vap}	kJ/mole	Enthalpy
ΔH_r	kJ/mole	Enthalpy of reaction
ΔS	J/K	Entropy
λ	-	O_2 stoichiometric ratio
ρ_{304ss}	kg/m^3	Density of 304 stainless steel

Abbreviations

Abbreviations

ACCR	Annualized capital charge ratio
ACM	Aspen custom modeler
AEA	Aspen energy analyzer
ASF	Anderson-Schulz-Flory
BtL	Biomass-to-Liquid
CEPCI	Chemical engineering plant cost index
CRV	Conversion reactor vessel
CSTR	Continuous stirred-tank reactor
D&E	Design and Engineering
DCFROR	Discounted chas-flow rate of return
ERV	Equilibrium reactor vessel
FT	Fischer-Tropsch
GBR	Gibbs reactor
HTE	High temperature electrolysis
IEA	International Energy Agency
IRR	Internal rate of return
ISBL	Inside battery limit
LHV	Lower heating value
NOK	Norwegian krone
NPV	Net present value
OS	Off-sites
OSBL	Off-site battery limit
RWGS	Reverse water gas shift
SMR	Steam methane reforming
SOEC	Solid oxide electrolysis cell
SPCEC	Solid proton conducting electrolysis cell
TAC	Total annualized cost
USD	United States dollar
WGS	Water gas shift
X	Contingency

1 Introduction

Renewable clean energy has recently attracted much attention due to the use of fossil fuels and increasing emission of greenhouse gases. Fossil fuel dominates the energy supply, but the reserves of fossil fuel are approximated to be emptied before 2088 [1]. However, the global energy demand will continue to increase due to the population growth, and therefore new energy sources must be developed. To accomplish the Paris agreement goal of a maximum global temperature increase of 2°C, renewable energy sources must replace some of the fossil fuel. Carbon based energy sources will still be important in the future as it will take time to replace all the transportation units using fossil fuel. Therefore the biofuel production must grow to meet the liquid hydrocarbon demands, and at the same time reduce the greenhouse gas emissions. Among the renewable energy sources, only biomass is carbon based and has the potential to replace fossil fuel in conventional combustion engines. However, biomass will often compete with food production and should ethically come from non-food sources like agricultural waste, algae, forest residue and municipal waste. Biomass gasification in combination with Fischer-Tropsch synthesis is considered as a highly applicable method for production of biofuels [2]. Synthesis gas is produced with high amounts of H_2 and CO, which after cleaning is synthesized to "green" biofuel. The fuel is of high quality and have little containments such as sulfur and aromatics, and can satisfy the strict environmental regulations imposed in Europe and US in recent years [3].

The main challenges for biomass-to-liquid Fischer-Tropsch plants is a low carbon efficiency and high investment, due to high CO_2 emission and low oil price. The current technology is therefore not economically profitable and must be improved to be able to compete with the fossil fuel price.

1.1 Project objective

The objective of this thesis is to develop a possible configuration of a biomass-to-liquid Fischer-Tropsch plant based on heat integration and economic optimization, with integrated hydrogen production by high-temperature electrolysis (HTE). The hydrogen will contribute to increase the carbon efficiency of the plant by converting CO_2 to CO in a reverse water gas shift reaction and adjusting the syngas ratio before each Fischer-Tropsch reactor to increase the production of hydrocarbons. The hydrogen enhanced plant is compared to a conventional BtL plant where steam is added to perform a water gas shift reaction to adjust the syngas ratio. However, this will decrease the carbon efficiency and production of hydrocarbons in the plant. The two cases are compared based on cost of production and profitability.

1.2 Overview of process

The objective of a Biomass-to-Liquid (BtL) process is to convert biomass into liquid fuel. An overview of the proposed process is shows in the blocksheet in Figure 1.1. First, the biomass is pretreated to make a suitable feed for the gasifier. This can be done by pyrolysis or torrefaction. In the gasifier, syngas is produced with controlled addition of oxygen to get an incomplete combustion of the biomass. The oxygen added to the gasifier is produced by high-temperature electrolysis (HTE) cells, together with hydrogen. After the gasification, the H_2/CO ratio in the syngas must be set to a ratio slightly below 2 to optimize selectivity in the Fischer-Tropsch (FT) synthesis. This is done in a reverse water gas shift (RWGS) reactor with addition of hydrogen produced by the HTE cells. The addition of hydrogen will also increase the carbon efficiency of the plant compared to conventional BtL plants, by converting CO_2 to CO. Impurities as hydrogen sulfide must be removed prior to the Fischer-Tropsch reactors to protect the catalyst from poisoning and deactivation. A Selexol process and guard beds of zinc-based absorbent media will purify the syngas. The Fischer-Tropsch reactors converts the synthesis gas by polymerization to hydrocarbons. Three FT reactors are placed in series with hydrogen addition in between to adjust the syngas ratio and increase the production of hydrocarbons.

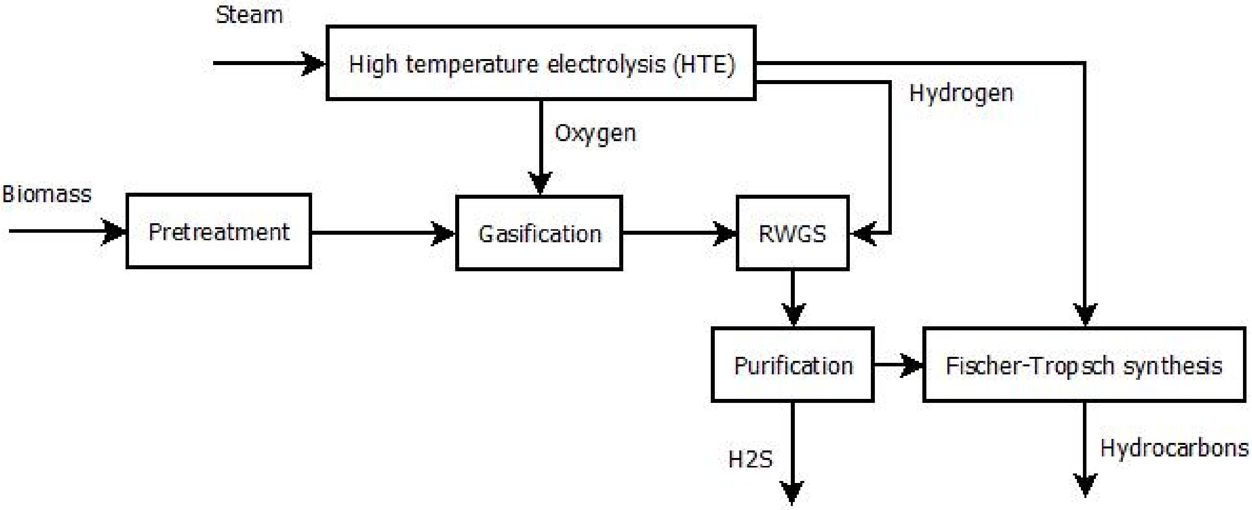

Figure 1.1: Blocksheet of the Biomass-to-Liquid process.

The model of the Biomass-to-Liquid plant was made using Aspen Hysys V9.0. The Fischer-Tropsch reactors were modeled in Hysys as CSTR using an ACM model made in Aspen Properties. Hysys provided component properties were used for the rest of the plant. Peng-Robinson was chosen as the thermodynamic fluid package to calculate the thermodynamic properties in the model.

2 Feedstock

A Biomass-to-liquid (BtL) plant converts biomass into liquid hydrocarbons. As the CO_2 emission from combustion of biomass is equal to the quantity consumed in photosynthesis by trees and plants, biomass is a carbon neutral energy source. However, biofuels will actually reduce the greenhouse gas emission because it will replace some of the fossil fuel. Since the discovery of the human impact on global warming through greenhouse gas emissions, the focus has been to increase the use of renewable energy sources compared to fossil fuel. It is possible to utilize various biomass feedstock in the production of biofuels. First-generation biofuels originating from sources like sugarcane and corn are enticing to use but represent an ethical problem due to the competition with food production. Second-generation biofuels on the other hand are based on forest residue, agricultural and municipal waste which are non-food sources. The process for converting biomass to biofuel must be adapted due to specific properties of different biomass. The pretreatment and the gasifier must be designed to optimize the utilization of the biomass in production of synthesis gas. Various feedstock are available, but forest residue is used in this report as it is cheap, have a high energy content and low amounts of impurities [4]. Table 2.1 shows the composition of the biomass used as feedstock basis in this report.

Table 2.1: Composition of the biomass feedstock.

Component	Wt% dry basis
C	51.8
H	6.04
N	0.17
S	0.09
O	41.9

The composition of the biomass in Table 2.1 is found in literature [5] [6]. To find the chemical formula of the biomass used in the simulation, the weight percent of each element is divided by their molecular weight: $C_{4.31}H_{6.04}O_{2.62}N_{0.012}S_{0.003}$. This is the chemical formula used for the inlet stream in the Hysys model. The energy content of the feed in the Hysys model is assumed to be torrefied biomass with a lower heating value (LHV) of 18747 kJ/kg [6]. An amount of 20000 tonne/day is used, corresponding to 434 MW biomass.

A biomass price of 15-30 US$/tonne is found in literature for forest residue [7]. The moisture content of the biomass is 30%-50%, which is important for the torrefaction process described in the next section.

2.1 Torrefaction

Torrefaction is a thermal treatment process of biomass at temperatures in the range of 200 - 300 °C [8]. The goal is to change the biomass properties to get a higher heating value and lower the moisture content before further processing of the biomass. During the torrefaction process, the biomass is converted into a brown-black uniform solid, steam and volatile gases. The solid product has higher calorific value than the original wood chips, and particle shape, size, and distribution is improved [5]. The moisture content of the torrefied biomass compared to wood is decreased from about 40-50 wt% to 1-5 wt%, while the energy content is increased from 10 MJ/kg to 18-24 MJ/kg [5]. Grinding energy of the torrefied biomass to reduce the particle size before further processing is reduced by about 80-90% compared to the original woody biomass [9]. As an example a reduction from 237.7 kWh/tonne to 24 kWh/tonne has been observed [8], [9]. In comparison to other biomass pretreatment technologies such as pyrolysis and pelletization, torrefaction has the highest process efficiency with 94% [3]. The torrefaction process consists of several steps, including:

- Pre-drying: Initial heating of biomass to evaporate free water from the biomass. This is done at around 100°C in a rotary dryer [9], [6]. Moisture content is decreased from 40-50% to about 12%. In this report, the heating medium is steam produced in the plant.
- Intermediate heating: Increasing the temperature to 200-300 °C. Some of the bound water and light volatiles evaporates.
- Torrefaction: The actual process where the biomass is torrefied at 200-300°C. Also here the heating medium is steam, and the moisture content is decreased to 1-5%.
- Cooling: Cooling of the biomass can be done if the biomass is used at another location than the torrefaction. This is not the case in this report and it is an advantage if the biomass is fed to the plant at a high temperature of 300°C.

The energy requirements for a torrefaction process have been studied in several reports. A report from the International Energy Agency (IEA) thoroughly analyzed the energy requirements for torrefaction of biomass and an overview can be seen in Table 2.2 [5].

Table 2.2: Energy consumption for torrefaction process in kWh/tonne product [5].

Components	Energy Consumption [kWh/tonne product]
Predryer	33
Torrefaction	60
Grinding [9]	24

The report also looks at the energy requirements for pelletization of the biomass, which is

150 kWh/ton product. This is however not relevant for this process as the torrefied biomass is fed to the gasifier without being pelletized. The pelletization energy is relevant if the torrefied biomass is produced off-site and needs to be transported to the BtL plant [5]. Other studies on the energy requirements which includes pre-drying, torrefaction, grinding and densification, report values in the range of 92-102 kWh/tonne input [10].

Torrefied biomass is particularly interesting to use in entrained-flow gasifiers because the biomass must be fed as a powder with a very small particle size. The torrefied biomass is also very energy dense, improving the efficiencies of the gasification system [8].

Different reactor technologies for torrefaction has been developed, and an overview can be seen in [8]. They all have their advantages, particularly for handling feedstocks with different particle size. If excess steam at temperatures above the operating temperature of a torrefaction unit is available, a rotating drum with indirect heating is highly relevant. A rotating drum pumps the biomass through a circular pipe and the process can be controlled by varying the rotational velocity, length of pipe, angle of the drum and temperature. This can be used as the predryer of the biomass, reducing the moisture content to 12%. A screw type reactor can use high-temperature steam as indirect heating medium, while screwing the biomass through the reactor. The heat transfer is determined by the length of the reactor and the rotational velocity of the screw. An example of an auger screw type reactor can be seen in Figure 2.1 [5].

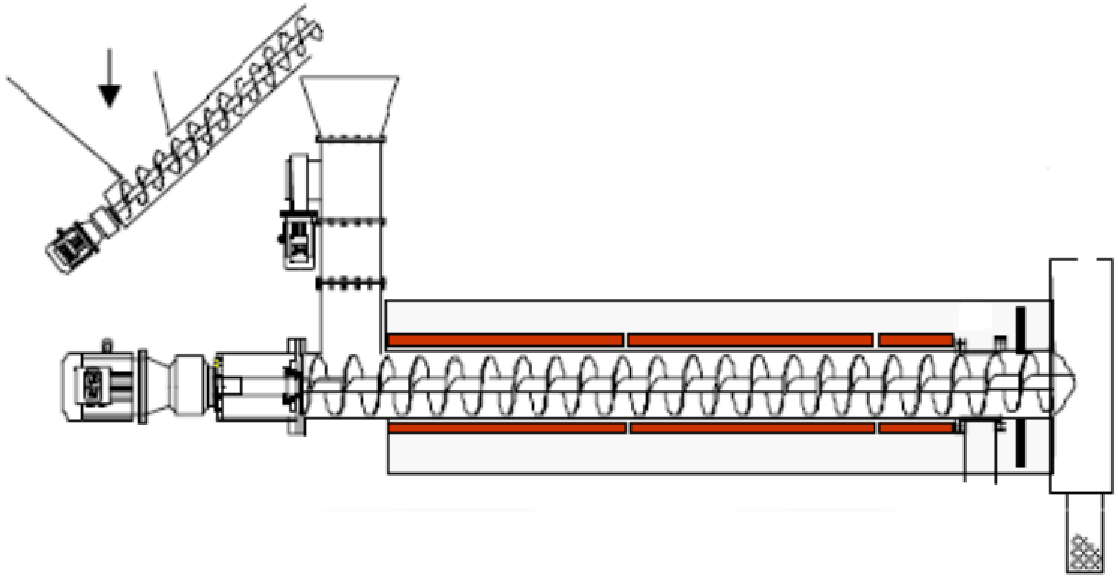

Figure 2.1: An auger screw type torrefaction reactor [5]. The red areas are the heat transfer zones where steam is condensed and the heat is transferred to the biomass.

3 Theory

3.1 Gasification of biomass

Gasification is a high-temperature and pressure operating process where carbonaceous materials, like biomass or coal, are converted mainly into a mixture of carbon monoxide, hydrogen, carbon dioxide and small amounts of methane, which is called syngas. The temperature is usually above 800°C to minimize the formation of methane and other byproducts. Production of methane will decrease the carbon efficiency of the plant as it will act as an inert in the conversion process of the syngas, and not be converted into high-weight hydrocarbons. The material reacts in the gasifier at high temperature and with limited amounts of a gasifier agent like oxygen, steam or air to get an incomplete combustion.

Various types of gasifiers have been designed, having different operating conditions, gasification agents and flow patterns. The main reactors are fixed bed gasifiers, fluidized bed gasifiers and entrained flow gasifiers [3]. Gasification can be operated at low (<1000°C) or high-temperature (>1200°C) based on the desired product. For high-temperature gasification, the main type is entrained flow gasifier [11]. The biomass will be completely converted into syngas, even with short residence time of only a few seconds. The entrained flow gasifier is operated with pressure of 20-50 bar and addition of gasifier agent like oxygen co-current to the feed. An advantage of high-temperature gasification is a more simple gas cleaning process as no organic impurities or slag are produced. However, the feed must be strictly pretreated to obtain a fine feed with particle size of 0.1-0.4 mm [3]. An example of an entrained flow gasifier is depicted in Figure 3.1. The commercially available gasifiers are compact in size because they operate under pressure [12]. The design of the vessel typically consists of refractory materials, as bricks, protecting the vessel metal from the high temperature and corrosion. It will also reduce the heat loss of the process.

For the gasification in this process, a gasifier with an additional space at the top of the reactor held for the reverse water gas shift reaction is proposed. The gasifier is extended with a separate zone where hydrogen is added and the reverse water gas shift reaction adjusts the H_2/CO ratio before further processing. No oxygen is present in this zone as the gasification reactions are finished before the gas enters this zone. An example of the gasifier can be seen in Figure 3.1.

Equation 3.1 is a general reaction equation for the biomass in the gasifier [3]. A more detailed description of all the reactions happening can be found in literature [3].

$$\text{Biomass} + O_2(\text{or } H_2O) \rightarrow CO, CO_2, H_2O, H_2, CH_4 + \text{other CHs} \tag{3.1}$$

The composition of the synthesis gas produced will depend on the feedstock composition, temperature, pressure, gasifying agents, etc.

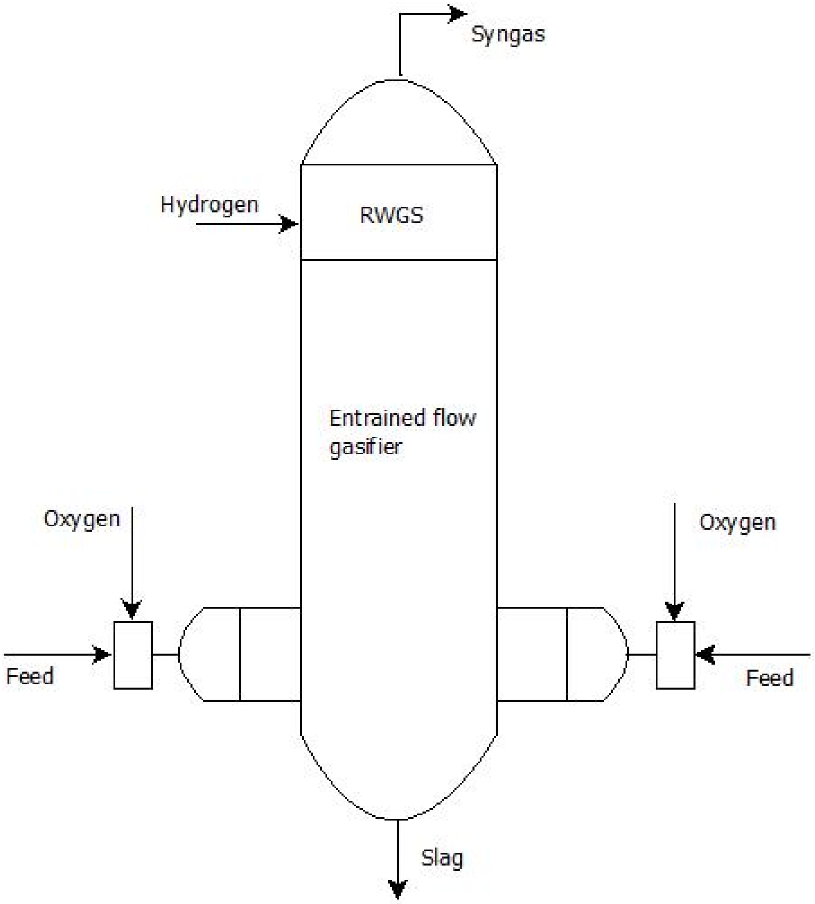

Figure 3.1: A representation of an entrained flow gasifier [3].

The temperature out of the gasifier must be above 1300°C to minimize the output of ash and soot, by melting it to vitreous slag which is easily disposed [13]. If the temperature is lower, solid particles must be removed from the syngas, which complicates the cleaning process. In this report, the temperature out of the gasifier is modeled as 1300°C. The temperature can also be even higher to ensure no solid particles are leaving the gasifier.

3.2 High-temperature electrolysis

Hydrogen is regarded as one of the most promising clean energy carriers for future energy production and has obtained much attention during the past years. The most common ways to produce hydrogen today is by steam methane reforming and alkaline water electrolysis. Steam methane reforming (SMR) uses steam to convert methane at high temperature into carbon monoxide and hydrogen. This is not an environmentally friendly process, as natural gas is used which emits greenhouse gases and contributes to global warming. However, it is the most commonly used process today because of the high efficiency (60-85 %) and low price of natural gas compared to electricity [14]. Alkaline water electrolysis is a low-temperature method producing hydrogen by use of electricity. The efficiency is low, about 27%, and the electricity usage is high, resulting in high operating cost [15].

Electrolysis of water is performed to produce hydrogen and oxygen gas using electrical energy. Low-temperature alkaline electrolysis is the most common process, but new technology as high-temperature electrolysis (HTE) shows great performance and uses less energy [16]. High-temperature electrolysis is divided into the use of solid oxide electrolysis cell (SOEC) and solid proton conducting electrolysis cell (SPCEC), which transports oxygen and hydrogen respectively through the cell. Both operates at high temperature (800 °C - 1000 °C) and uses electrical energy to split steam into H_2 and O_2 gas. If HTE processes use waste heat from other processes to convert water into steam and heat to the operating temperature, the energy efficiency of the process will increase considerably. The HTE has favorable thermodynamic and electrochemical conditions at the high temperature compared to low-temperature electrolysis [16]. This can be explained by equation 3.2, where ΔH represents the total energy demand, ΔG the electrical energy demand, and TΔS the heat energy demand. The thermodynamic advantage is that the Gibbs energy (ΔG) required to split the water is reduced from 237 kJ/mol to 183 kJ/mol when the temperature increases from 25 °C to 900 °C. This can be seen in Figure 3.2. However, the molar enthalpy of the reaction, ΔH, remains constant at 249 kJ/mol at all temperatures as seen from the red line in the same figure. Therefore the consumption of electrical energy to produce hydrogen drops significantly if the heat energy is provided from waste heat from high-temperature streams.

$$\begin{gathered} \Delta H = \Delta G + T\Delta S \\ \text{Total Energy} = \text{Electrical Energy} + \text{Heat energy} \end{gathered} \tag{3.2}$$

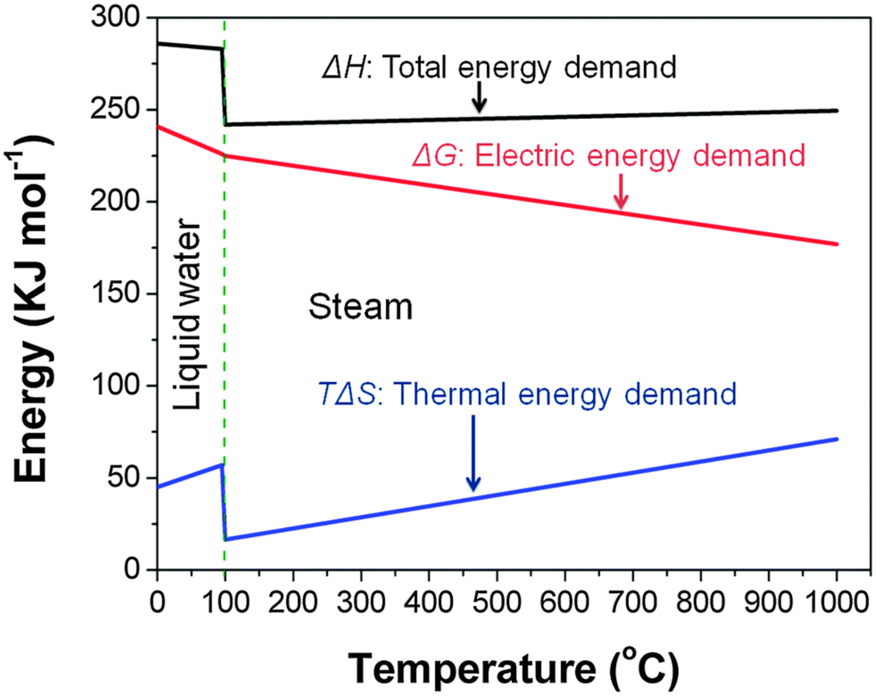

Figure 3.2: A representation of the total energy demand for electrolysis of water at different temperatures. The electrical energy demand drops significantly at high temperatures [17].

Solid proton conducting electrolysis cells (SPCEC) are a relatively new technology producing pure hydrogen in contrast to solid oxide electrolysis cell (SOEC), where the hydrogen product is mixed with the unconverted water vapor. The operating concept of SOEC is seen in Figure 3.3 and SPCEC in Figure 3.5. Both processes operate at high temperature and splits the steam according to equation 3.3 with use of electricity.

$$\mathrm{H_2O} \longrightarrow \mathrm{H_2} + \frac{1}{2}\mathrm{O_2} \tag{3.3}$$

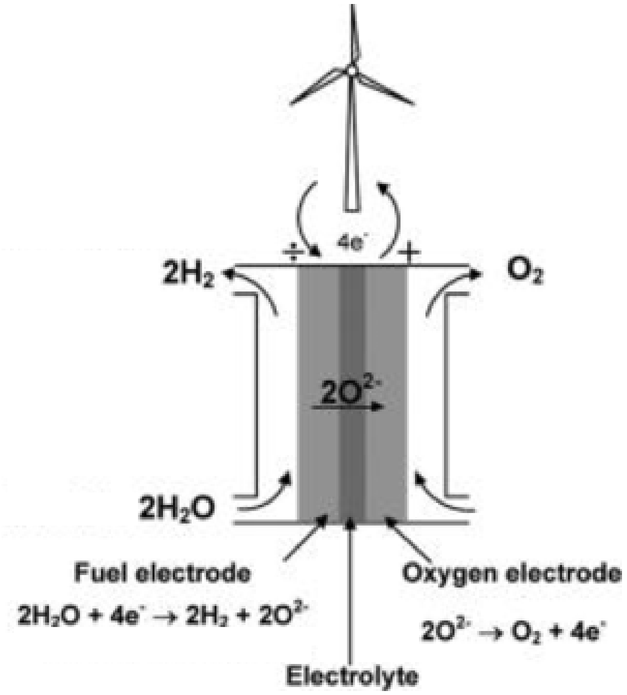

Figure 3.3: A representation of the mechanism in a high-temperature solid oxide electrolysis cell [17].

In a SOEC like the example in Figure 3.3, steam is added on the cathode side where it is reduced to oxygen and hydrogen ions. The oxygen ions pass through the electrolyte membrane where it releases two electrons and forms pure oxygen gas which leaves the process. The hydrogen gas will not permeate through the membrane and will leave the process together with the unconverted steam. A standard cell setup consists of a Ni/Zr cermet with a strontium doped lanthanum manganite perovskite anode and a yttrium-stabilized zirconia electrolyte as seen in Figure 3.4 [18]. The technology of high-temperature electrolytic membranes is suffering from ohmic losses due to ionic conductivity through the cell. This will reduce the efficiency in producing hydrogen and more research must be conducted to increase the performance of the cell. The high operating temperature of the cells can be an issue and cause drawbacks on the stability, lifetime and material [19]. It will also require much energy to heat the steam, so development of well operating HTE cells at lower temperature is important to reduce the energy usage.

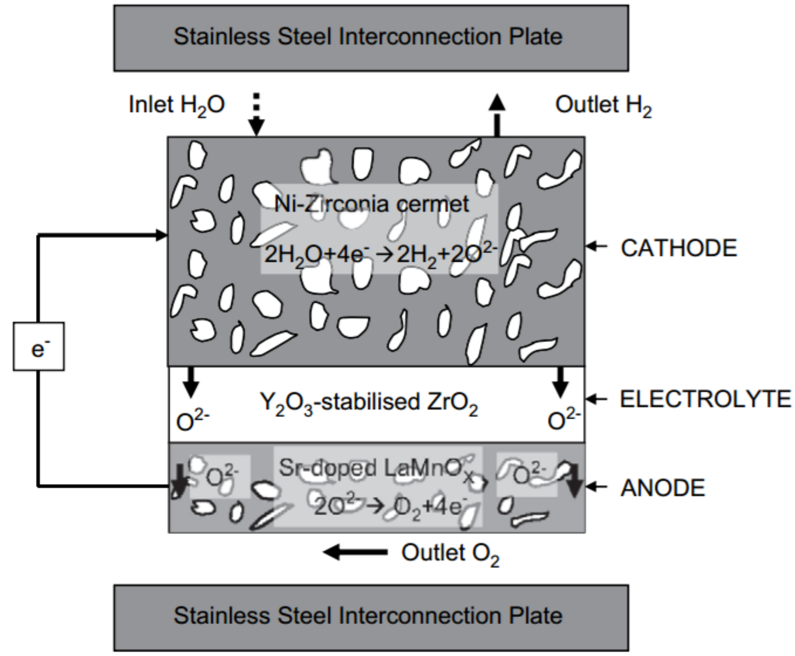

Figure 3.4: A representation of the mechanism in a high-temperature electrolysis cell [18].

Figure 3.5 shows how the SPCEC is working. The hydrogen ions permeate through the electrolyte and form pure hydrogen gas by reduction on the permeate side of the cell. The oxygen ions will not permeate through the electrolyte and will leave the cell together with the unconverted steam. The SPCEC consists of a proton-conducting electrolyte to transport hydrogen through the cell.

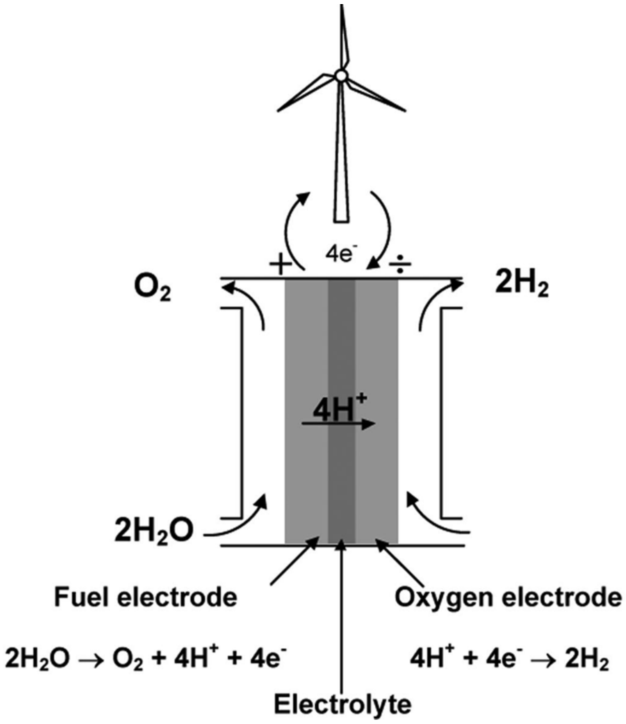

Figure 3.5: A representation of the mechanism in a high-temperature solid proton conducting electrolysis cell [17].

The electricity consumption of a HTE cell is important for evaluation of the profitability of the process. Values found in literature range from 28-39 kWh/kg H_2, which is up to 50% lower than conventional alkaline processes [20]. The current technology of HTE cells operates with a steam conversion of 80-90% but cells with higher conversions are under development [21]. Cells with operating conditions lower than 800°C are also under development and will be important to reduce the electricity consumption even further. Ohmic loss is observed in the cells, but lab research must be conducted to evaluate the exact impact of the loss on electricity consumption. It is assumed that the referred electricity consumption includes this loss.

3.3 Biosyngas conditioning by Reverse Water Gas Shift Reaction

The water gas shift reaction converts carbon monoxide and water to hydrogen and carbon dioxide as seen in equation 3.4. The reaction is an exothermic reversible reaction, and at temperatures above 820°C the equilibrium is shifted to the reverse of the reaction (reverse water gas shift (RWGS)) [14].

$$CO + H_2O \longleftrightarrow H_2 + CO_2 \qquad \Delta H_r = -41 \frac{kJ}{mole} \tag{3.4}$$

The water gas shift reaction is often used to adjust the H_2/CO ratio in syngas before further processing. This is done to convert CO to H_2 which can be used e.g. in a fuel cell [22]. However, sometimes the desired product is carbon monoxide and the reaction can be reversed. To get the optimal H_2/CO ratio in the syngas of 1.8-2.1 before a Fischer-Tropsch synthesis, the reverse water gas shift reaction can be used if hydrogen is added.

As seen from the reaction in equation 3.4, the forward water gas shift reaction reduces the carbon efficiency of a plant because CO is converted to CO_2. However, if the temperature is high and/or hydrogen is added to the syngas, the equilibrium is shifted towards CO. This will increase the carbon efficiency as more synthesis gas is produced.

3.4 Synthesis gas cleaning: Sulfur removal

The major components of synthesis gas are hydrogen, carbon monoxide, carbon dioxide, and water. However, there will always be small amounts of other components because the biomass contains sulfur and nitrogen. Different upgrading processes require different gas composition and quality. The catalyst used for synthesis gas conversion are often very sensitive to sulfur components due to poisoning. Removal of acid gases from synthesis gas, known as acid gas treating or gas sweetening, is an important process to clean the gas and prevent deactivation and catalyst poisoning. The main goal is to remove CO_2, H_2S and other sulfur compounds. Different methods exist to clean the synthesis gas, e.g. wet scrubbing and dry adsorption [11]. Wet scrubbing is divided into physical and chemical adsorption. For physical adsorption, Selexol and Rectisol can be used as adsorbent, and in chemical absorption amines like MEA and DEA is widely used. Dry processes use metal oxides like ZnO or activated carbon to remove impurities. However, dry processes are more expensive and mainly used as guard beds when the sulfur concentration is low. An advantage of using biomass instead of coal as the carbon source is the sulfur content in the syngas, which can be 50 times lower [23]. However, sulfur compounds still represent a problem for the conversion of the syngas as the purity requirements are strict.

In a Selexol process the syngas is entering an absorber column where Selexol is fed at the top of the absorber. H_2S is absorbed by the Selexol and sent to a stripper, while clean fuel exits the at the top of the absorber. The bottoms of the absorber containing H_2S is then let down to a low pressure to reduce the amount of co-absorbed CO_2 led to the stripper. In the stripper the Selexol is regenerated by using steam in the reboiler. The overhead of the stripper contains high amounts of sulfur and a very lean solvent is routed back to the absorber [24].

After the chemical/physical adsorption, a dry process can be used to remove the rest of the sulfur components. The mostly used adsorbents are ZnO or activated carbon. The main drawback of using guard beds as ZnO is that the adsorbent has to be disposed because regeneration is highly energy consuming and not economically profitable. Due to economic reasons, dry adsorption is mainly used to clean syngas with sulfur concentrations below 50 ppm [11]. The following equation describes the reaction between zinc oxide and H_2S [23]:

$$\mathrm{ZnO(s) + H_2S(g) \leftrightarrow ZnS(s) + H_2O(g)} \tag{3.5}$$

The maximum sulfur content requirements of the syngas are different for various processes and are also reported different for the same type of process. 5 ppm, less than 1 ppm and as strictly as 5 ppb is found in literature when the syngas is used in Fischer-Tropsch synthesis [11], [25], [26].

3.5 Fischer-Tropsch

Fischer-Tropsch synthesis is a catalytic chemical process used to produce liquid hydrocarbon fuels from synthesis gas. n-paraffins and 1-olefins are produced by a surface catalyzed polymerization following reaction 3.6 and 3.7 [27].

$$\mathrm{nCO} + (2n+1)\mathrm{H_2} \longrightarrow \mathrm{C_nH}_{2n+2} + \mathrm{nH_2O} \qquad n = 1, 2, ..., \infty \tag{3.6}$$

$$\mathrm{nCO} + 2\mathrm{nH_2} \longrightarrow \mathrm{C_nH}_{2n} + \mathrm{nH_2O} \qquad n = 2, 3, ..., \infty \tag{3.7}$$

The process is named after the scientists Hans Tropsch and Franz Fischer who developed the process in the 1920s and has been used to process coal and natural gas to liquid fuel. In the recent years, conversion of syngas from biomass has become a relevant topic of use of Fischer-Tropsch synthesis to meet the environmental emission goals. Plants which previously were based on coal can now be customized to use biomass.

From almost a century of improvement of the Fischer-Tropsch technology the mainly used catalysts today are transition metals like iron- or cobalt-based catalysts. The cobalt catalyst has the advantage relative to iron catalyst of being more selective to C_{5+} hydrocarbons, more active at lower temperature, less selective to olefins and less active to the water gas shift reaction [28], [27]. A cobalt catalyst is more expensive than an iron catalyst, but provide a better compromise between price and production of hydrocarbons from a syngas mixture. A cobalt catalyst also has the advantage of longer lifetime and thereby need for less frequently replacement [27]. Iron catalysts however are cheaper and have a higher tolerance for sulfur, but have a lifetime limited to only eight weeks in commercial plants [2]. The operating temperature range from 150-300 °C, where higher temperature leads to faster reaction and production of lighter hydrocarbons such as methane. High molecular weight hydrocarbons are preferred as products from the Fischer-Tropsch process so it can be used as fuel. Depending on operating conditions as the type of catalyst, temperature, pressure and type of reactor, hydrocarbons with a broad range of molecular weight can be synthesized. Production of C_{5+} hydrocarbons is also favored by using a slightly understoichiometric ratio of H_2/CO in the syngas entering the FT reactors [29]. The condensation polymerization of CO to hydrocarbons taking place in the Fischer-Tropsch reactors follows an Anderson-Schulz-Flory (ASF) distribution of the molecular weight of the hydrocarbons [30]. M_n is the molar fraction of various hydrocarbons, and can be described by [3]:

$$M_n = (1 - \alpha)\alpha^{n-1} \tag{3.8}$$

α is a chain growth probability. The ASF distribution in mole fraction and mass fraction can be seen in figure 6 in [3].

The catalyst used in FT synthesis is very sensitive to impurities in the syngas. Even small amounts of e.g. sulfur components can poison and deactivate the catalyst. The economic consideration for a plant is whether to invest in gas cleaning technology or accept a decreasing production rate and eventually replace the catalyst. Therefore, there is no clear definition of the maximum amounts of impurities in the syngas; it varies from plant to plant. However, some of the impurities need to be removed regardless. Some specifications on Fischer-Tropsch gas feed are presented in section 3.4.

Various FT reactors are commercially available and have different operating conditions. A slurry reactor is used in this report, which operates at low temperature (220°C) and with a cobalt catalyst.

4 Simulation Setup

4.1 Flowsheet and design basis

The objective is to improve the carbon and energy efficiency of a biomass to liquid Fischer-Tropsch plant by integration of renewable production of hydrogen. A blocksheet of the proposed process can be seen in Figure 1.1. Biomass is the feedstock of the plant and is described in section 2. The basis is 83.33 tonne/h or 20 000 tonne/day biomass.

A detailed flowsheet of the plant can be seen in Figure 4.1. Appendix C shows a complete overview of all the streams in the plant with molar composition. The biomass is initially dried to remove the free water in the biomass. This will reduce the moisture content significantly, but the main removal occurs in the torrefaction unit. The content decreases to about 1-5% and is assumed to be 4% in this report. Then, the torrefied biomass is fed to an entrained flow gasifier at the outlet temperature from the torrefaction which is about 300°C. By under-stoichiometric combustion with oxygen, the biomass is reacting to form synthesis gas (syngas), a mixture of mainly hydrogen, carbon monoxide, carbon dioxide and steam. The added oxygen is produced by high-temperature electrolysis in a solid electrolysis cell. A recycle stream with unconverted syngas is also mixed into the gasifier. After the gasifier, a reverse water gas shift reaction is occurring at high temperature with addition of hydrogen. This will convert some of the CO_2 to CO and at the same time adjust the H_2/CO ratio in the syngas to 1.9. The high-temperature syngas is heat exchanged with water at the boiling point and at high pressure to cool the gas and concurrently produce steam. The steam is then superheated in another heat exchanger. The steam can be used in the high temperature electrolysis cells and the torrefaction unit as seen in Figure 5.1. Subsequently, the water in the syngas is removed at low temperature, before the syngas is cleaned in an acid gas removal unit with Selexol. Here, most of the sulfur-containing components are removed. Guard beds of ZnO are also used to purify the gas to the requirements of a syngas entering Fischer-Tropsch reactors. The gas is heated to the operating temperature of the synthesis before the reactors and a cooling system controls the temperature inside the reactor. Low-pressure steam is produced in the cooling unit in the FT reactors and used to produce electricity. The heavy hydrocarbons are removed before the gas is heat exchanged with the feed stream to the reactor and cooled. Light hydrocarbons and water are separated from the unconverted syngas in a three-phase separator. Hydrogen is added to the syngas to adjust the H_2/CO ratio before the next FT reactor. This procedure is repeated for all the three FT reactors. The hydrocarbons produced are collected as product, while the unconverted syngas is recycled to the gasifier. Some of the recycled gas is purged to prevent accumulation of inerts like nitrogen. The purge is used for supplementary heating of the steam used in the HTE cell by complete combustion.

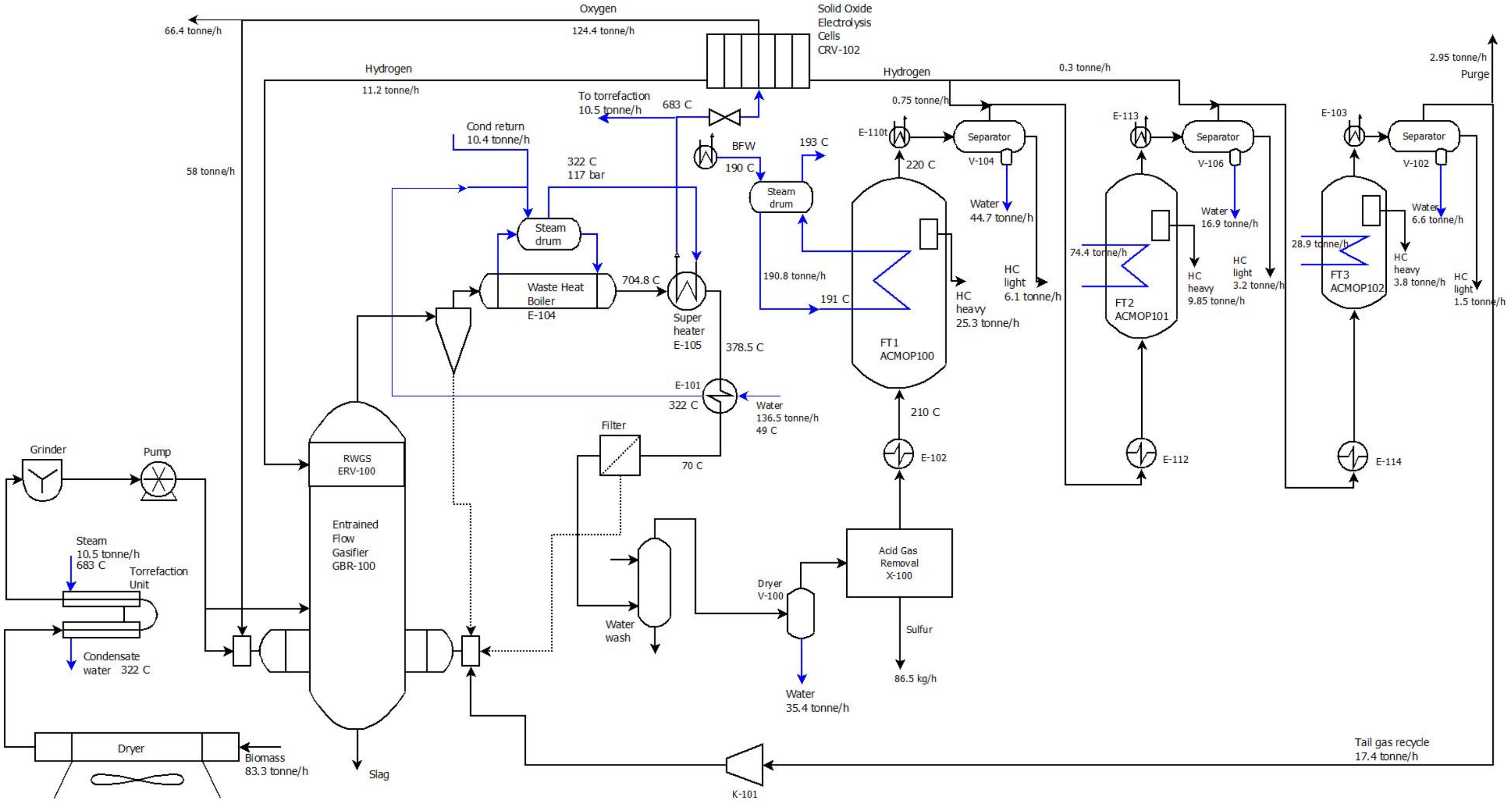

Figure 4.1: Flowsheet of the Biomass-to-Liquid process with tag names of the most important components and mass flows. A detailed overview of every stream and equipment can be found in appendix A.2 and C.

Table 4.1 shows the tag-name of the main components in the process. A Hysys flowsheet with all names on every stream and equipment can be found in appendix A.2.

Table 4.1: Important components in Hysys with their tag-names. The components can be found in Figure 4.1 and in the flowsheets in appendix A.2.

Component	Tag-name
Entrained flow gasifier	GBR-100
Water gas shift reactor	ERV-100
Water separator after RWGS	V-100
Acid gas cleaning (AGC)	X-100
HTE cell	CRV-102
Fischer-Tropsch 1	ACMOP100
Fischer-Tropsch 2	ACMOP101
Fischer-Tropsch 3	ACMOP102
Waste heat boiler	E-104
Superheater	E-105
Pre-heater	E-101

4.2 Design basis and assumptions

Some assumptions have been used in the simulations in Hysys:

- The torrefied biomass is assumed to have a moisture content of 4%, which is within reported values in literature [5]. To obtain this value in the simulations, a dry stream of torrefied biomass is mixed with steam, adjusted to 4 wt% of the biomass weight.
- Different steam conversions have been reported for HTE cells. Everything from 55% up to almost 100% appears to be possible, but a steam conversion rate value of 80% has been chosen [21]. This implies that 20% of the steam in unconverted and leaves the HTE cell with the oxygen.
- A constant temperature out of the gasifier of 1300°C is used to minimize the output of ash and soot. This is controlled by the oxygen addition to the gasifier. The gasifier is assumed to operate at equilibrium.
- The reverse water gas shift reactor is assumed to be at equilibrium and is modeled with an equilibrium reactor directly after the gasification in Hysys.
- A H_2/CO ratio in the syngas of 1.9 at the inlet of each FT reactor has been chosen. The hydrogen addition to the plant is adjusted to obtain this value.

- Three slurry CSTRs modeled in Aspen Custom Modeler are used as FT reactors. The conversion is kept between 60-61% in the simulations, however this must be done manually and some differences are observed between the simulations.
- The hydrocarbon product in this report is not assumed to be upgraded to fuel. Normally the hydrocarbons need to be recovered and separated into gasoline, diesel and jet fuel. The price of the product is set at the output from the Fischer-Tropsch reactors.
- The Hysys model had problems to converge when the recycle stream was connected to the gasifier. This was solved by modifying the stream added to the gasifier to be similar to the recycle stream. A Hysys flowsheet can be seen in appendix A.2 and the compositions of the tailgas and recycle in the workbook in appendix B.

5 Results

The task of this report is to investigate different operating parameters for a BtL plant to obtain maximal hydrocarbon production in an economical view. The following sections evaluates the performance of the BtL plant.

5.1 Comparison of BtL plants with and without H_2 addition

An initial case study of a BtL plant was done to get an indication of how much additional fuel it is possible to produce with addition of hydrogen to the process. A flowsheet of the case with conventional steam addition to the WGS reactor instead of hydrogen addition can be seen in appendix A.2 Figure A.3. The numbers in Table 5.1 are retrieved from the simulations in Hysys. To compare the cases, the electrical energy consumption needed to produce hydrogen in an HTE unit is included as seen in Table 5.1.

Table 5.1: Hydrocarbon production and electricity consumption for a BtL plant with and without adjustment of the syngas ratio with hydrogen. The reference case uses steam instead of hydrogen to adjust the syngas ratio.

	Reference case with steam addition	Optimized case
Hydrocarbons [L/h]	30723	70887
Electricity [MW]	0	419

With a hydrogen addition corresponding to 419 MW electricity consumption, 40.2 m^3/h additional hydrocarbons are produced compared to a BtL plant without hydrogen addition. As seen from Table 5.2, 0.1 L additional syngas is produced per kWh of electricity used to produce hydrogen. With the current electricity price in Norway of 0.3 NOK/kWh [31], the cost will be 3.13 NOK per liter additional syngas produced, (see Table 5.2). This estimate does not include the higher investment of the plant due to larger syngas flow, as seen in Table 5.1. More syngas produced in the gasifier and RWGS reactor requires larger process equipment, as e.g. FT reactors, to handle the increased flow. A HTE unit is also needed to produce the hydrogen. The enhancement with hydrogen addition shows a great reduction in the production cost of fuel compared to a report from Avinor/Rambøll in 2013. This report estimated a possible price of 11 NOK/L fuel from a conventional BtL plant [32]. The price found in this study is only a rough estimate of the cost of the additional hydrocarbons produced. A more thorough price estimate has been conducted in section 8.

Table 5.2: Additional hydrocarbon product produced by adding hydrogen to the BtL plant compared to a reference plant without hydrogen addition, as seen in Table 5.1. The electricity consumption is given, and the additional product is calculated into L/kWh electricity added. The production price with an electricity price of 0.3 NOK/kWh is given [31].

Additional product [L/h]	40164
Electricity consumption [MW]	419
L/kWh	0.10
NOK/L	3.13

5.2 Torrefaction energy requirements

The energy requirements for a torrefaction unit is important when designing the plant. In this report use of excess steam is assumed produced in a waste heat boiler heat exchanged with hot syngas from the RWGS reactor. It is also assumed that the torrefied biomass is produced at the same location as the BtL plant. This will save the cost of pelletization and transportation. The biomass is already heated to around 300°C, and if it is fed to a gasifier directly no cooling or pelleting is required [8],[9].

A calculation of the energy requirement for the torrefaction process was performed. An overview of the energy requirements can be seen in Table 2.2. The pre-dryer is assumed to use 33 kWh/tonne product, and the torrefaction unit to use 60 kWh/tonne product [5],[10]. The grinding energy of 24 kWh/tonne product is either supplied by electricity produced from excess steam in the plant or imported electricity. The pre-dryer and torrefaction unit is indirectly heated with steam.

The steam used indirectly as the heating medium is produced by heat exchange with the hot syngas leaving the gasifier as seen in Figure 5.1. After condensing and heating the biomass, the water is reused in a closed loop to cool the syngas in a waste heat boiler.

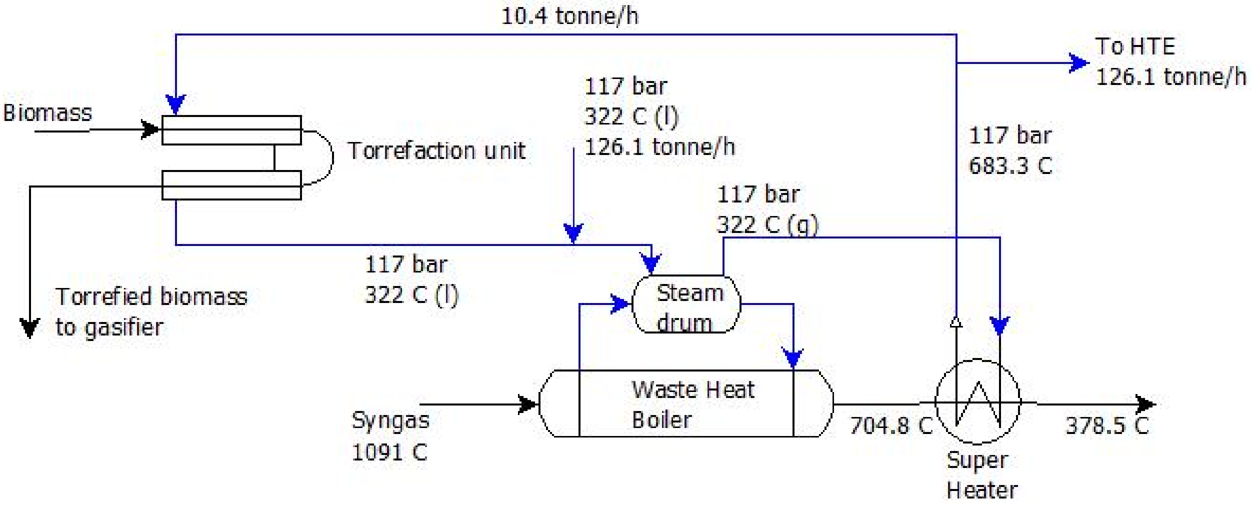

Figure 5.1: Steam production for torrefaction. The blue streams are water while the black contains carbon based material.

The required amount of steam for heating the biomass is calculated by using the specific heat of steam at 683°C and the heat of vaporization (released when the steam is condensing). The values can be found in Table 5.3. The biomass feed is 83.33 tonne/h, so with an energy requirement of 93 kWh/tonne as seen in Table 2.2, the required heat energy is 7.75 MW. This corresponds to 10.4 tonne/h of steam at 683°C and 117 bars, cooled to the boiling point at 322°C, and then condensed to liquid water. This can be seen in Figure 5.1.

Table 5.3: Properties of steam at 683°C and 322°C. The numbers are taken from the Hysys simulation.

Specific heat of steam at 683°C [kJ/kgK]	2.5
Heat of vaporization at 322°C [kJ/kg]	1251

5.3 Evaluation of type of High-Temperature Electrolysis cell used to produce hydrogen.

The high-temperature electrolysis cell can either be oxide conducting or proton conducting. In a SOEC, the oxide ion permeates through the membrane, and in a SPCEC the proton (H^+) permeates. This means that the unconverted steam is either in the oxygen stream added to the gasifier or in the hydrogen stream added to the RWGS as seen in Figure 4.1. Water acts as a gasifier agent and will influence the amount of syngas produced in the gasifier. Two simulations were conducted, and the results can be seen plotted in Figure 5.2.

1. The HTE cell is a SPCEC producing pure hydrogen, and the oxygen stream contains the 20% unconverted steam. This oxygen/steam stream is added to the gasifier.
2. The HTE cell is a SOEC producing pure oxygen, and the hydrogen stream contains the 20% unconverted steam.

The size of the oxygen stream is adjusted so the temperature out of the gasifier is kept constant at 1300°C. The size of the hydrogen stream is adjusted so the H_2/CO ratio is kept constant at 1.9 before the first Fischer-Tropsch reactor. The result is collected from the outlet stream of the gasifier in Hysys. Only hydrogen, carbon monoxide, water and carbon dioxide is considered as they represent 99.8 mol% of the stream in both cases. The concentration of other minor components as e.g. H_2S will not differ in the two cases.

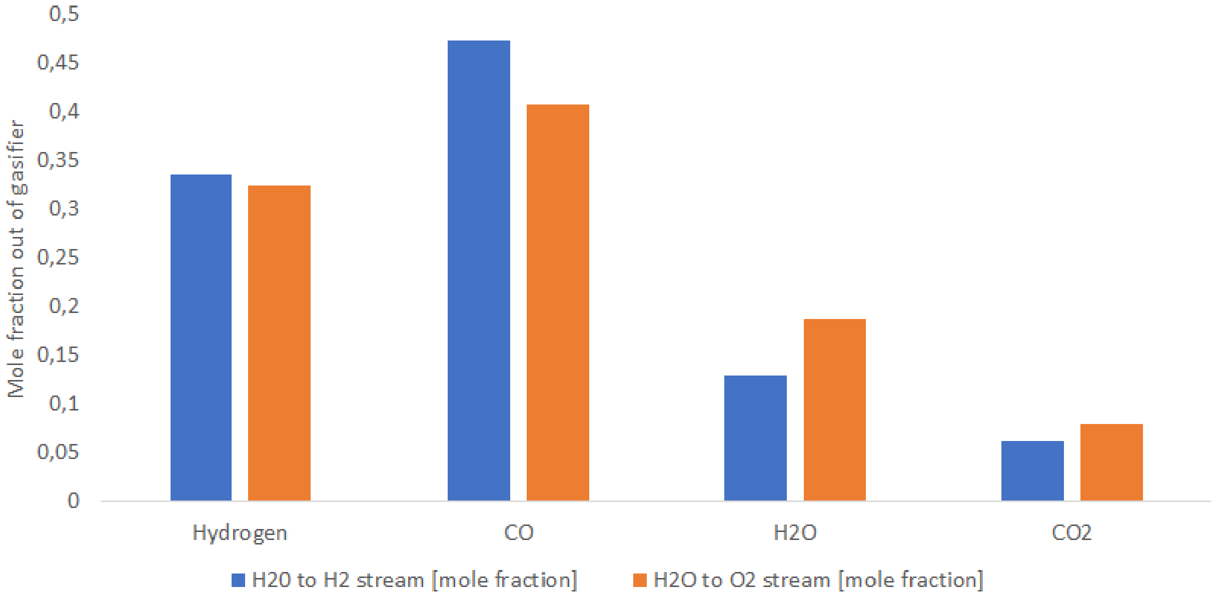

Figure 5.2: Differences in composition out of gasifier when the unconverted steam from the HTE is added in the O_2 stream and in the H_2 stream.

From the result in Figure 5.2 it is clear that the mole fraction of hydrogen and carbon monoxide is higher out of the gasifier when the unconverted steam is added with the hydrogen stream to the plant. This means that pure oxygen is added to the gasifier. Less water and carbon dioxide will also leave the gasifier. The composition of syngas out of the gasifier is however not the only consideration that needs to be made. The most important parameter is how much syngas entering the Fischer-Tropsch reactors. Equation (5.1) has been used to evaluate the economic profitability of the cases. The electricity ($Q_{electricity}$) used in the equation is retrieved from the Hysys simulation and is the electricity used in the HTE cell to split steam into oxygen and hydrogen.

$$M_{\text{products}} \cdot P_{\text{products}} - Q_{\text{electricity}} \cdot P_{\text{electricity}} = Z \tag{5.1}$$

M_{products} is the volume stream in L/h of products produced in the FT synthesis, P_{products} is the price of products, $Q_{\text{electricity}}$ is the number of kWh electricity used to split steam in the HTE cell, $P_{\text{electricity}}$ is the price of electricity per kWh (0.3 NOK/kWh), and Z is the objective function value. This case study was conducted before the complete design of the plant was finished, so some assumptions were made: The conversion in the FT reactors is 90%, producing products with a density of 0.8 kg/L. By using these numbers the volume flow of products can be calculated from the mass flow of syngas before the FT reactors. A price of 11 NOK/L product was used.

To investigate the two options, equation 5.1 was used in Hysys and an optimization was performed to maximize the equation while keeping the H_2/CO ratio at 2.1 at the inlet of the first FT reactor. A ratio of 2.1 was used so the production of hydrogen corresponds to the total hydrogen added both before and in between the FT reactors. A ratio of 1.9 would have been correct if only one FT reactor was used, but with a 2.1 ratio the hydrogen added in between the three reactors are also included. The results from the inlet to the first FT reactor can be seen in Table 5.4.

Table 5.4: Amount of syngas entering the FT reactor for the two cases when steam is added with the oxygen to the gasifier or with the hydrogen to the RWGS reactor.

	H_2O in O_2 stream	H_2O in H_2 stream
H_2 molar flow [kmol/h]	8 192	8 094
CO molar flow [kmol/h]	3 901	3 854
Total syngas molar flow [kmol/h]	**12 092**	**11 948**
Steam to HTE [tonne/h]	132 900	128 900
Energy HTE [kW]	408 455	396 244
Objective function (Z)	1 433 919	1 418 941

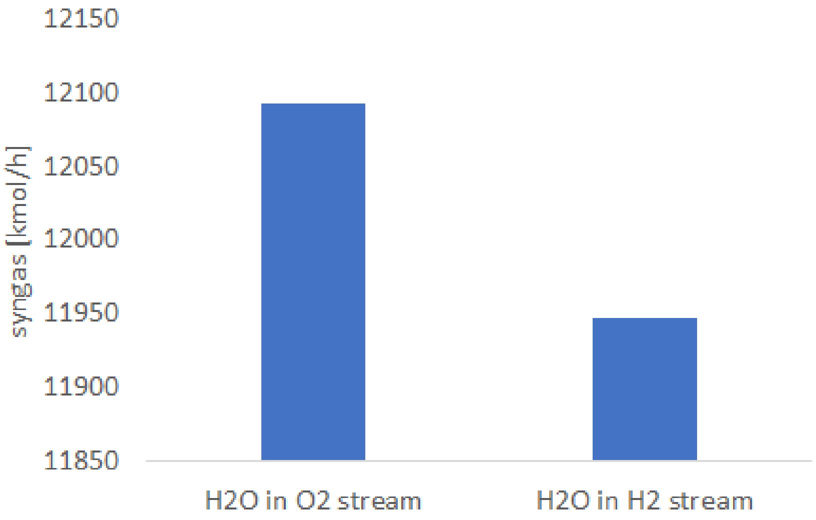

Figure 5.3: Total syngas flow when steam is in the O_2 stream and in the H_2 stream.

As seen from Table 5.4 and Figure 5.3 the syngas production has increased by 150 kmole/h when the unconverted steam from the HTE is added in the oxygen stream to the gasifier instead of in the hydrogen stream. However, more hydrogen needs to be produced when the steam is added in the oxygen stream and hence more electricity must be used to split the water. This will increase the electricity consumption, but with a price of 0.3 NOK/kWh the objective function value indicates that it is more economical to have the water in the oxygen stream. The value of the objective function can however not be used to determine any other economic aspects of the process as revenue and income, because the price of the syngas is an assumed value used in the optimization in Hysys. The values of electricity consumption in the HTE cells and syngas flow is slightly different from other parts in this report. This is because this evaluation was done at an early stage in the development of this process and some parameters have changed since that time. However, the evaluation is still valid.

5.4 Influence of oxygen in gasifier

The amount of oxygen to the gasifier is an important parameter to be decided. The following results are obtained when using a SPCEC to produce the added oxygen, which means that there is 20% steam in the stream. To optimize the production of syngas in the gasifier the oxygen input should be controlled, so the production of hydrogen and carbon monoxide is maximized. A case with varying amount of oxygen stream to the gasifier was simulated in Hysys, and the results can be seen in Figure 5.4. To produce carbon monoxide, the amount of oxygen added must be under-stoichiometric to get an incomplete combustion. The ratio of the oxygen feed (λ) to the gasifier can be calculated by equation 5.2.

$$\lambda = \frac{\text{Mass flow of oxygen stream at gasifier inlet } (\frac{\text{kg}}{\text{h}})}{\text{Mass flow of oxygen stream for stoichiometric combustion } (\frac{\text{kg}}{\text{h}})} \tag{5.2}$$

The oxygen stream in the equation refers to the stream with a mixture of oxygen and steam added to the gasifier from the HTE cell. The stoichiometric value is found by increasing the added oxygen amount until oxygen is observed in the outlet stream of the gasifier.

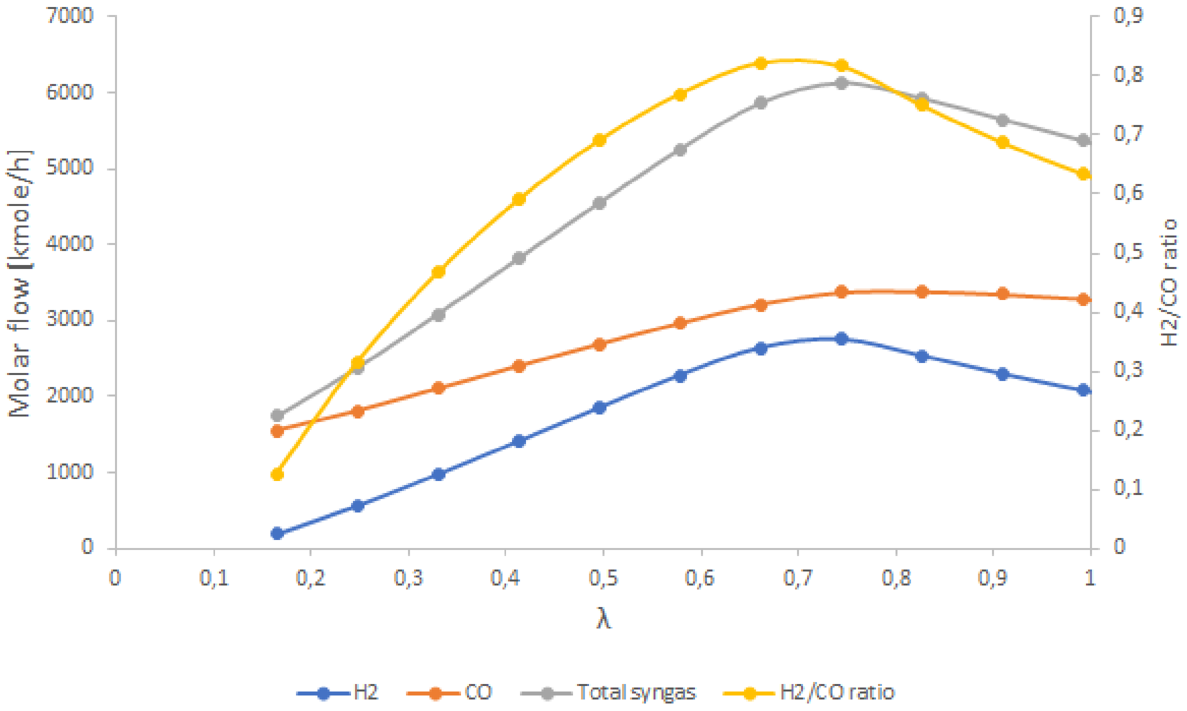

Figure 5.4: Production of H_2, CO and total syngas flow as function of the oxygen ratio added to the gasifier. The H_2/CO ratio is also shown.

A value of λ below 1 must be used to get incomplete combustion and maximize the production of CO. The figure shows that the optimal addition of the oxygen stream is when $\lambda \approx 0.75$. Both the hydrogen and carbon monoxide molar flow are maximized in that point.

The temperature out of the gasifier must be at least 1300°C to convert ash and soot into slag [12], [13]. From Figure 5.5 it can be seen that the temperature is 1300°C or above when λ is 0.805 or above. This will cause a slight decrease in production of syngas, but the benefit of reducing the production of slag in the process will compensate for this decrease [13]. This is because the slag and soot must be removed from the syngas stream before it enters the FT reactors, which complicates the cleaning process. The slag also represents a carbon loss for the process.

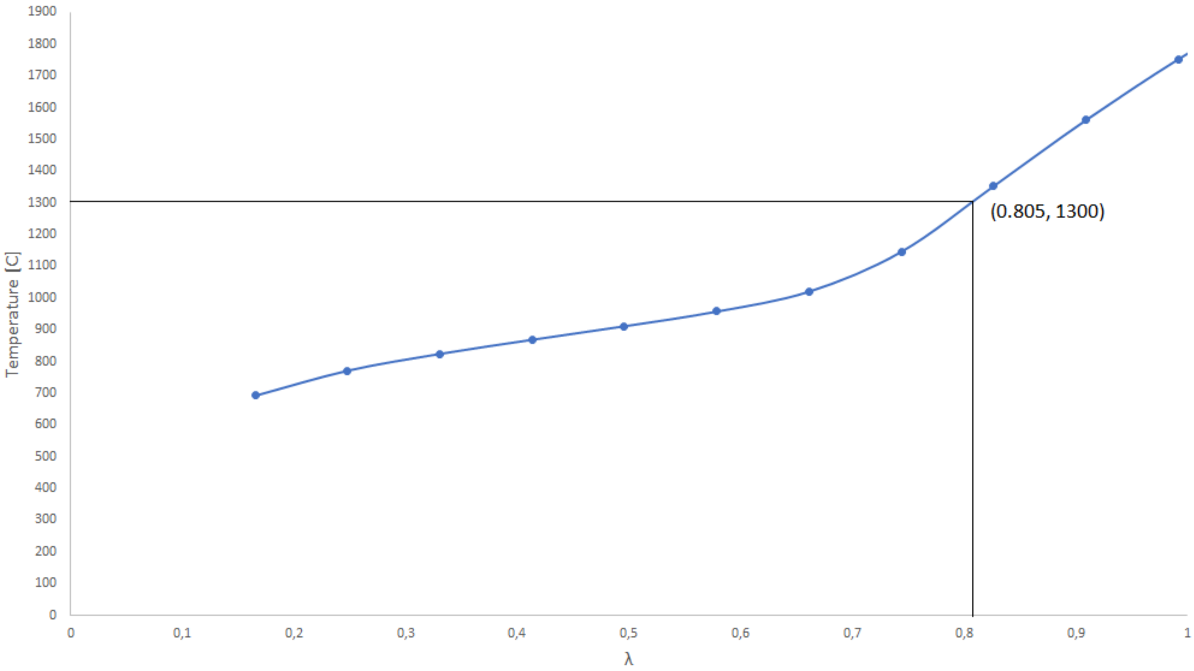

Figure 5.5: The temperature of the syngas leaving the gasifier as a function of oxygen ratio. The highlighted point is where the temperature of the outlet stream from the gasifier is 1300°C.

5.5 High temperature electrolysis cell energy

The HTE is modeled with a conversion reactor in Hysys to simulate the splitting of water. Prior to the HTE cell, the water is heated in a heat exchanger with the syngas leaving the gasifier. The water enters the exchanger as liquid and is vaporized in a waste heat boiler at constant temperature. The steam is then superheated to over 650°C by the syngas (see Figure 5.1 and 6.2 for exact temperatures). The temperature of the steam must be increased to the operating temperature of the HTE cell of 800°C. An alternative is to utilize the purge stream from the process by burning it. About 14% of the recycle stream is purged to prevent accumulation of inerts as nitrogen, CO_2 and CH_4. By burning the purge in a fired heater, the steam can be further heated to the operating temperature of the HTE cell. A simulation in Hysys showed that burning the purge produced enough heat to increase the temperature of the steam to 800°C.

Table 5.5 shows the hydrogen production and the energy requirement for the electrolysis of steam in the Hysys simulation. The energy required per kg hydrogen matches the previous referred value from literature [20].

Table 5.5: The simulated energy consumption for HTE in Hysys.

Parameter	Value
Duty [kW]	419000
Hydrogen [kg/h]	12228
kWh/kg H_2	34.27

5.6 Optimal distribution of hydrogen in the plant

The hydrogen produced in the HTE process must be optimally distributed in the plant to maximize the product outcome of hydrocarbons. The addition of hydrogen in the RWGS will contribute to the shift of CO_2 to CO and increase the amount of syngas entering the FT process. The amount of hydrogen added must be controlled to obtain a H_2/CO ratio slightly below 2 to favor the production of high weight hydrocarbons in the FT reactors.

The optimal hydrogen distribution was obtained by deciding a H_2/CO ratio at the inlet of each FT reactor. Then an optimization was done in Hysys by evaluating equation 5.1, with the constraints of a H_2/CO ratio of 1.9 at the inlet of each FT reactor.

Table 5.6: An overview of the hydrogen distribution in the BtL plant. The added amount is optimized to get a H_2/CO ratio of 1.9 at the inlet of each FT reactor.

Hydrogen	[kmole/h]	%
To RWGS	5530.0	91.17
Before FT2	385.0	6.35
Before FT3	150.6	2.48

Table 5.6 shows the amount of hydrogen in kmole/h and the percentage of the total amount of hydrogen being added at the various places in the plant. Most of the hydrogen is added to the RWGS, and less is needed to adjust the H_2/CO ratio between the FT reactors.

5.7 Acid gas removal

Table 5.7 shows the composition of the syngas after the RWGS reactor and after the syngas moisture is removed. The hydrogen sulfide content is 0.02% or 200 ppm. As previously stated, this value must be significantly reduced before the syngas enters the Fischer-Tropsch reactors to avoid catalyst poisoning and deactivation.

Removal of constituents in the FT feed such as CO_2, N_2 and CH_4 is mainly done due to economic considerations. These gases are inerts in the FT synthesis, and not removing them will require larger reactors and a higher investment. A maximum of 15 mol% of these gases in the feed to the FT reactors is suggested in literature [2]. As seen in Table 5.7, the carbon dioxide content in the syngas is only 1.89 mol%. Together with N_2 and CH_4 the total mole fraction is 3.12, significantly below the suggested maximum level of 15 mol%. It is therefore not considered necessary to include a process to remove these components. They will be inerts in the FT reactors and be recycled to the gasifier in the tail gas. This may be an advantage based on carbon efficiency because more CO is produced in the gasifier and in the RWGS when some CO_2 is present due to the shift in equilibrium. However, sulfur will cause deactivation of catalysts in the process and must be removed.

Table 5.7: Composition of the synthesis gas in percent after water removal and before Fischer-Tropsch reactors. The total stream is 11374 kmole/h.

Component	[Mole fraction]
Methane	0.0001
Hydrogen	0.6354
H_2O	0.0091
CO_2	0.0189
H_2S	0.0002
Nitrogen	0.0018
CO	0.3345

To remove as much sulfur as possible from the syngas, it is proposed to first use a physical adsorbent process and then remove the rest of the sulfur with ZnO guard-beds as seen in Figure 5.6. The figure shows a general cleaning process of syngas in the industry [2]. The syngas is first quenched with water to remove solid particles like dust and slag. For the process in this case, the hydrolysis of COS and HCN, and water wash of NH_3 may not be necessary due to the low concentration of these compounds. These components can be captured in guard beds which may be economically more attractive.

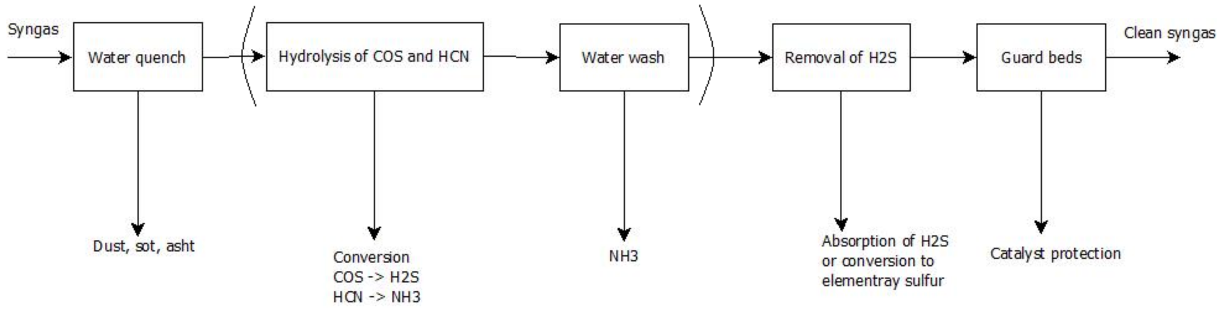

Figure 5.6: General cleaning of syngas in the industry [2]. The hydrolysis and water wash may be unnecessary in this case due to low concentrations of COS, HCN and NH_3.

R. Grainger did a case study by comparing syngas cleaning with MDEA and Selexol [24]. This is highly relevant for this case to evaluate the economics of different cleaning processes. The report compared both combined and separate recovery of CO_2 and H_2S, with each solvent. The selexol process performed better considering both energy consumption and selectivity than the MDEA process. The MDEA process did not meet the required purity for FT synthesis after the cleaning and used ten times more steam in the stripper reboiler for recovering of the solvent.

Of the two selexol processes, the selective purification of CO_2 and H_2S in a two stage process performed best with respect to energy consumption. The investment cost is clearly higher due to the larger plant, but with separate recovery there is a possibility to recycle the CO_2. The purification results from the report is listed in Table 5.8. These numbers are used further in the Hysys simulation. It must also be decided whether to capture the CO_2 or not. The low concentration may not cause a significant increase in the investment cost of larger FT reactors. If the CO_2 is not captured, it will pass through the FT reactors and be recycled to the gasifier. This will increase the production of CO both in the gasifier and in the reverse water gas shift reactor. It will also increase the size of the syngas stream fed to the FT reactors, requiring of larger reactors and thereby causing higher investment.

Table 5.8: Removal specifications by selective selexol cleaning [24].

Component	Removal [%]
CO_2	89
H_2S	99

By not capturing CO_2, the total volume of the three FT reactors increases by 81.5 m^3. This corresponds to an increase of 7% of the total volume. The production of hydrocarbons increases by over 2000 kg/h at the same time. In this report, it is assumed not to capture but recycle the CO_2 to the gasifier. The selective Selexol process is a two stage process where the first part captures H_2S and the second captures CO_2. By only implementing the first part in the BtL plant, H_2S is captured while CO_2 is left in the syngas.

With the proposed design used in this report, the sulfur removal is 99% [24]. As the syngas inlet in this case contains 200 ppm, the outlet will contain 2 ppm. This is a significant decrease, however the concentration should preferably be even less. In the industry this is achieved by using guard beds. H. Boerrigter et. al [2] did a simulation of using guard beds to polish the syngas after the adsorption process. The H_2S is removed to a level below 10 ppb by the ZnO guard beds, achieving acceptable levels for FT synthesis of the syngas [2]. Active carbon after the ZnO beds can be considered to remove impurities of COS and NH_3 if present in the syngas [3]. This is not considered in this report.

To estimate the energy requirements of the first part of the selexol process, a simulation with the design by D. Grainger [24] was performed in Hysys. The energy requirements for the simulation are listed in Table 5.9. The duty of the H_2S stripper is stated in the report as 7.8 MJ/kg S. A removal of 99% corresponds to 83.75 kg/h of sulfur captured. The energy usage in the stripper will then be 182 kW.

Table 5.9: Obtained energy requirements for sulfur removal with selexol based on the report by D. Grainger [24].

Parameter	Duty [kW]
Pumping duty	350.1
Compression duty	70.8
Stripper duty	182.0

A small part of the CO_2 in the syngas will be co-absorbed with H_2S in the selexol absorber [24]. This effect can be coped with, but not totally avoided, by operating the sulfur-cleaning process at higher temperature [33]. 2% of the CO_2 entering the sulfur gas cleaning unit is assumed to be co-absorbed in the process.

The ZnO guard beds are not simulated in Hysys but are assumed to remove the rest of the sulfur in the syngas before the FT reactor. The syngas cleaning system is simulated with a component splitter in Hysys, where the cleaning results from this discussion are defined.

In the investment analysis performed in the following sections, the price of the ZnO guard beds must be calculated as a variable cost, because they need to be shifted due to saturation of the beds [11].

5.8 Carbon efficiency of the biomass-to-liquid plant

With the previously obtained results, the plant is evaluated based on carbon efficiency and energy efficiency. The energy efficiency evaluation is presented in the next section. The carbon efficiency is defined as how much of the added carbon in the biomass is converted to hydrocarbons. From Figure 4.1 it can be seen that the main carbon loss is from the purge stream.

The carbon efficiency of the plant is defined as:

$$C_{\text{eff}} = \frac{C_{\text{biomass}} - C_{\text{purge}} - C_{\text{selexol}}}{C_{\text{biomass}}} \cdot 100\% \tag{5.3}$$

The C_{selexol} is as previously stated 2% of the carbon dioxide entering the selexol sulfur removal process. This corresponds to $0.02 \cdot 223.5$ kmol/h CO_2 = 4.47 kmol/h CO_2. The inlet of biomass is 83.33 tonne/h or 832.4 kmol/h with a composition as stated in section 2.

The purge represents the main loss of carbon in the process. As previously stated, the purge is sized to prevent accumulation of inerts in the process. The purge is also sized to release enough heat when burned to increase the steam inlet of the HTE to the operating temperature. The amount of purge needed to heat the steam to 800°C represents 14.7% of the total tail gas stream, as seen in Figure 5.7. The heating is simulated in Hysys by using a fired heater fed with the purge and heat exchanged with the steam. After a complete combustion with excess oxygen from the HTE, the purge is released as CO_2.

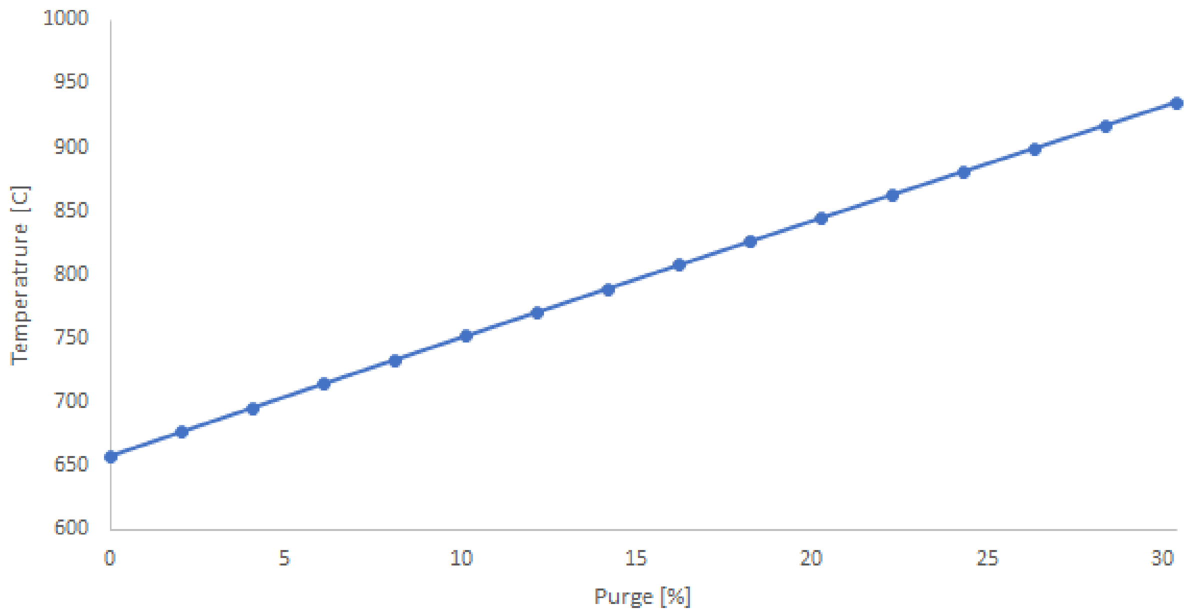

Figure 5.7: Temperature of the steam to the HTE as a function of percent of tailgas combusted in a fired heater and heat exchanged with the steam. Just under 15% is needed to get a steam temperature of 800°C.

The amount of carbon released after the combustion of the purge is 97 kmol/h. Inserting the numbers into equation 5.3, the carbon efficiency of the process is calculated as:

$$C_{\text{eff}} = \frac{3587.6 - 97.0 - 2.5}{3587.6} \cdot 100\% = 97.2\% \tag{5.4}$$

Compared to conventional BtL-FT plants, the carbon efficiency obtained here is much higher [34],[35]. This is due to the possibility of converting even more of the carbon in the biomass into hydrocarbons by using three FT reactors in series and a RWGS reaction with hydrogen addition.

6 Heat Integration

6.1 Heat integration of the BtL plant

Heat integration of the plant is important to recover as much energy as possible and minimize the need for imported energy. Aspen Energy Analyzer (AEA) V9 has been used to heat integrate the BtL plant.

It was chosen to split the heat exchanging of the plant in two parts; one part is the FT part of the plant seen in Figure 6.1, while the other is the rest of the plant including torrefaction, gasification, RWGS, HTE and sulfur removal. This is also done due to problems in Aspen Energy Analyzer when the whole plant is heat exchanged simultaneously.

6.2 Heat integration of the plant excluding FT reactors

The first part of the plant covers the torrefaction, gasifier, RWGS, HTE (and purge burning), and acid gas removal. The proposed design to obtain the optimal heat exchanging in this part of the plant is to heat exchange the steam used in the HTE with the hot syngas after the RWGS reactor. It will be important to cool the syngas rapidly to avoid backward reaction of CO to CO_2 by forward water gas shift reaction. If this happens, the carbon efficiency of the plant decreases due to production of CO_2. The heat exchanger network will consist of a waste heat boiler vaporizing water at high pressure, and a superheater to increase the temperature of the steam further. Figure 5.1 illustrates the proposed design.

After the network described above, the syngas must be further cooled before it enters the acid gas cleaning. This is done by preheating water as seen in Figure 6.2. Syngas moisture must be removed to achieve the best operating conditions for the FT reactors. More water in the syngas will shift the equilibrium in the FT reactors, and less hydrocarbons will be produced [27].

6.3 Heat exchanger network in FT part of the plant

Figure 6.1 shows the proposed heat exchanger network from the analysis of the Fischer-Tropsch part of the plant in Aspen Energy Analyzer, with the temperature of each stream. The heat exchanger network from Aspen Energy Analyzer can be seen in appendix B.

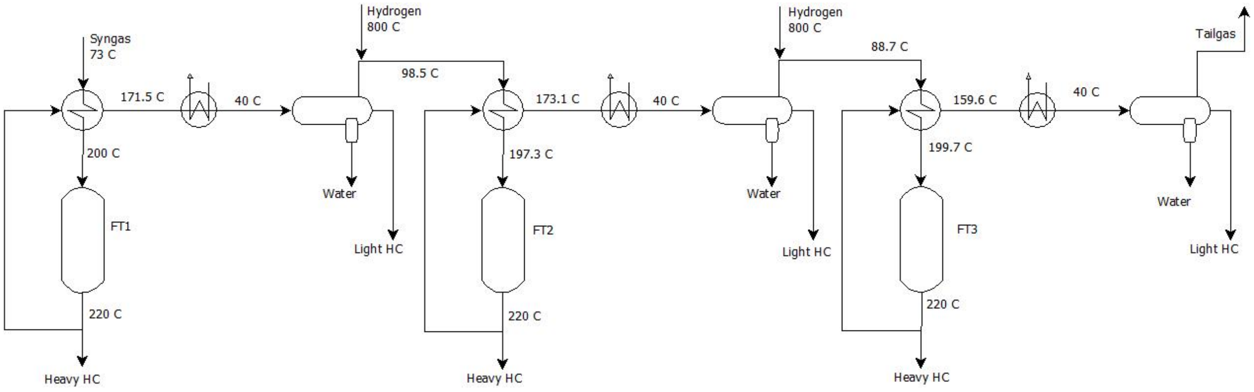

Figure 6.1: Proposed heat exchanger network for the FT part temperatures of each stream.

This part of the plant is self-sufficient with heat if the syngas is only heated to 200°C before entering the FT reactors. The outlet streams from the FT reactors must be cooled to condense the water and extract the light hydrocarbons from the unconverted syngas. The amount of heat removed from the streams can be seen in Table 6.1. This is low-temperature syngas which is not possible to utilize by producing steam, so it will be cooled by using low-temperature cooling water.

Table 6.1: Cooling requirements for the syngas after the three Fischer-Tropsch reactors to condense the water in the streams at 40°C.

Cooler after	Cooling [kW]
FT1	29200
FT2	12500
FT3	4980

6.4 Cooling of Fischer-Tropsch reactors

The Fischer-Tropsch reactors operate at a temperature of 220°C. This is to optimize the production of hydrocarbons when using a cobalt catalyst [27]. The synthesis reaction is highly exothermic, so the reactors need a good operating cooling system. A U-tube with water at the boiling point ensures sufficient cooling. The cooling water is at 13 bars and 190°C, vaporizing to steam at constant temperature. The mass flow of water required to cool the FT reactors has been calculated by using the heat of vaporization of water at 190°C seen in Table 6.2. The produced steam is used in electricity generation as seen in section 7.13.

Table 6.2: Overview of the amounts of heat removed by the cooling water in the Fischer-Tropsch reactors. The mass heat of vaporization is obtained from water property tables [36].

	Mass Heat of Vap. [kJ/kg]	Heat removed by cooling water [MW]	Massflow [kg/h]
FT1	1970	104.4	190800
FT2	1970	40.7	74400
FT3	1970	15.8	28900
Total			294100

6.5 Excess heat removed

As previously written excess heat in the system must be removed to condense water from the outlet streams of the FT reactors, and remove syngas moisture. In section 6.3 the cooling requirements for the syngas after the FT reactors are specified. The syngas must also be cooled after the RWGS and before the acid gas cleaning to remove the syngas moisture in the stream. Low temperature is necessary to condensate the vapor in the syngas and separate water, light hydrocarbons and unconverted syngas into separate streams.

The syngas leaving the superheater has a temperature of 378.5°C. This excess heat can be used to preheat the water stream before it enters the waste heat boiler. The byproduct water from the FT reactors is assumed to be cleaned and then reused in the HTE cell. These FT water streams and the water stream from the syngas dryer are cleaned and pressurized. The total water stream is then heat exchanged with the excess heat in the syngas after the superheater. Figure 6.2 shows the complete heat exchanger network for heating water to steam and cooling the syngas. No additional cooler is needed after the last heat exchanger, implying that all the heat energy in the syngas is recovered.

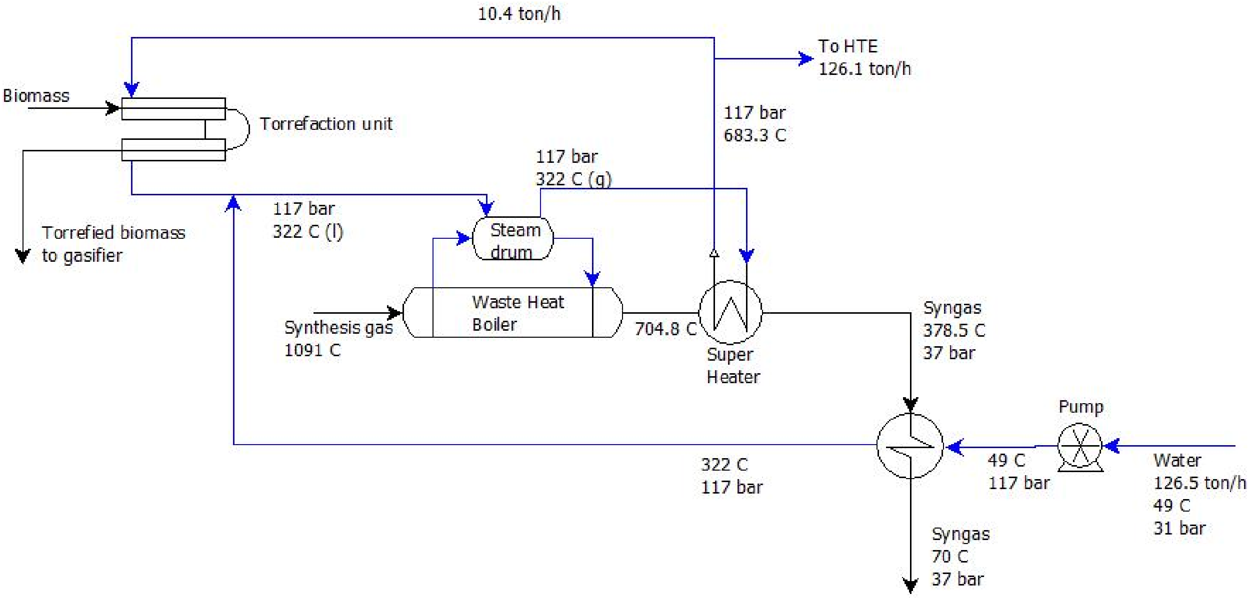

Figure 6.2: Heat exchanger network cooling the syngas and heating water to steam, which is used in the torrefaction and in the high temperature electrolysis. The blue steams are water or steam, while the black are synthesis gas.

6.6 Overall energy efficiency of the plant

To calculated the energy efficiency of the plant, mass and energy flows calculated by Hysys is used. The energy referred to in equation 6.1 is the mass flow (kg/s) multiplied with the lower heating value (MJ/kg) of the streams. Electricity is the electrolyser input (MW_E) required to split steam in the HTE cell.

$$E_{\text{eff}} = \frac{\text{Energy}_{\text{products}}[\text{kW}]}{\text{Energy}_{\text{biomass}}[\text{kW}] + \text{Energy}_{\text{electricity}}[\text{kW}]} \cdot 100\% \tag{6.1}$$

By inserting numbers, the energy efficiency is calculated to 70.4%. Compared to results for a conventional BtL plant using steam to adjust the syngas ratio the energy efficiency is higher [37].

7 Cost Estimation

7.1 Estimating equipment cost

The cost estimation of the BtL plant follows the method described in Sinnott & Towler [38]. This method gives a preliminary estimate of the investment and total production costs. First, the hydrogen enhanced BtL plant is evaluated thoroughly, then the conventional BtL plant shown in appendix A.1 is estimated based on the same methods. The annual operating time is assumed to be 99% of the year, or 361 days per year. The estimation is mainly done in united states dollar (USD), as the values in most literature are given in USD.

Table 6.6 in [38] is used together with equation 7.1,

$$C_e = a + bS^n \tag{7.1}$$

where C_e is the purchased equipment cost on a US Gulf Coast basis per January 2007. a, b and n are constants from Table 6.6 in [38], and S is a size parameter from the same table. Since the equipment costs are calculated based on a 2007 index, it can be scaled by equation 7.2 to a 2016 value.

$$C_{2016} = C_{2007}\frac{I_{2016}}{I_{2007}} \tag{7.2}$$

C_{2016} is the costing in 2016, C_{2007} are the estimated price in 2007 found by equation 7.1. I_{2016} and I_{2007} are the cost indices in 2016 and 2007 respectively. These numbers originate from the Chemical Engineering Plant Cost Index (CEPCI) [39]. The numbers for 2007 and 2016 can be seen in Table 7.1.

Table 7.1: Chemical Engineering plant cost index (CEPCI) for 2007 and 2016 [39].

Cost index	Value
I_{2016}	541.7
I_{2007}	509.7

The total capital cost of the plant can be calculated by equation 7.3.

$$C = \sum_{i=1}^{i=M} C_{e,i}[(1 + f_p) + (f_{er} + f_{el} + f_i + f_c + f_s + f_l)/f_m] \tag{7.3}$$

The cost estimation factors are listed in Table 7.2.

Table 7.2: Installation factors [38].

Cost estimation factor	Tag-name
$C_{e,i}$	Purchased equipment cost of equipment i in carbon steel
M	Total number of pieces of equipment
f_p	Installation factor for piping
f_{er}	Installation factor for equipment erection
f_{el}	Installation factor for electrical work
f_i	Installation factor for instrumentation and process control
f_c	Installation factor for civil engineering work
f_s	Installation factor for structures and buildings
f_l	Installation factor for lagging, insulation or paint
f_m	Material cost factor

The material factor f_m is defined as [38]:

$$f_m = \frac{\text{Purchased cost of item in exotic material}}{\text{Purchased cost of item in carbon steel}} \tag{7.4}$$

To avoid corrosion, the plant is designed in 304 stainless steel, see Table 7.3. When designing pressure vessels, the shell mass must be calculated and used as a size parameter in equation 7.1. The thickness is calculated by equation 7.5.

$$t = \frac{P_i \cdot D_i}{2SE - 1.2P_i} \tag{7.5}$$

P_i is the internal design pressure, D_i is the internal diameter, S is the maximal allowable stress and E is the welded-joint efficiency (assumed to be 1). The mass of the pressure vessel is:

$$\mathrm{m_{shell}} = \pi \cdot D_i \cdot H \cdot t \cdot \rho_{\mathrm{304SS}} \tag{7.6}$$

where H is the height of the vessel in meters, and ρ_{304SS} is the density of 304 stainless steel.

If historical data for similar equipment is available, an economic estimate can be made by scaling the data to present value with equation 7.7.

$$C_2 = C_1(\frac{S_2}{S_1})^n \tag{7.7}$$

Table 7.3 shows the factor cost of material relative to carbon steel. Table 7.4 shows typical factors used in equation 7.3 for estimating fixed capital cost of a project [38].

Table 7.3: Factorial cost factors, f_m, relative to plain carbon steel [38].

Material	f_m
Carbon steel	1.0
Aluminum and bronze	1.07
Cast steel	1.1
304 Stainless Steel	1.3
316 Stainless Steel	1.3
321 Stainless Steel	1.5
Hastelloy C	1.55
Monel	1.65
Nickel and Inocel	1.7

Table 7.4: Typical factors for estimation of project fixed capital cost [38].

Item	Process type Fluids
Major equipment, total purchase cost	C_e
f_{er} Equipment erection	0.3
f_p Piping	0.8
f_i Instrumentation and control	0.3
f_{el} Electrical	0.2
f_c Civil	0.3
f_s Structures and buildings	0.2
f_l Lagging and paint	0.1
ISBL cost, $C = \sum C_e \times$	3.3
Offsites (OS)	0.3
Design and Engineering (D&E)	0.3
Contingency (X)	0.1
Total fixed capital cost C_{FC} = C(1+OS)(1+D&E+X)	
= C ×	1.82
$= \sum C_e \times$	6.00

7.2 Torrefaction

The sizing and costing of the torrefaction part of the plant are based on numbers presented in a case study by Topell [5], [10]. The output capacity of the torrefaction unit in that case is however seven times less than this case. The assumed output capacity of torrefied biomass for the plant in this case is about 722 000 tonne/year. Based on the published cost of the torrefaction unit, the price is scaled to this case with a scaling factor of 0.6. By use of equation 7.7, the capital cost of the torrefaction part of the plant is:

$$C_2 = 16.3 \cdot (\frac{722000}{100000})^{0.6} = \text{M\$ } 54.35 \tag{7.8}$$

This includes the cost of the predryer and the torrefaction unit. Pelleting is not included as the torrefied biomass is assumed to be fed to the gasifier without further processing. There are however some differences between the two compared plants. The lower heating value (LHV) of the torrefied biomass is assumed to be 21.70 GJ/tonne in the Topell case, but it is only 18.75 in this case. A product with higher specific energy will reduce the need for production capacity in the plant, for the production of the same amount of energy in the biofuel. This will reduce the capital cost of the torrefaction part of the BtL plant due to investment in smaller equipment. However, the calculated price for the torrefaction equipment in equation 7.8 is used in the further study.

7.3 Gasifier

Due to unrealistic size and cost estimation of the gasifier by methods presented in Sinnott & Towler [38], the gasifier is estimated based on results presented of similar equipment in other reports. An estimation of a gasifier with a capacity of 483 MW_{LHV} biomass costs 150 million dollars in 2007 [40]. The feed of torrefied biomass to the gasifier used in this thesis has a lower heating value of 434 MW. With a scaling factor of 0.5 as given in the report, the cost of the gasifier will be 151.1 million dollars in this case. The sizing of the gasifier is not specified in the report, however an external diameter of around 3 meters and internal diameter of 2 meters appears to be conventional in the industry [41]. The height of the same gasifiers is about 4.5-5 meters.

Other reports give other numbers for the gasifier. In a report by I. Hannula [42] the price of a gasifier based on 100 MW_{LHV} biomass is calculated to be 17 M€. Upscaled with a scaling factor of 0.6 and converted to USD (19. June 2017) this equals 41 M$. The original price in the report is assumed to be on a 2016 basis as nothing else is mentioned.

The latter is taken as the price of the gasifier in the economic evaluation because this price is assumed to represent the newest type of gasifier.

7.4 Reverse water gas shift reactor

The water gas shift reactor can be seen as an extension of the gasifier, as seen in Figure 3.1. The reaction is spontaneous when the temperature is above 800 °C, so no catalyst is required [14]. Hydrogen from the HTE cell is fed to the RWGS reactor contributing to the conversion of CO_2 to CO and adjusting the syngas ratio to 1.9.

A simulation done with the Cantera software using the GRI 3.0 kinetic model has been used to estimate the sufficient residence time of the syngas in the RWGS reactor, and the volume of the reactor. The syngas from the gasifier is fed to the reactor, and hydrogen is added. The reaction is happening at 1118°C and 40 bars, and the results from the simulation are shown in Figure 7.1.

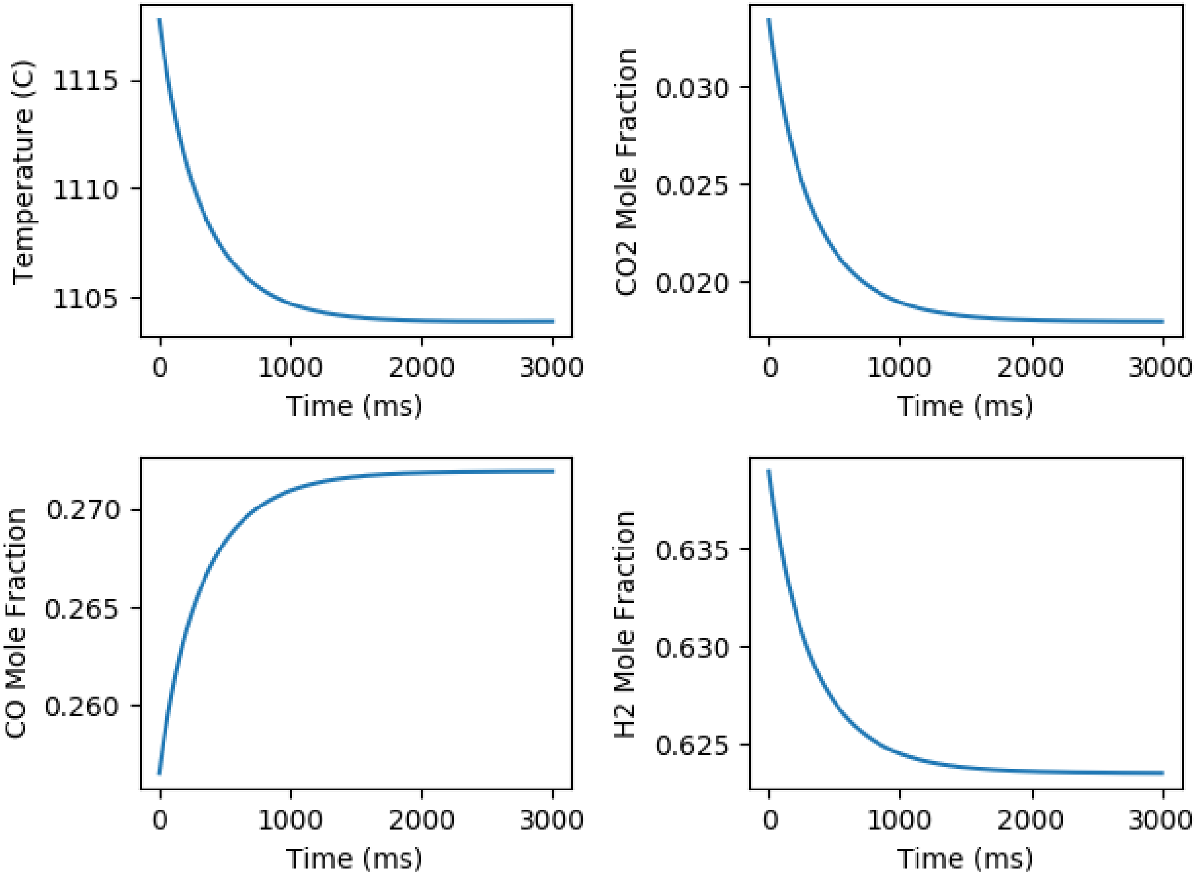

Figure 7.1: Dynamic profile of important parameters for the RWGS reaction at 40 bars.

From the figure, the sufficient residence time is estimated to 1.5 seconds when equilibrium is reached, which gives a volume of the reactor of 17.3 m^3. By using a height to diameter ratio of 2, the diameter, thickness of the shell and the shell mass of the vessel can be calculated. The results are summarized in Table 7.5. The estimation is difficult to verify as no example of a RWGS reactor as an extension of the gasifier has been found in literature.

Table 7.5: Sizing results for the RWGS reactor. It is assumed to be an extension of the gasifier.

Diameter [m]	2.22
Height [m]	4.44
Thickness of shell [m]	0.06
Shell mass [tonne]	14

By cost estimating it as a pressure vessel with previously mentioned equations, the price will be \$114 000.

A simulation has been done for a case where the pressure is 20 bar, instead of 40. The rest of the parameters are equal to the other case. The results can be seen in Figure 7.2.

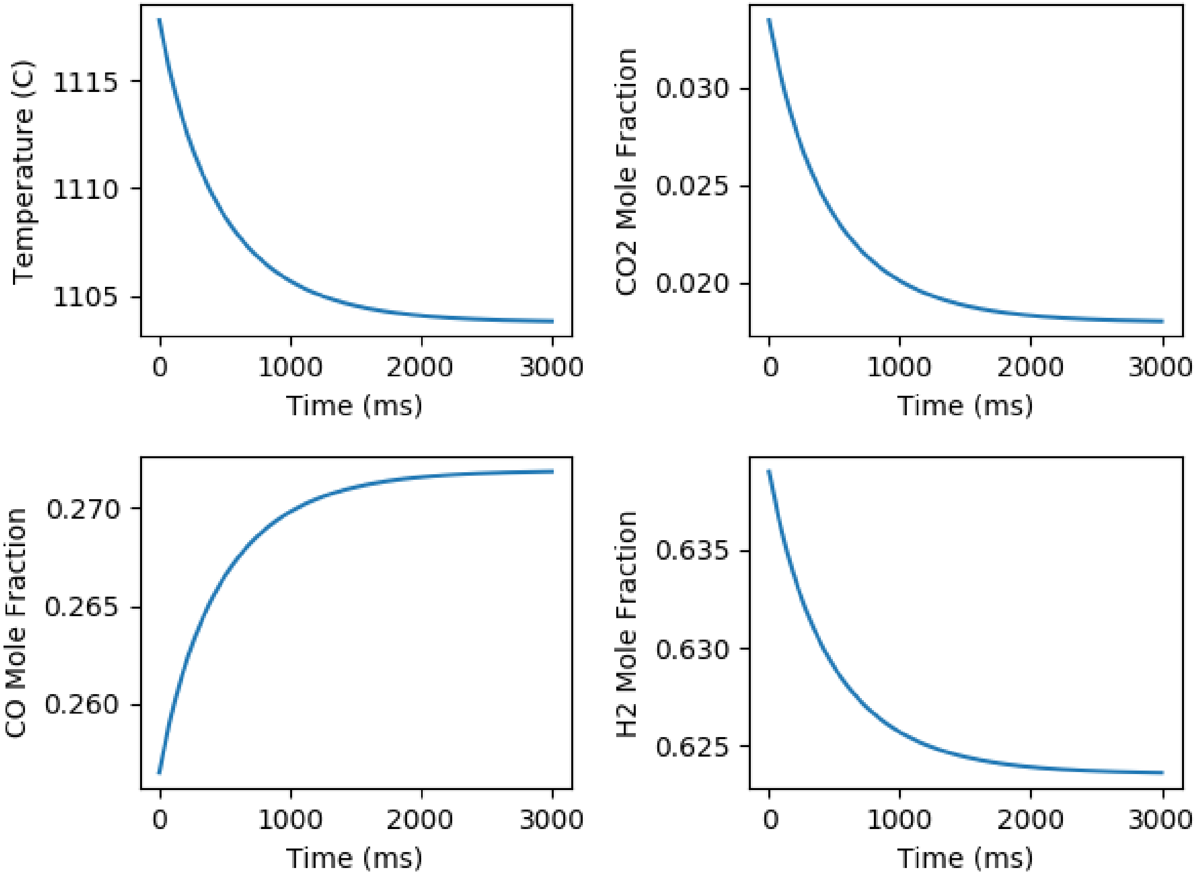

Figure 7.2: Dynamic profile of important parameters for the RWGS reaction at 20 bars.

With lower pressure, the reaction rate is slower, and a residence time of 2.5-3 seconds is necessary to obtain equilibrium. The reactor volume must also be increased to 70 m^3, leading to a higher investment cost of \$351 000. Clearly, the most economically is to operate at the high pressure of 40 bar. However, the pressure cannot be too high, as the FT reaction is conducted at 20-50 bar.

7.5 Fischer-Tropsch reactors

7.5.1 Sizing

A FT reactor can be sized based on the size of the inlet stream, q_{in}. The diameter of the reactor can be calculated from equation 7.9, where A is the cross-sectional area and v is the gas inlet velocity. The velocity of the gas used in literature varies between 0.1-0.3 m/s [43]. In this model, an average value of 0.2 m/s is chosen.

$$q_{in} = v \cdot A \tag{7.9}$$

The diameter is then:

$$D = \sqrt{\frac{4 \cdot q_{in}}{\pi \cdot v}} \tag{7.10}$$

From the diameter and the volume of the reactor, the height can be calculated by equation 7.11. The volume of the reactors in the simulation required to obtained the specified conversion of syngas is calculated by the ACM models in the Hysys simulation.

$$H_{cstr} = \frac{4 \cdot V_{cstr}}{\pi D^2} \tag{7.11}$$

Now the thickness of the shell is calculated by equation 7.5 and the mass from equation 7.6. The price of the three FT reactors can be calculated by using the equations for a pressure vessel stated above. The FT reactors in Hysys are modeled with a slurry volume of 67% of the reactor where 20 wt% of the slurry is catalyst. The weight of the catalyst is given by the ACM model in Hysys. The ACM model is based on a specific area of heat transfer which is 50m^{-1}. To find the area of the required cooling system, this value is multiplied by the volume of the reactor. The results are shown in Table 7.6.

Table 7.6: Calculated parameters for the three Fischer-Tropsch reactors.

Parameter	FT1	FT2	FT3
Volume [m^3]	713	306	139
Diameter [m]	4.7	3.1	2.1
Height [m]	40.3	40.0	39.1
Thickness [m]	0.112	0.069	0.045
Mass of shell [tonne]	536.5	217.5	93.3
Area of heat transfer [m^2]	35650	15300	6975
Mass of catalyst [tonne]	79.0	33.9	15.5

7.5.2 Cost estimation

When cost estimating the reactors, the cobalt catalyst and the cooling system must also be included. By using the equations for a pressure vessel and the mass of the shell in Table 7.6, the cost of the reactors are given in Table 7.7. As the method of cost estimating heat exchangers is limited to the maximum size of 1000 m^2 in [38], the total area of each heat exchanger, as seen in Table 7.6, is split into several 1000 m^2 exchangers which is cost estimated and the values are added together. The numbers can be seen in the following table.

Table 7.7: The cost of the FT reactors calculated by use of equations in Sinnott & Towler[38]. All the prices are in million dollars.

	FT1	FT2	FT3
Vessel	2.30	1.07	0.53
Catalyst	2.32	0.99	0.46
U-tube	7.38	3.17	1.44
Total	12.00	5.23	2.43

The calculated values are higher than reported values in literature. K. Holmgren (2015) reported a price of 28.6 M€ for a Fischer-Tropsch slurry reactor producing 2420 MW of products [40]. Here, a catalyst was not included. The price was scaled by using a scaling factor of 0.75, and the calculated cost can be seen in Table 7.8. Each of the reactors are scaled individually.

Goellner et al. [44] reported a price of 20.3 M€ for a FT slurry reactor including heat exchangers, but not catalyst. The scaling is done based on the size of the inlet flowrate to the reactors. The price of the FT reactors scaled to this case can be seen in Table 7.8. For both cases, the price of the catalyst in the reactors needs to be calculated. In K. Holmgren (2015), the cost of the catalyst is given based on the energy (MW) of the products. The price is scaled to the reactors in this case, and is included in Table 7.8. The catalyst price will be equal for both of the reactor cost calculations mentioned above. The energy amount in the products from the three FT reactors can also be seen in the table.

Table 7.8: Cost estimation of the three Fischer-Tropsch reactors based on numbers found in [40] and [44].

	FT1	FT2	FT3	Total
Product [MW]	380	157	64	601
FT slurry reactor [M$] [40]	8.0	4.1	2.1	14.2
FT slurry reactor inc. heat exchangers [M$] [44]	6.3	3.4	1.9	11.6
Catalyst [M$] [40]	0.088	0.036	0.015	0.14

Worth reflect on is why the price of FT reactors with heat exchangers is cheaper than the reactors without. Both the reactors in K. Holmgren and Goellner are reported to be slurry reactors. However, the scaling basis is different in the two cases which may give different results. In the following sections, the price of the FT reactors including heat exchangers from [44], and the price of the catalyst is used. This is because the price of the heat exchangers is difficult to estimate without knowing the exact configuration and type of reactor.

7.6 Acid gas removal: Selexol process

As no economic evaluation of the sulfur removal is done in the report from D. Grainger [24] other sources are used. In a report from I. Hannula, the price for acid gas removal equipment of hydrogen sulfide is given in euros based on a 100 MW_{LHV} feed of biomass. The price of the equipment is reported to be 10 M€. Scaled up with a scaling factor of 0.6, this equals 24.12 M€ or 27 M$ (19. June 2017). This value is used as the price of the acid gas cleaning. Even though the price is not for exactly the same equipment as used in this report, it gives a good estimate on the cost of gas cleaning equipment.

7.7 ZnO guard beds

The amount and cost of ZnO guard beds are based on the procedure described in Hofbauer [11]. The properties of ZnO beds are presented in Table 7.9.

Table 7.9: Capacity and price of ZnO [11].

Sorbent	Capacity [gS/100g sorbent]	Price [$/kg]
ZnO	13 - 22	1.1 - 2.2

As 99% of the H_2S is removed by the selexol process, only 0.84 kg/h of H_2S is left in the syngas stream. By using the numbers in Table 7.9, the required amount of ZnO is calculated and the price can be seen in Table 7.10. The capacity of the sorbent is assumed to be 22 gS/100 g sorbent and the price 1.5 \$/kg. The beds must be replaced once they are saturated with sulfur compounds.

Table 7.10: Estimated amount of ZnO guard beds needed for purification, adjusted to the amount of sulfur in the syngas.

ZnO [kg/year]	Price [\$/year]
33440	50170

With the ZnO-beds placed after the selexol process the syngas is polished down to under 10 ppb H_2S [2].

7.8 Compressors and pumps

The cost estimation of pumps and compressors in the plant is performed with numbers given in [38]. A pump is required after the torrefaction to pressurize the biomass before it enters the gasifier. A compressor is required to pressurize the tailgas recycled to the gasifier. The total cost of compressors and pumps are estimated to M\$ 1.

7.9 Heat Exchangers

7.9.1 Sizing

With the heat exchanger design in Figure 4.1, 6.1 and 6.2 it is necessary to use ten heat exchangers and coolers in the plant. Some of the exchangers have been size estimated in AEA (Aspen Energy Analyzer), and some are estimated manually based on the cooling requirements. When manually calculated, the method described in Sinnott and Towler is used [38]. The sizes can be seen in Table 7.11.

Table 7.11: Result from sizing of the heat exchangers and coolers in the BtL plant.

Heat exchangers	Area [m^2]
Waste heat boiler (E-104)	457
Superheater (E-105)	3704
Preheater of water (E-101)	890
Before FT1 (E-102)	2894
Before FT2 (E-112)	1064
Before FT3 (E-114)	556
Coolers	
After FT1 (E-110)	207
After FT2 (E-113)	106
After FT3 (E-103)	52

7.9.2 Cost estimation

The cost of the heat exchangers is estimated based on numbers in Table 6.6 in Sinnot and Towler [38]. The result can be seen in Table 7.12.

Table 7.12: Cost estimation of the heat exchangers in USD.

Heat exchangers	Price [k$] 2016
Waste Heat boiler (E-104)	108
Superheater (E-105)	1 023
Preheater of water (E-101)	207
Before FT1 (E-102)	768
Before FT2 (E-112)	250
Before FT3 (E-114)	130
Coolers	
Cooler After FT1 (E-110)	58
Cooler After FT2 (E-113)	41
Cooler After FT3 (E-103)	33

7.10 High temperature electrolysis cells

The economic analysis of the electrolysis cells is based on previously published results [45], [46]. The investment of electrolysis cells is currently high with an assumed cost of 0.86 M€/MW (MW electricity) for 2020. However, the price is expected to decrease rapidly to

0.28 in 2030 and 0.21 in 2050 [45]. This report is focusing on a BtL plant being built in the future, but not immediately, and using state of the art technology. As HTE cells are a relatively new technology with a lot of research still to be conducted, the price in ten years is more relevant than the price today. Therefore, the assumed price of the cells in this report is 0.28 M€/MW.

The electricity consumption is 419 MW for this case with production of H_2 and O_2 at 800°C. This gives an investment cost of the HTE cells of 117.3 M$.

7.11 Separators

7.11.1 Vertical separator (syngas dryer)

A vertical separator is needed to separate the syngas moisture after the RWGS. The diameter of the separator must be large enough to slow down the gas below the settling velocity of the water droplets [38]. The diameter is given by:

$$D_v = \sqrt{\frac{4V_v}{\pi u_s}} \tag{7.12}$$

where D_v is the minimum vessel diameter, V_v is the vapor volumetric flow rate and u_s is the settling velocity of liquid droplets given by:

$$u_s = 0.07((\rho_L - \rho_v)/\rho_v)^{0.5} \tag{7.13}$$

ρ_L is the liquid density and ρ_v is the vapor density. From numbers obtained in Hysys for the gas and the liquid:

$$u_s = 0.07((975.8 - 15.17)/15.17)^{0.5} = 0.56 \text{ m/s}$$

With this result, the diameter in equation 7.12 becomes 2.4 meters. With a holdup time of 10 minutes for the liquid, the height of the liquid becomes 1.34 meters. The height of the separator is calculated using the recommended dimensions in Sinnott & Towler [38]:

$$H = 0.4 + D_v + 0.5D_v + H_{\text{liquid}} = 5.34 \text{ m} \tag{7.14}$$

By estimation as a pressure vessel the thickness is 0.056 meters and the mass of the shell is 18040 kg. The price of the separator will be 147000 $.

7.11.2 Horizontal separators

Three three-phase separators are used to separate the unconverted syngas from the water and the light hydrocarbons after the FT reactors. The vessels are designed with the equipment design tool in Hysys, based on the light liquid and heavy liquid residence time. Recommended residence time is 2466 seconds and 600 seconds respectively. A length to diameter ratio of 3 is used. The dimensions of the three separators are calculated by Hysys, while the wall thickness and shell mass are calculated by assuming a pressure vessel. The sizing can be seen in Table 7.13.

Table 7.13: Sizing of the horizontal separators.

Separator	Diameter [m]	Height [m]	Wall Thickness [m]	Shell mass [kg]
V-104	1,98	6,93	0,0439	15186
V-106	1,37	4,80	0,0286	4748
V-102	1,06	3,73	0,0209	2094

The price of the separators based on pressure vessel cost are seen in Table 7.14.

Table 7.14: Investment cost of horizontal separators.

Separator	$
V-104	128 700
V-106	55 00
V-102	33 100

7.12 Electricity consumption

HTE is the main source of electricity consumption in the plant. The required amount is however reduced by pre-heating the steam with waste heat from the process to the operating temperature of the cells. The electricity is then only used to split the water in the HTE cell. With a steam conversion of 80% in the cell, the required amount of steam to produce hydrogen to the plant is 126.1 tonne/h. This can be seen in Table 7.16. In the Hysys simulation, 419 MW of electricity is used to split the steam at 800 °C. 12.2 tonne/h of hydrogen is needed in the process to obtain a H_2/CO ratio of 1.9 before each FT reactor. The electricity usage corresponds to 34.26 kWh/kg H_2 produced. This matches the reported values in literature of 28-39 kWh/kg H2 [20]. The HTE electricity consumption can be seen in Table 7.15.

Table 7.15: Electricity consumption in the BtL plant.

	[MWh/year]
HTE	3 600 000

7.13 Water and steam balance

To cool the BtL plant, water is vaporized to steam which can be used in production of electricity. The low-temperature streams are cooled without steam production. The syngas after the RWGS is dependent on rapid cooling to prevent a backward reaction of CO. This is achieved by a waste heat boiler and a superheater as shown in Figure 6.2. The Fischer-Tropsch reactors are also cooled by pressurized water at the boiling point vaporizing to steam. An overview of the required water streams can be seen in Table 7.16.

The water usage can be categorized into recyclable and un-recyclable water. The steam used for electricity production can be pressurized and reused as cooling water in the FT reactors. The syngas moisture removed from the syngas after the RWGS reactor and the byproduct water produced in the FT synthesis is, after cleaning, reused in the process. Some of the water is lost due to production of hydrogen and oxygen. This water will not be possible to recycle. A water balance of the BtL plant can be seen in Table 7.16. The cooling water for the FT synthesis is vaporized to steam and used to generate electricity in a turbine.

Table 7.16: An overview of the water usage in the process.

Not recyclable	Mass flow [tonne/h]
Water to HTE	136.6
AGC	0.3
Recyclable after waste water treatment	
Dryer	35.4
Separator after FT1	44.7
Separator after FT2	16.9
Separator after FT3	6.6
Recyclable	
FT cooling water	294.1
Torrefaction	10.5

The water from the dryer and the FT separators has been in contact with syngas and hydrocarbons and must be cleaned. According to [38], the cost of waste water treatment is typically \$1.5/tonne of water.

Steam for electricity production is produced by cooling of each of the FT reactors. The steam produced is used to generate electricity. A simulation in Hysys with the amounts of steam from the FT reactors as seen in Table 7.16 generated the electricity seen in Table 7.17.

Table 7.17: Electricity generation from the steam production in the BtL plant.

Source	Electricity produced [MW]
FT cooling system	27.1

This energy is assumed to be used by compressors, pumps and other equipment. It may also be used to reduce the need for importation of electricity to the HTE unit.

7.14 Total cost of the plant

After each component is sized and cost estimated, the fixed capital cost of the plant can be calculated. The fixed capital cost is given as a function of purchased equipment calculated by equation 7.3 with the installation factors in Table 7.4 for fluids. The total fixed capital cost is then [38]:

$$C_{FC} = \mathrm{C(1{+}OS)(1{+}D\&E{+}X)} \tag{7.15}$$

OS, D&E and X are defined in Table 7.4. The equipment is assumed to be made of stainless steel, so a material factor of 1.3 is used for the equipment which is in contact with the syngas.

In addition to the total fixed capital cost, working capital is needed to get the plant running [38]. This is the money needed to buy feedstock and pay bills until the plant starts providing income. The amount can be estimated by a range of different methods, but a simple method is to use a value of 5-30% of the fixed capital (ISBL + OSBL). In this report the working capital is assumed to be 10% of the fixed capital cost. Then the total investment is:

$$\text{Investment} = C_{\mathrm{FC}} + \text{Working capital} \tag{7.16}$$

Table 7.18 shows the investment required for the various parts of the plant adjusted to 2016 dollars.

Table 7.18: The price of all the equipment in the plant. The prices are given in 2016 dollars.

Equipment	M$
Heat exchangers	2.5
Torrefaction unit	54.3
Gasifier + RWGS	41.8
HTE cells	117.3
Acid gas cleaning (AGC)	24.1
Separators	0.7
FT reactors	11.6
Compressors & pumps	1.0
Total	**253.3**

A graphic representation of the investment cost can be seen in Figure 7.3.

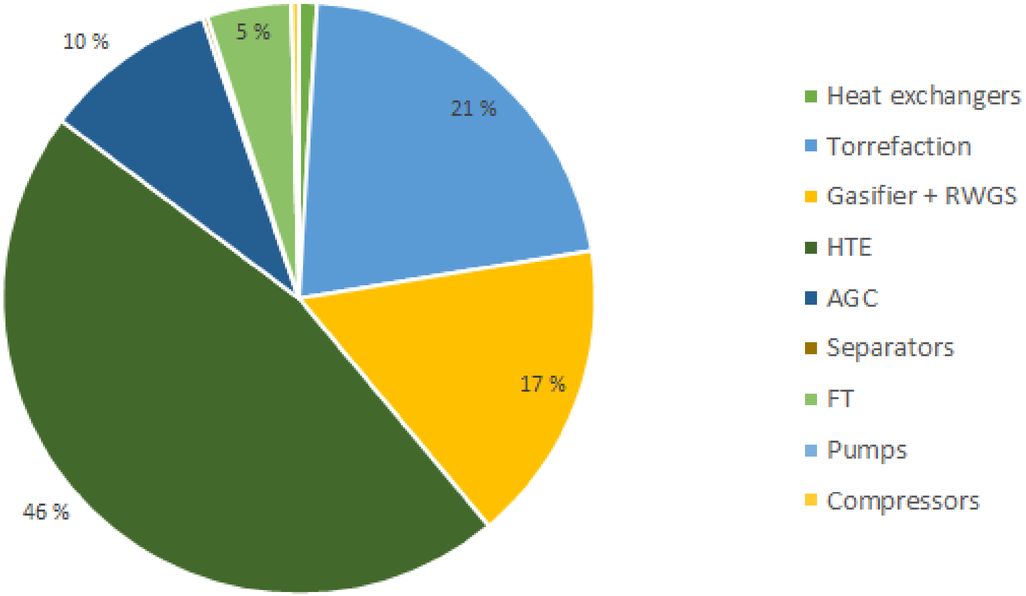

Figure 7.3: A graphic representation of the investment cost of various equipment.

When calculating the total fixed capital investment, constructing, designing, purchasing and installing must be considered. The investment can be divided into inside and outside battery limit investment (ISBL & OSBL), engineering costs and contingency costs. By using the procedure in Table 7.4, the ISBL is calculated as:

$$\text{M\$ } 253.3 \cdot ((1 + 0.8) \cdot 1.1 + (0.3 + 0.2 + 0.3 + 0.3 + 0.2 + 0.1)) = \text{M\$ } 947.3$$

The OSBL is the cost concerning the off-site development and cost not directly associated with the process. This may be adding infrastructure to the plant, offices, pipes, security etc. The OSBL is estimated as a fraction of ISBL dependent on the type of process, normally between 10-50% [38]. The OSBL taken as 15% of ISBL for this case giving a cost of 142.1 M$.

Engineering cost and contingency are both taken as 10% of ISBL plus OSBL. The exact numbers are presented in Table 7.19.

Table 7.19: Estimated values of ISBL, OSBL, engineering cost and contingency, working capital and investment for the plant.

	M$
ISBL	947.3
OSBL (15% of ISBL)	142.1
Engineering (10% of ISBL+OSBL)	109.0
Contingency (10% of ISBL+OSBL)	109.0
Fixed capital cost	1 308.5
Working capital	109.0
Investment	**1 416.4**

7.14.1 Variable cost of production

The variable costs or operating costs of production are proportional to the production volume. This includes the cost of raw material as biomass and water, electricity, shifting of catalyst and cleaning of waste water. The waste water cleaning is assumed to cost 1.5$/tonne water. The electricity consumption of the plant can be seen in Table 7.15. The biomass price varies based on the type of biomass used. Forest residue has a price of 15-30 $/tonne [7], [6]. In this report it has been assumed to cost 30$/tonne. The electricity has been assumed to have a price of 0.3 NOK/kWh or 0.035 $/kWh [31]. The water produced in the FT reactors and from the separator(dryer) of the syngas needs to be treated. After the treatment it is assumed to be used in the HTE cell to produce hydrogen. The additional water supply to the plant needs to be 33 ton/h to compensate for the loss of water in the electrolysis. The water is assumed to cost 9.77 NOK/m^3 or 1.15 $/$m^3$ [47]. A summary of the total variable costs can be seen in Table 7.20.

Table 7.20: An overview of the variable costs of production for the BtL plant.

Variable	M$/year
Biomass	21.7
Electricity	129.0
Process Water	0.3
Waste water treatment	1.3
ZnO guard beds	0.05
Total	**152.3**

As expected the costs of electricity and biomass are the main contributors to the operating costs with 84% and 14% respectively.

7.14.2 Fixed cost of production

The fixed costs of production are costs not dependent on the operation rate or output of the plant [38]. This includes everything listed in Table 7.21. How they are estimated is also explained in the table.

7.14.3 Labor

Equation 7.17 is used to calculate the required number of operators as a function of the number of major process equipment [38].

$$\mathrm{N_{operators}} = (6.29 + 0.23\mathrm{N_{units}})^{0.5} \tag{7.17}$$

A total of 25 units can be counted when including all the major units. This gives four operators per shift, and with a four shift rotation with an average salary of $60,000 per shift per year, the total cost is just under one million dollar, $960 000.

Table 7.21: An overview of the fixed cost of production.

Factor of fixed cost of production	Estimate	M$/year
Operating labour	See section 7.14.3	0.96
Supervision	25% of operating labor	0.24
Direct salary overhead	50% of operating labor+supervision	0.72
Maintenance	4% of ISBL investment	37.92
Property taxes and insurance	1%-2% of ISBL fixed capital	14.22
Rent of land	1%-2% of ISBL+OSBL investment	16.36
General plant overhead	65% of total labor+maintenance	39.18
Total fixed costs of production		**109.60**

7.14.4 Total cost of production

When the variable and fixed costs of production are calculated, the total cost of production is found by adding them together. The total costs of production, or annual operating costs, are then M$261.9.

7.14.5 Revenues

The revenue of the plant is one of the most important numbers when evaluating if a plant is economically profitable and a feasible project. From the Hysys simulation, 70884 L of hydrocarbons is produced every hour. This corresponds to 10700 barrels/day. The most interesting aspect in a study like this is to look at how sales price of the products making the plant profitable. This is done in the next section with a sensitivity analysis. No other products are assumed sold than hydrocarbons. Some electricity is produced, but it is assumed to be used internally in the plant for pumps and compressors.

7.15 Conventional BtL plant

To compare the results from the hydrogen enhanced BtL plant (H-BtL), a conventional BtL plant with steam (S-BtL) added to the water gas shift reactor is cost estimated with the similar procedure as for the H-BtL plant. A flowsheet of the plant can be seen in Figure A.3. The plant consist almost of the same equipment and components as the H-BtL plant. However, no HTE cells are used to produce hydrogen and oxygen. Instead, an air separation unit (ASU) is used to produce oxygen to the gasifier. Instead of using hydrogen to adjust the H_2/CO ratio in the syngas, steam is added in a water gas shift reactor, converting CO and water into CO_2 and hydrogen. This will decrease the carbon efficiency of the plant because the CO_2 must be removed in a acid gas removal unit. The torrefaction, gasifier and WGS reactors are assumed to be equal in both cases. Smaller FT reactors are needed because of the reduced amount of syngas, but a larger acid gas removal unit is necessary to remove CO_2 and H_2S.

An overview of the cost estimation of the components in the plant can be seen in Table 7.22. The cost estimation is performed based on the same assumptions in both cases, but the ASU is cost estimated based on numbers in [42]. An ASU producing oxygen to a plant based on 100 MW_{LHV} biomass is scaled to the current plant with 434 MW_{LHV} biomass. The original cost is 15 M$, giving a 36.2 M$ ASU for the S-BtL plant with a scaling factor of 0.6. Also the acid gas cleaning (AGC) unit is based on numbers in [42]. With the same calculation as above, a 23 M$ AGC will cost 55.5 M$ for the S-BtL plant. The FT reactors are cost estimated in the same way as for the H-BtL plant, however with updated input volume flow rates.

Table 7.22: Calculated equipment cost for the conventional BtL plant using steam to adjust the syngas ratio.

Equipment	M$
Heat exchangers	2.5
Torrefaction	54.3
Gasifier + WGS	41.1
ASU	36.2
AGC	55.5
Separators	0.7
FT	6.3
Compressors + pumps	1.0
Sum	**197.6**

The cost of equipment will be lower than for the H-BtL plant, mainly due to the high cost of HTE cells compared to an ASU. However, in this case the acid gas cleaning unit will be significantly more expensive because both H_2S and CO_2 must be removed.

By using the same method and calculations as for the H-BtL plant, the investment is shown in Table 7.23.

Table 7.23: Estimated values of ISBL, OSBL, engineering cost and contingency, working capital and investment for the plant.

	M$
ISBL	739.5
OSBL (15% of ISBL)	110.9
Engineering (10% of ISBL+OSBL)	85.1
Contingency (10% of ISBL+OSBL)	85.1
Fixed capital cost	1 020.6
Working capital	85.1
Total fixed capital investment	**1 105.7**

The variable cost of production will also be different. The biomass expenses will be the same, but the electricity consumption will be significantly lower. About 0.8 kWh of electricity is needed per kilo oxygen produced in an ASU [42],[48]. The process needs 43 tonne/h of oxygen, giving a consumption of 34.4 MW. Also, the torrefaction unit needs 7.75 MW of electricity. By using numbers in [42] of 1 MW for the acid gas cleaning energy consumption, this is added to the total electricity consumption. Process water and waste water treatment is also included with the same cost per tonne as seen in section 7.14.1. The removed CO_2 does also have a disposal cost of 5.44$/tonne [49]. Table 7.24 summarizes the variable cost of production.

Table 7.24: Variable cost of production.

Variable	M$/year
Biomass	21.7
Electricity	13.3
Process Water	2.7
Waste water treatment	1.4
CO_2	4.1
ZnO guard beds	0.05
Total	**43.2**

Then the fixed cost of production can be calculated and are shown in Table 7.25.

Table 7.25: Overview of the fixed cost of production.

Factor of fixed cost of production	Estimate	M$/year
Operating labor	See section 7.14.3	0.96
Supervision	25% of operating labor	0.24
Direct salary overhead	50% of operating labor+supervision	0.72
Maintenance	4% of ISBL investment	29.62
Property taxes and insurance	1%-2% of ISBL fixed capital	11.11
Rent of land	1%-2% of ISBL+OSBL investment	12.77
General plant overhead	65% of total labour+maintenance	30.87
Total fixed cost of production		**86.30**

The total annual cost of production for the plant is then 129.5 M$.

The revenues from the plant is dependent on production of hydrocarbons. 31 390 liter/hour of hydrocarbons are produced, corresponding to 4 740 barrels/day.

8 Sensitivity Analysis

8.1 Operating costs per liter fuel

An interesting aspect of the plants is the cost of production of one liter hydrocarbons based on the annual operating cost. An overview of the annual production of hydrocarbons in liter and the annual operating costs for both cases is shown in Table 8.1. Only the variable and fixed costs are included in the annual operating costs (Table 7.20 and 7.21). The cost of one liter hydrocarbons is calculated by dividing the annual cost with the amount of products.

Table 8.1: The production costs of one liter fuel in NOK and dollars based on the production of hydrocarbons and annual cost of production.

	H-BtL	S-BtL
Products [L/year]	614 738 000	272 269 000
Annual cost of production [M$/year]	261.9	129.5
$/L	0.43	0.48
NOK/L	3.62	4.08

The price of producing one liter of hydrocarbons from the H-BtL plant is $0.43 or 3.62 NOK, while for the S-BtL plant the price is $0.48 or 4.08 NOK. Compared to the production price of 11 NOK/L estimated in a report from Rambøll and Avinor, both values are significantly lower. However, the results are very uncertain as the operating costs are calculated based on a general procedure presented in Sinnott & Towler [38]. To get a more exact and realistic estimation, numbers from similar plants already up and running should be considered. The two evaluated plants are cost estimated based on the same procedure, so a comparison of the two is valid.

8.2 Total annualized cost

The estimation just conducted does not include the investment of the plants. This can be done by an annualized cost method. The annual capital charge ratio is defined as [38]:

$$\mathrm{ACCR} = \frac{[i(1+i)^n]}{[(1+i)^n - 1]} \tag{8.1}$$

where i is the interest rate of the investment and n is the number of years of repayment. This value can be used to calculate the total annualized cost (TAC):

$$\text{TAC} = \text{operating costs} + \text{ACCR} \times \text{total capital cost} \tag{8.2}$$

By choosing an interest rate of 0.07 and a payment period of 20 years the TAC can be calculated for both cases.

Now the price of producing one liter of hydrocarbons can be calculated based on TAC. The results can be seen in Table 8.2.

Table 8.2: The production cost of one liter fuel in NOK and dollars based on the production of hydrocarbons and total annualized cost(TAC).

	H-BtL	S-BtL
Products [L/year]	614 738 000	272 269 000
TAC [M$/year]	385.7	225.9
$/L	0.63	0.83
NOK/L	5.32	7.04

Compared to the previous result the cost of producing one liter of hydrocarbons has increased by 1.7 NOK/L to 5.32 NOK/L for the H-BtL case. Still this is below the result from the Rambøll/Avinor report of 11 NOK/L. The numbers are not completely comparable because the report also includes upgrading of the hydrocarbons. Regardless of including the upgrading process in the calculation the number will most likely be lower, because the major parts of the plant are included in the investment calculation. The S-BtL case is significantly more expensive with a price of 7.04 NOK/L products. From this evaluation it is possible to conclude that the H-BtL plant is more profitable than the S-BtL case based on the total annualized cost.

8.3 Net Present Value

A sensitivity analysis examines whether the project is profitable and economically feasible based on various sales prices and operating costs. Net present value (NPV) has been used to evaluate H-BtL project. A positive NPV indicates a profitable project while a negative NPV indicates an economic loss [38]. Equation 8.3 can be used to calculate the NPV.

$$NPV = CF_0 + \sum_{n=1}^{t} \frac{CF_n}{(1+i)^n} \tag{8.3}$$

CF_0 is the initial investment cost, CF_n is the cash flow in year n, t is the project lifetime in years and i is the interest rate.

The production price per liter shown in Table 8.1 is clearly not viable as product sales price because then the production costs and revenues are equal. To calculate the NPV, the total investment, total operating costs and annual revenues are used. The project is evaluated over a lifetime of 20 years, with a depreciation of 20%, a tax of 28% and an interest rate of 7%. Figure 8.1 shows the NPV of the plant as a function of product sales price in NOK/L.

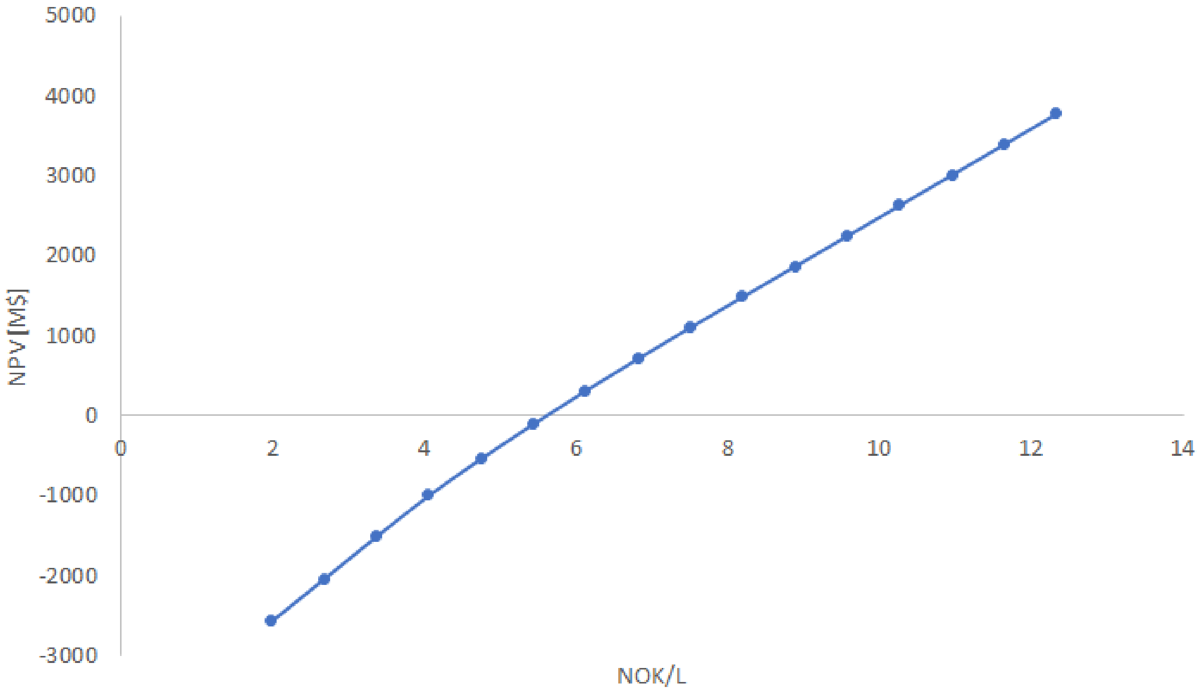

Figure 8.1: NPV evaluated as function of sales price in NOK/L for the H-BtL case.

As seen from the figure, a product price of more than 5.6 NOK/L will give a positive NPV at the end of the 20 year period.

A sales price of 7 NOK/L product is studied with respect to the cash flow of the plant. As seen in Figure 8.1 will this price give a NPV larger than 0. A graph showing the cash flow over twenty years is seen in Figure 8.2.

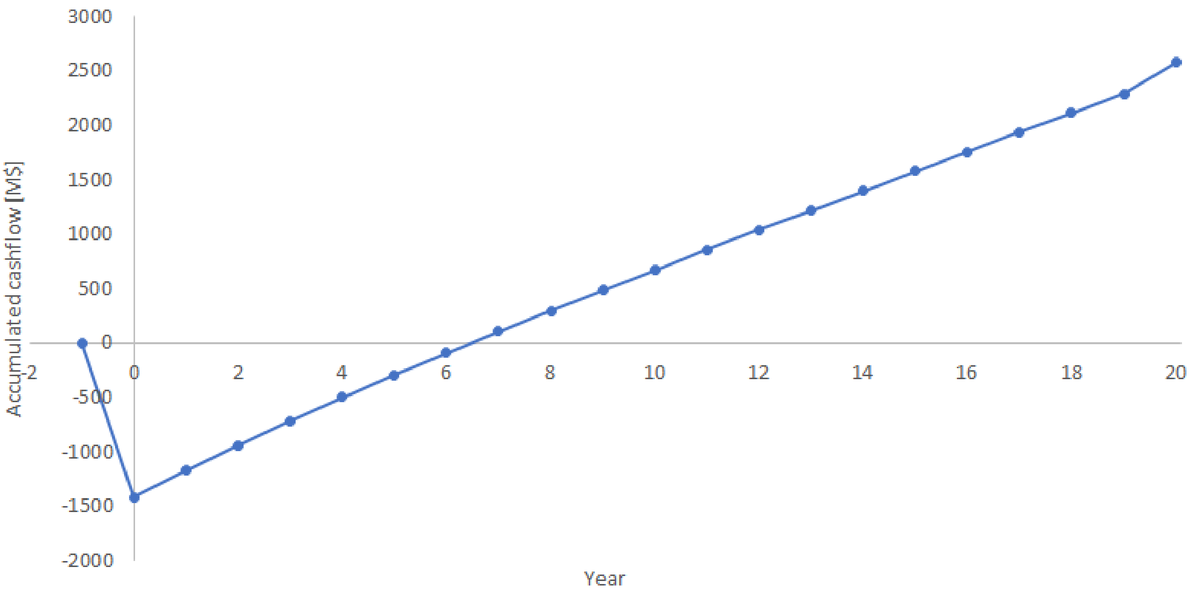

Figure 8.2: The accumulated cashflow of the plant evaluated with a sales price of 7 NOK/L and a interest rate of 7%.

The payback time of the project with 7% interest rate and a product price of 7 NOK/L is just over 6 years as seen in Figure 8.2.

By using the NPV formula the two BtL plants can be compared based on the maximum interest rate the projects could pay and still break even at the end of the project lifetime. This rate is called the "discounted cash-flow rate of return" (DCFROR) [38]. By using a lifetime of 20 years, a product price of 7 NOK/L and investment and annual operating costs as stated earlier in the report, the DCFROR is calculated to 15% for the H-BtL plant and 5% for the S-BtL plant. A higher DCFROR indicates a more profitable project because it will be able tolerate a higher interest rate and still break even at the end of the project. Clearly the H-BtL plant is the most profitable of the two plants.

Figure 8.3 shows how the NPV of the project changes with varying product price and electricity price in percent of the base price. The base point (0% in the graph) is taken as 0.3 NOK/kWh electricity and 7 NOK/L product. The base point will increase or decrease on the y-axis if the base prices is changed. The interest rate is kept constant at 7 %. The effect of tax on the plant is also included. Different places in the world have various tax rate, so it is interesting to see the effect of the rate on the NPV.

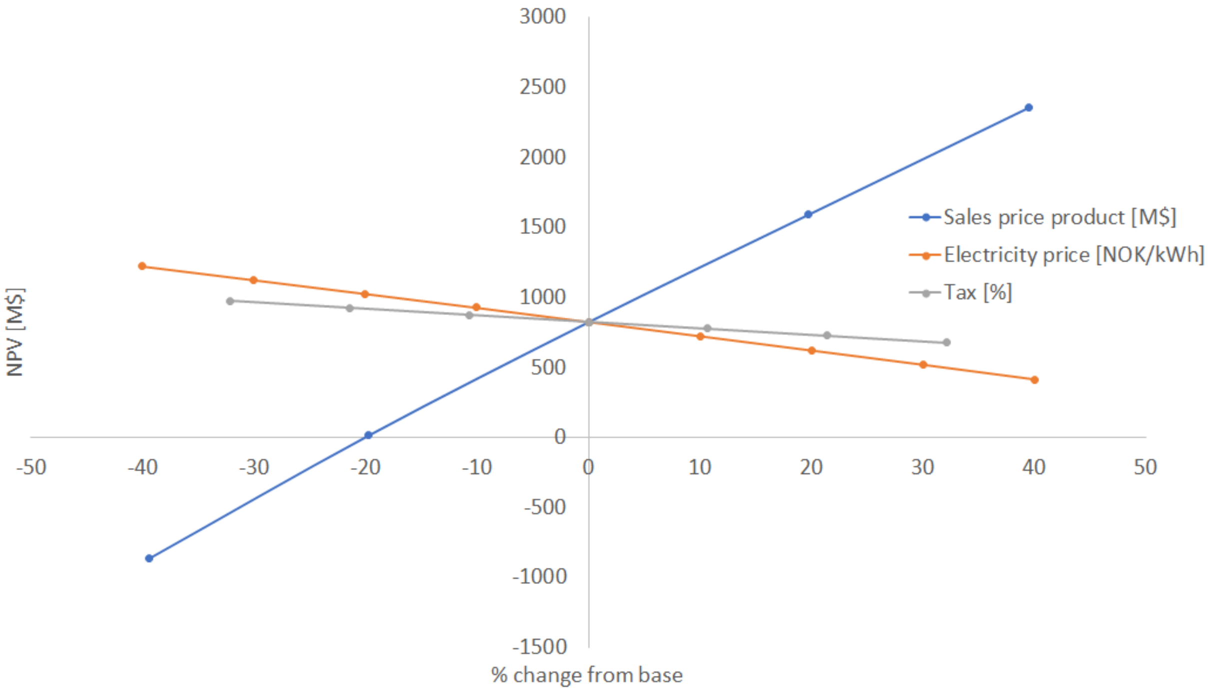

Figure 8.3: A sensitivity diagram of the NPV as a function of the electricity price, product price and tax on the plant in percent of the base price. The base price is 0.3 NOK/kWh electricity, 7 NOK/L product and 28% tax.

As seen from the figure, the product sales price has the largest effect on the NPV of the plant. A 20% decrease in the price would make the plant have a negative NPV. The electricity price and the tax however have less impact on the NPV, but both are important in a complete economical perspective of the plant.

9 Discussion

The evaluation of a hydrogen enhanced BtL plant by simulations in Hysys has shown a reduction in production price of hydrocarbon products compared to a conventional BtL plant. The plant has been optimized based on production of hydrocarbons, and evaluated based on heat integration and economic profitability. A torrefaction pretreatment of the biomass has been included in the evaluation of the plant, and torrefied biomass has been used in the simulations. An energy content of 18.75 kJ/kg has been assumed for the biomass, which is in the lower range of values found in literature for forest residue [5], [6]. If the energy content of the biomass is higher, the amount of biomass required to produce a product with the same energy content will be lower. This will cause lower investment costs for smaller equipment and lower purchase cost of biomass. So, for investment in a real plant it is important to know the exact energy content of the feedstock. Other biomass sources may also be considered, based on availability.

The evaluation is based on the assumption of production of torrefied biomass at the same location as the rest of the BtL plant. If that is not the case, transportation and pelletization of the biomass must be included in the economical analysis. This can add a fair bit on the feedstock price, as pelletization is highly energy demanding and transportation is expensive, particularly deep sea transportation with ships [5]. However, the investment cost of a torrefaction unit is high, calculated to 55.5 M$ in this case, so there may be savings in buying imported torrefied biomass. This must be carefully evaluated before a comparison can be made. In this thesis, one of the goals was to integrate a torrefaction unit in the plant and evaluate the possible heat integration of the unit with the rest of the plant. An energy reducing parameter for this case is the possibility to use steam produced in the plant as heating medium in the torrefaction unit. By doing this, the plant is found to produce enough steam to power the torrefaction unit without the need for additional electricity.

It is found that the most optimal operation regarding syngas production is achieved when using SPCEC for the high temperature electrolysis to split the steam. In this case the unconverted steam is added with the oxygen to the gasifier, and pure hydrogen will be available to add at desired locations in the plant. However, the technology of a SOEC is more developed than the SPCEC and may therefore be cheaper. No price estimate of a SPCEC is found, so the investment cost compared to SOEC is difficult to analyze.

The assumed price of a HTE cell used is 0.28 M€/MW$_{el}$ [45], and is an estimated price for the cells in 2030. The current price is 0.86 M€/MW$_{el}$, but the assumption is presumed valid because the price of the cells will drop significantly due to development of the technology before this plant will be realized and built. The conversion of steam in the cells is assumed to be 80% [21]. Improvement of the conversion rate may significantly influence the investment cost of the plant, as the price of HTE cells corresponds to almost 50% of the equipment cost. If the conversion is improved, fewer cells are necessary to get the same production of oxygen and hydrogen. The electricity consumption of the cells will also be reduced, causing a decrease in the variable cost of production for the plant. It is found that the electricity consumption of the cells is almost 85% of the variable costs, so developing new and improved cells will be important for the overall economics of the plant. In this simulation, it is also assumed to use some of the tailgas to heat the steam to the operating temperature of the HTE cells. This is the only carbon loss in the process which reduces the carbon efficiency to 97.2%. However, some of the tailgas must be purged in order to avoid accumulation of inerts. Therefore, burning the purge will actually improve the energy efficiency of the plant, as electricity usage to heat the steam is avoided.

The necessary oxygen addition to the gasifier is found to be slightly higher than the optimal oxygen ratio for syngas production [13]. This is because the outlet temperature must be high to decrease the ash and soot contaminants in the output syngas. In this simulation, 1300°C has been used as the outlet temperature, but a higher temperature may be necessary based on the exact configuration of the gasifier. The temperature can be varied by adjusting the added amount of oxygen to the gasifier.

Addition of hydrogen to the RWGS reactor will be favorable with a high temperature of the hydrogen stream. This is because the reverse water gas shift reaction is happening spontaneously at temperatures higher than 820°C [14]. This is also important in between the FT reactors where syngas at 40°C is mixed with high-temperature hydrogen, and the temperature is increased to 100°C. This will improve the heat integration and make the plant more self-sufficient with energy. If the hydrogen is added at a lower temperature, it may be necessary to use imported energy to heat the streams.

The analysis proves that it is not beneficial to remove the CO_2 content in the syngas stream. This is because removing the CO_2 will decrease the production of hydrocarbons in the plant. A H_2S removal unit with following ZnO guard beds is preferred when additional hydrogen is used in a RWGS reactor to convert CO_2 to CO in the syngas [42]. However, it is important to remove sulfur components as they will deactivate the catalyst in the FT reactors. It is found that a Selexol process will remove the major part of the H_2S, and using following ZnO guard beds will polish the stream. The sizing of the ZnO guard beds is not performed in this study, but they are usually sized based on industrial standards of the beds and preferred replacement frequency. However, the yearly average cost will be the same regardless of the replacement frequency.

The plant is found to be self-sufficient with heat. Electricity to the HTE is the only imported energy used in the plant. By heat integrating the hot syngas with the production of steam to the HTE unit, all the energy from the stream is recovered. Some of the steam is also used in the torrefaction unit as heating medium, which covers the energy requirement for this process. The FT part of the process is heat integrated as seen in Figure 6.1, and no additional heating is required. By combining cooling of the FT reactors with steam production, electricity can be generated. In the economic analysis, this electricity is assumed to be used by compressors, pumps and other equipment and is not included as an economic income.

The cost estimation of the equipment in the plant is based on a method described in [38]. Additionally, numbers from literature are used for more advanced process equipment. The values found in literature are often specific to the process analyzed, and might not be a perfect fit for the components in this process. The torrefaction unit proved to be more expensive than expected with a cost corresponding to 21% of the total equipment cost, while the Fischer-Tropsch reactors proved to be cheaper than expected. The technology of Fischer-Tropsch reactors is more complex than the torrefaction, and a higher cost was therefore expected. The torrefaction technology is relatively new which might explain the high cost related to the torrefaction unit.

From the comparison of the two cases, H-BtL and S-BtL, in section 8 it is found that the H-BtL is the most economically profitable project. The total annualized cost of production of one liter hydrocarbons is over 1.7 NOK (almost 25%) cheaper than for the S-BtL plant. The cost estimations are done based on the same assumptions both with respect to hydrocarbon production and equipment cost. The result is confirmed by calculation of the discounted cash-flow rate of return, which is 15% for the H-BtL plant and 5% for the S-BtL plant. As the H-BtL plant can withstand a higher rate, this is the more profitable plant. The parameters used in the evaluation can be found in section 8.3. A production cost of 5.32 NOK/L product is calculated based on the total annualized cost, and is lower than the cost found by Avinor/Rambøll of 11 NOK/L [32]. They have also included upgrading of the hydrocarbons, so the comparison is not based on the exact same assumptions. However, the price is a good indication of the production price as the major parts of the plant are included in the evaluation. The S-BtL plant is found to have a production price of 7.04 NOK/L hydrocarbons. This is based on an evaluation of a similar plant as in the Avinor/Rambøll report, without the hydrocarbon upgrading process included. As this price is almost 4 NOK/L cheaper, there may be some errors in the economic evaluation of the plant. For the H-BtL plant, the NPV is strongly dependent on the sales price of the product as seen in Figure 8.3. The electricity price is also important as it represents almost 85% of the calculated variable cost of production, mainly due to the high electricity consumption of the HTE cells. A 20% increase of the electricity price will reduce the NPV with almost 25%. The electricity price is assumed as the current price from Statistics Norway [31], which strongly depends on the water reservoir filling rate. The cost may however be planned for a long term if a fixed price contract is signed.

The imposed tax of the plant is also interesting to assess. The parliament may give tax reduction or subsidies to environmentally friendly processes with low greenhouse gas emissions [52]. However, from the evaluation in this report it is found not to have a significant influence on the NPV of the project.

The economic analysis is done based on a general approach in [38]. The installation factors and other parameters in the model might not be an exact fit to the plant evaluated here. There might also be some specific costs related to this plant which are not captured by the general approach. Still, the analysis give a good indication of the overall economics of the plant.

10 Conclusion

A biomass to liquid plant has been analyzed and optimized based on hydrocarbon production, energy efficiency and economics by simulations in Aspen Hysys. A conventional BtL plant has been enhanced by addition of hydrogen produced by HTE cells to increase the carbon efficiency and production rate.

The hydrogen enhanced biomass to liquid plant shows great improvements of carbon efficiency, and better economic profitability than conventional BtL plants using steam. The total annualized cost of the plant per liter hydrocarbons produced is estimated to be reduced by 25% while the carbon efficiency is increased to 97%. The plant will only have a NPV greater than zero when the product price to is larger than 5.6 NOK/L. However, this is a significant reduction of the minimum price compared to similar evaluations of BtL plants converting syngas with Fischer-Tropsch reactors. A report from Avinor/Rambøll predicted a price of 11 NOK/L for the plant to be economically feasible [32]. The investment cost of the plant is expected to decrease in the future as the technology is improved and becomes cheaper. The plant is found to be self-sufficient with heat and the only imported energy is the electricity used for high temperature electrolysis. This gives an energy efficiency of 70.4%.

10.1 Further work

The evaluation performed in this report is based on values found in literature in addition to the achieved results from the simulation in Hysys. To get a more realistic and correct estimation of the economic feasibility of the plant, equipment prices from up and running plants should be considered. Prices from equipment manufacturers should also be procured.

For further work the performance of the HTE cells might be researched and improved. This may include lab work to develop the technology further. Also, the reverse water gas shift reaction should be investigated to study the reaction at high temperatures above 1100 °C. Examples of RWGS reactors combined with the gasifier in a single vessel has not been found in literature, but has been assumed in this report. This should be researched to find out if it's chemically and physically possible.

In this report, the upgrading of hydrocarbons to fuel has not been considered. This should be included to get a more complete cost estimation of the plant.

References

[1] Ecotricity.co.uk. (2017). The End Of Fossil Fuels - Our Green Energy - Ecotricity. [online] Available at: `https://www.ecotricity.co.uk/our-green-energy/energy-independence/the-end-of-fossil-fuels` [Accessed 8 May 2017].

[2] Boerrigter, H et al. "Gas Cleaning For Integrated Biomass Gasification (BG) And Fischer -Tropsch (FT) Systems". ECN Report ECN-C–04-056. Energy research Centre of the Netherlands (ECN): Petten, The Netherlands, 2004.

[3] Hu, J., Yu, F. and Lu, Y. (2012). Application of Fischer–Tropsch Synthesis in Biomass to Liquid Conversion. Catalysts, 2(4), pp.303-326.

[4] Demirbas, A. (1997). Calculation of higher heating values of biomass fuels. Fuel, 76(5), pp.431-434.

[5] Koppejan, J., Sokhansanj, S., Melin, S. and Madrali, S. (2012). Status overview of torrefaction technologies. IEA Bioenergy Task 32.

[6] Spath, P., Aden, A., Eggeman, T., Ringer, M., Wallace, B. and Jechura, J. (2005). Biomass to Hydrogen Production Detailed Design and Economics Utilizing the Battelle Columbus Laboratory Indirectly- Heated Gasifier. Technical Report. National Renewable Energy Laboratory.

[7] International Renewable Energy Agency, Biomass for power generation. (2012). IRENA working paper, vol. 1 1/5.

[8] Shankar Tumuluru, J., Sokhansanj, S., Hess, J., Wright, C. and Boardman, R. (2011). REVIEW: A review on biomass torrefaction process and product properties for energy applications. Industrial Biotechnology, 7(5), pp.384-401.

[9] van der Stelt, M., Gerhauser, H., Kiel, J. and Ptasinski, K. (2011). Biomass upgrading by torrefaction for the production of biofuels: A review. Biomass and Bioenergy.

[10] Uslu, A., Faaij, A. and Bergman, P. (2008). Pre-treatment technologies, and their effect on international bioenergy supply chain logistics. Techno-economic evaluation of torrefaction, fast pyrolysis and pelletisation. Energy, 33(8), pp.1206-1223.

[11] Hofbauer, Hermann, Reinhard Rauch, and Karl Ripfel-Nitsche. "Report On Gas Cleaning For Synthesis Applications". (2007): n. pag. Print.

[12] Schulzke, T. (2016). Synergies from direct coupling of BtL- and PtL-plants. Chemical Engineering & Technology.

[13] Qin, K., Jensen, P., Lin, W. and Jensen, A. (2012). Biomass Gasification Behavior in an Entrained Flow Reactor: Gas Product Distribution and Soot Formation. Energy & Fuels, 26(9), pp.5992-6002.

[14] Ebbesen, S., Jensen, S., Hauch, A. and Mogensen, M. (2014). High Temperature Electrolysis in Alkaline Cells, Solid Proton Conducting Cells, and Solid Oxide Cells. Chemical Reviews, 114(21), pp.10697-10734.

[15] Mingyi, L., Bo, Y., Jingming, X. and Jing, C. (2008). Thermodynamic analysis of the efficiency of high-temperature steam electrolysis system for hydrogen production. Journal of Power Sources, 177(2), pp.493-499.

[16] Helmeth.eu. (2017). High temperature electrolysis cell (SOEC). [online] Available at: `http://www.helmeth.eu/index.php/technologies/high-temperature-electrolysis-cell-soec` [Accessed 6 May 2017].

[17] Koh, J., Yoon, D. and Oh, C. (2010). Simple Electrolyzer Model Development for High-Temperature Electrolysis System Analysis Using Solid Oxide Electrolysis Cell. Journal of Nuclear Science and Technology, 47(7), pp.599-607.

[18] Brisse, A., Schefold, J. and Zahid, M. (2008). High temperature water electrolysis in solid oxide cells. International Journal of Hydrogen Energy, 33(20), pp.5375-5382.

[19] Bi, L., Boulfrad, S. and Traversa, E. (2014). Steam electrolysis by solid oxide electrolysis cells (SOECs) with proton-conducting oxides. Chem. Soc. Rev., 43(24), pp.8255-8270.

[20] Hydrogen Production & Distribution. (2007). IEA Energy Technology Essentials. [online] Available at: `https://www.iea.org/publications/freepublications/publication/essentials5.pdf` [Accessed 7 Jun. 2017].

[21] Mougin, J., Di Lorio, S., Chatroux, A., Donnier-Marechal, T., Palcoux, G., Petitjean, M. and Roux, G. (2017). Development of a Solid Oxide Electrolysis Stack Able to Operate at High Steam Conversion Rate and Integration into a SOE System. [online] Available at: `https://ecs.confex.com/ecs/sofc2017/webprogram/Paper101153.html` [Accessed 30 May 2017].

[22] Callaghan, C. (2006). Kinetics and Catalysis of the Water-Gas-Shift Reaction: A Microkinetic and Graph Theoretic Approach. Worcester Polytechnic Institute.

[23] Dutta, A., Cheah, S., Bain, R., Feik, C., Magrini-Bair, K. and Phillips, S. (2012). Integrated Process Configuration for High-Temperature Sulfur Mitigation during Biomass Conversion via Indirect Gasification. Industrial & Engineering Chemistry Research, 51(24), pp.8326-8333.

[24] Grainger, D. (n.d.). A comparison of MDEA- and Selexol®-based acid gas removal for pre-combustion CO2 capture in an IGCC process.

[25] Hunpinyo, P., Cheali, P., Narataruksa, P., Tungkamani, S. and Chollacoop, N. (2014). Alternative route of process modification for biofuel production by embedding the Fischer–Tropsch plant in existing stand-alone power plant (10MW) based on biomass gasification – Part I: A conceptual modeling and simulation approach (a case study in Thailand). Energy Conversion and Management, 88, pp.1179-1192.

[26] Xu, J., Yang, Y. and Li, Y. (2015). Recent development in converting coal to clean fuels in China. Fuel, 152, pp.122-130.

[27] Iglesia, E. (1997). Design, synthesis, and use of cobalt-based Fischer-Tropsch synthesis catalysts. Applied Catalysis A: General, 161(1-2), pp.59-78.

[28] Ostadi, M., Dalane, K., Rytter, E. and Hillestad, M. (2015). Conceptual design of an autonomous once-through gas-to-liquid process — Comparison between fixed bed and microchannel reactors. Fuel Processing Technology, 139, pp.186-195.

[29] Rafiee, A. and Hillestad, M. (2012). Staging of the Fischer–Tropsch reactor with an iron based catalyst. Computers & Chemical Engineering, 39, pp.75-83.

[30] Hillestad, M. (2015). Modeling the Fischer–Tropsch Product Distribution and Model Implementation. Chemical Product and Process Modeling, 10(3).

[31] "Elektrisitetspriser, 4. Kvartal 2016". SSB. 2017. Web. 22 May 2017.

[32] Killingland, Magnus et al. "Utredning: Bærekraftig Biodrivstoff For Luftfart". (2013): n. pag. Print.

[33] Nicholas, D. and Wilkins, J. (1983). Optimize acid gas removal. Hydrocarbon Process, 62:9.

[34] Rytter, E., Ochoa-Fernández, E. and Fahmi, A. (2013). Biomass-to-Liquids by the Fischer-Tropsch Process. Catalytic Process Development for Renewable Materials, pp.265-308.

[35] Bour, H. (2016). Modelling and Optimization of a Process from Biomass to Liquid Fuels via Fischer-Tropsch Synthesis.

[36] Engineeringtoolbox.com. (n.d.). Properties of Saturated Steam - SI Units. [online] Available at: `http://www.engineeringtoolbox.com/saturated-steam-properties-d_101.html` [Accessed 5 Jun. 2017].

[37] E. Samuelsen (2016). Integration of renewable production of hydrogen in current Biomass-to-Liquid Biofuels production systems, Specialization project. NTNU

[38] Sinnott, R. and Towler, G. (2009). Chemical engineering design. 5th ed. Oxford: Butterworth-Heinemamn.

[39] Chemengonline.com. (2017). Current economic trends: CEPCI January (prelim.) and December (final). [online] Available at: `http://www.chemengonline.com/current-economic-trends-cepci-january-prelim-and-december-final/` [Accessed 16 Jun. 2017].

[40] Holmgren, K. (2015). Integration aspects of biomass gasification in large industrial or regional energy systems. 1st ed. Gøteborg: Chalmers University of Technology.

[41] Basu, P. (2010). Biomass gasification design handbook. London: Academic.

[42] Hannula, I. (2016). Hydrogen enhancement potential of synthetic biofuels manufacture in the European context: A techno-economic assessment. Energy, 104, pp.199-212.

[43] Schweitzer, J. and Viguié, J. (2009). Reactor Modeling of a Slurry Bubble Column for Fischer-Tropsch Synthesis. Oil & Gas Science and Technology - Revue de l'IFP, 64(1), pp.63-77.

[44] Goellner JF, Shah V, Turner MJ, Kuehn NJ, Littlefield GC and Marriott J (2013). Analysis of Natural Gas-to-Liquid Transportation Fuels via Fischer-Tropsch. Office of Strategic Energy Analysis and Planning, National Energy Technology Laboratory DOE/NETL- 2013/1597, U.S.A

[45] Ridjan, I., Mathiesen, B. and Connolly, D. (2014). Synthetic fuel production costs by means of solid oxide electrolysis cells. Energy, 76, pp.104-113.

[46] Mathiesen, B. V., Ridjan, I., Connolly, D., Nielsen, M. P., Vang Hendriksen, P., Bjerg Mogensen, M., ... Dalgaard Ebbesen, S. (2013). Technology data for high temperature solid oxide electrolyser cells, alkali and PEM electrolysers. Department of Development and Planning, Aalborg University.

[47] Oslo kommune. (2017). Vann- og avløpsgebyrer. [online] Available at: `https://www.oslo.kommune.no/vann-og-avlop/priser-og-beregning/vann-og-avlopsgebyrer/` [Accessed 19 Jun. 2017].

[48] Beysel, G. (2009). Enhanced Cryogenic Air separation, A proven Process applied to Oxyfuel, Future Prospects. 1st Oxyfuel Combustion Conference.

[49] investing.com. (2017). Carbon Emissions Futures Price - Investing.com. [online] Available at: `http://www.investing.com/commodities/carbon-emissions` [Accessed 19 Jun. 2017].

[50] Aneke, M. and Wang, M. (2015). Potential for improving the energy efficiency of cryogenic air separation unit (ASU) using binary heat recovery cycles. Applied Thermal Engineering, 81, pp.223-231.

[51] Eia.gov. (2017). Spot Prices for Crude Oil and Petroleum Products. [online] Available at: `https://www.eia.gov/dnav/pet/pet_pri_spt_s1_d.htm` [Accessed 20 Jun. 2017].

[52] Tax Policies to Reduce Greenhouse Gas Emissions. (2008). Pew Center on Global Climate Change.

A Flowsheets

A.1 Steam BtL plant

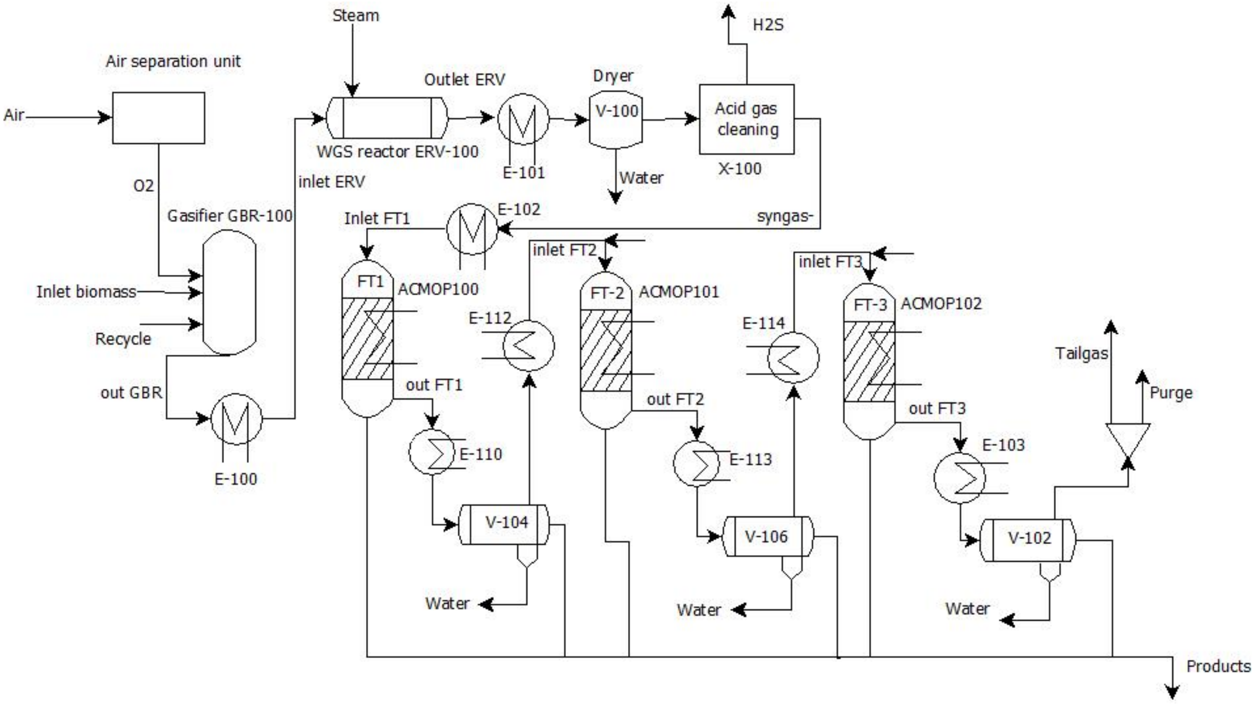

Figure A.1: A flowsheet of the Biomass-to-Liquid process with steam addition.

A.2 Hysys flowsheets

The following pages shows the simulation flowsheet made in Hysys. A complete overview of the stream properties in the flowsheet can be found in appendix C.

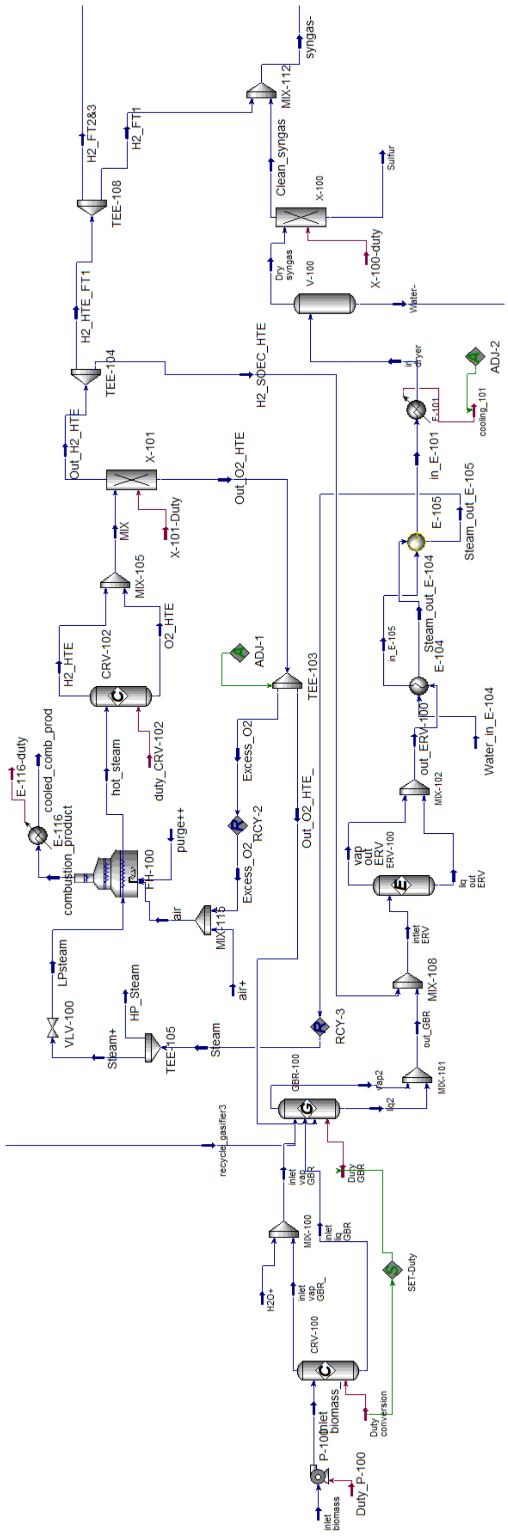

Figure A.2: A Hysys flowsheet of the first part of the Biomass-to-Liquid process.

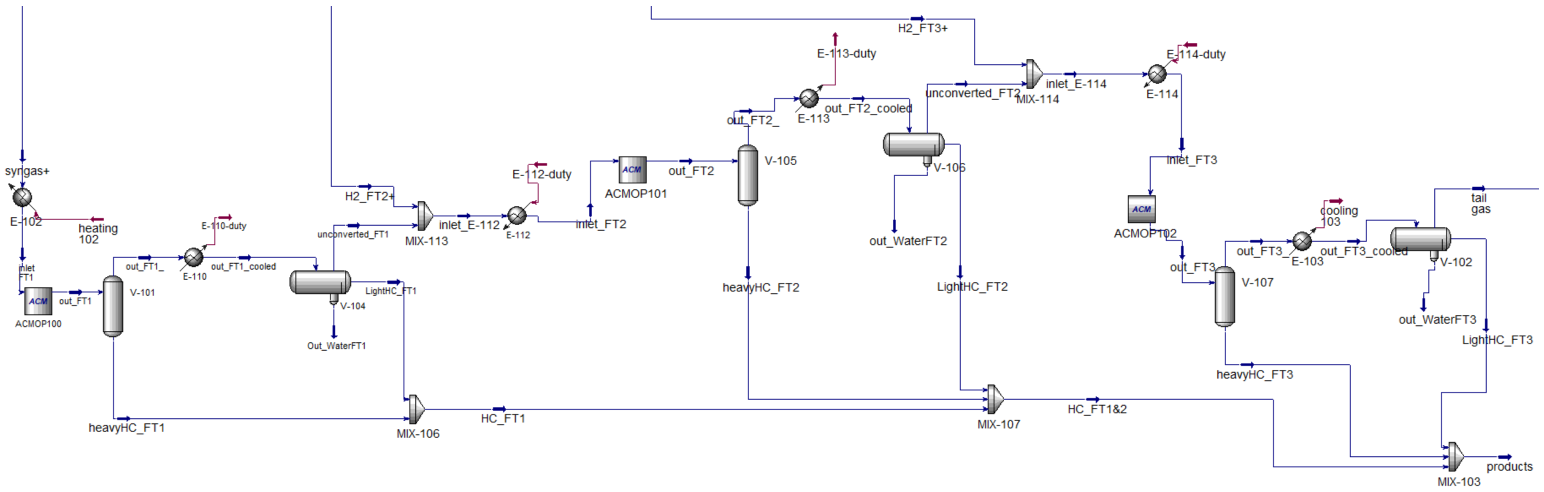

Figure A.3: A Hysys flowsheet of the second part of the Biomass-to-Liquid process.

B Heat integration by Aspen Energy Analyzer

On the next page is the proposed heat exchanger network by Aspen Energy Analyzer. The green lines and circles are heat exchangers, while the blue and red are coolers and heaters respectively. The setup can also be seen in Figure 6.1.

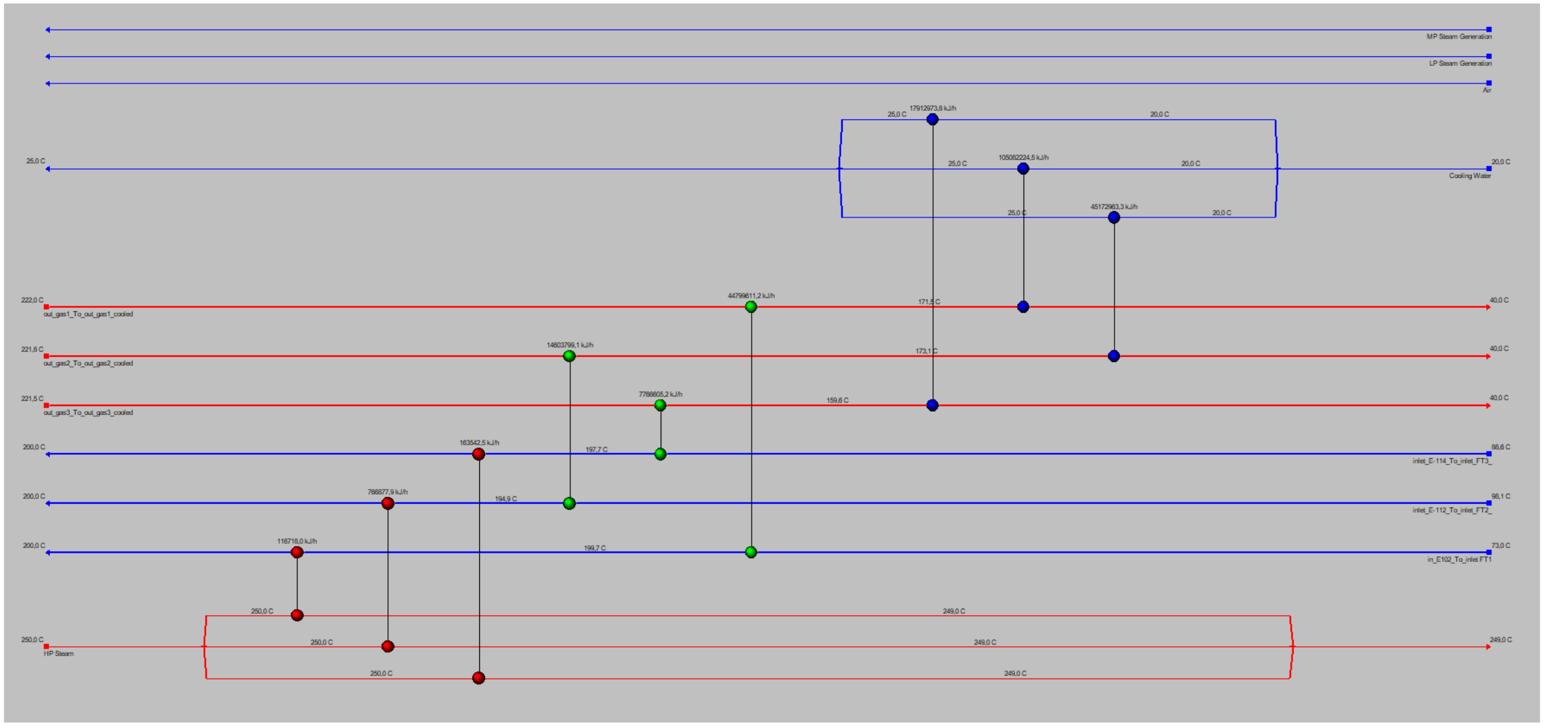

Figure B.1: Proposed heat exchangers network by Hysys.

C Hysys Workbooks

C.1 Material workbook from Hysys

The material workbook with stream properties can be seen on the next pages.

Workbook: Case (Main)

Material Streams

Fluid Pkg: All

Name		inlet biomass	inlet vap GBR_	inlet liq GBR	inlet vap GBR	vap2	liq2
Vapour Fraction		0.0000	1.0000	0.0000	1.0000	1.0000	0.0000
Temperature	(C)	300.0 *	800.0 *	800.0	799.5	1299	1299
Pressure	(kPa)	100.0 *	4000	4000	4000	3900	3900
Molar Flow	(kgmole/h)	832.4 *	3611	3590	3796	8255	0.0000
Mass Flow	(kg/h)	8.333e+004	4.016e+004	4.317e+004	4.349e+004	1.626e+005	-0.0000
Liquid Volume Flow	(m3/h)	117.9	103.4	26.28	106.8	260.8	0.0000
Heat Flow	(kJ/h)	-4.255e+008	8.537e+007	4.841e+007	4.594e+007	-6.786e+008	-0.0000
Name		H2O+	intlet ERV	vap out ERV	out_GBR	liq out ERV	Dry syngas
Vapour Fraction		1.0000	1.0000	1.0000	1.0000	0.0000	1.0000
Temperature	(C)	800.0 *	1124	1091	1299	1091	67.34
Pressure	(kPa)	4000 *	3900	3900	3900	3900	3700
Molar Flow	(kgmole/h)	185.0 *	1.379e+004	1.379e+004	8255	0.0000	1.182e+004
Mass Flow	(kg/h)	3333 *	1.737e+005	1.737e+005	1.626e+005	-0.0000	1.384e+005
Liquid Volume Flow	(m3/h)	3.340	420.4	405.5	260.8	0.0000	370.1
Heat Flow	(kJ/h)	-3.943e+007	-5.513e+008	-5.513e+008	-6.786e+008	-0.0000	-5.376e+008
Name		Water-	in_E-105	in dryer	Sulfur	out_FT3_cooled	LightHC_FT3
Vapour Fraction		0.0000	1.0000	0.8575	1.0000	0.7259	0.0000
Temperature	(C)	67.34	704.8	67.34	73.00 *	40.00 *	40.00
Pressure	(kPa)	3700	3800	3700	3700	3100	3100
Molar Flow	(kgmole/h)	1964	1.379e+004	1.379e+004	2.568	1390	13.20
Mass Flow	(kg/h)	3.540e+004	1.737e+005	1.737e+005	86.49	2.958e+004	1455
Liquid Volume Flow	(m3/h)	35.48	405.5	405.5	0.1100	64.57	1.923
Heat Flow	(kJ/h)	-5.556e+008	-7.334e+008	-1.093e+009	-5.325e+004	-2.286e+008	-3.492e+006
Name		out_WaterFT3	tail gas	heavyHC_FT1	out_FT1_	out_FT1	tail gas recycle
Vapour Fraction		0.0000	1.0000	0.0000	1.0000	0.9878	1.0000 *
Temperature	(C)	40.00	40.00	222.0	222.0	222.0	40.00 *
Pressure	(kPa)	3100	3100	3700	3700	3700	3100 *
Molar Flow	(kgmole/h)	367.9	1009	86.08	6972	7058	987.0 *
Mass Flow	(kg/h)	6628	2.150e+004	2.528e+004	1.130e+005	1.383e+005	2.040e+004
Liquid Volume Flow	(m3/h)	6.641	56.00	28.05	292.3	320.4	54.76
Heat Flow	(kJ/h)	-1.047e+008	-1.204e+008	-4.707e+007	-8.352e+008	-8.823e+008	-1.118e+008
Name		purge-	Clean_syngas	inlet FT1	syngas+	recycle_gasifier	recycle_gasifier2
Vapour Fraction		1.0000	1.0000	1.0000	1.0000	1.0000	1.0000
Temperature	(C)	40.00	73.00 *	200.0 *	73.00	40.00	66.82
Pressure	(kPa)	3100	3700	3700	3700	3100	4000 *
Molar Flow	(kgmole/h)	98.70	1.182e+004	1.182e+004	1.182e+004	888.3	888.3
Mass Flow	(kg/h)	2040	1.383e+005	1.383e+005	1.383e+005	1.836e+004	1.836e+004
Liquid Volume Flow	(m3/h)	5.476	370.0	629.1	629.1	49.29	49.29
Heat Flow	(kJ/h)	-1.118e+007	-5.355e+008	-4.900e+008	-5.350e+008	-1.006e+008	-9.978e+007
Name		recycle_gasifier3	recycle gas	products	Water_in_E-104	Out_H2_HTE	Out_O2_HTE
Vapour Fraction		1.0000	1.0000	0.0117	0.0000 *	1.0000	1.0000
Temperature	(C)	74.51	40.00	185.7	322.0 *	800.0 *	800.0 *
Pressure	(kPa)	4000	3100	3100	1.174e+004	1.154e+004 *	1.154e+004 *
Molar Flow	(kgmole/h)	883.7	888.3	212.3	8163 *	6066	4549
Mass Flow	(kg/h)	1.798e+004	1.836e+004	4.963e+004	1.471e+005	1.223e+004	1.244e+005
Liquid Volume Flow	(m3/h)	35.50	49.29	56.94	147.4	175.0	112.7
Heat Flow	(kJ/h)	-9.927e+007	-1.006e+008	-9.620e+007	-2.117e+009	1.396e+008	-2.467e+008
Name		MIX	Out_WaterFT1	unconverted_FT1	out_FT1_cooled	LightHC_FT1	HC_FT1
Vapour Fraction		1.0000	0.0000	1.0000	0.6381	0.0000	0.0006
Temperature	(C)	794.2	40.00	40.00	40.00 *	40.00	189.6
Pressure	(kPa)	4000	3500	3500	3500	3500	3500
Molar Flow	(kgmole/h)	1.061e+004	2480	4449	6972	43.02	129.1
Mass Flow	(kg/h)	1.366e+005	4.469e+004	6.224e+004	1.130e+005	6054	3.134e+004
Liquid Volume Flow	(m3/h)	287.7	44.77	239.8	292.3	7.688	35.74
Heat Flow	(kJ/h)	-1.090e+008	-7.060e+008	-2.657e+008	-9.851e+008	-1.341e+007	-6.048e+007

* Specified by user.

Workbook: Case (Main) (continued)

Material Streams (continued)

Fluid Pkg: All

Name	inlet_FT2	out_FT2	out_FT2_	heavyHC_FT2	out_FT2_cooled	out_WaterFT2
Vapour Fraction	1.0000	0.9892	1.0000	0.0000	0.6724	0.0000
Temperature (C)	200.0 *	221.8	221.8	221.8	40.00 *	40.00
Pressure (kPa)	3500	3500	3500	3500	3300	3300
Molar Flow (kgmole/h)	4834	2975	2943	32.24	2943	938.1
Mass Flow (kg/h)	6.302e+004	6.302e+004	5.317e+004	9845	5.317e+004	1.690e+004
Liquid Volume Flow (m3/h)	260.5	139.9	129.0	10.92	129.0	16.93
Heat Flow (kJ/h)	-2.414e+008	-3.943e+008	-3.762e+008	-1.807e+007	-4.360e+008	-2.670e+008
Name	unconverted_FT2	LightHC_FT2	inlet_FT3	out_FT3	heavyHC_FT3	out_FT3_
Vapour Fraction	1.0000	0.0000	1.0000	0.9915	0.0000	1.0000
Temperature (C)	40.00	40.00	200.0 *	221.5	221.5	221.5
Pressure (kPa)	3300	3300	3300	3300	3300	3300
Molar Flow (kgmole/h)	1979	25.84	2129	1402	11.88	1390
Mass Flow (kg/h)	3.312e+004	3157	3.342e+004	3.342e+004	3835	2.958e+004
Liquid Volume Flow (m3/h)	107.9	4.105	116.0	68.82	4.251	64.57
Heat Flow (kJ/h)	-1.617e+008	-7.222e+006	-1.503e+008	-2.099e+008	-6.933e+006	-2.030e+008
Name	HC_FT1&2	Out_O2_HTE_	Excess_O2	H2_SOEC_HTE	H2_HTE_FT1	out_ERV-100
Vapour Fraction	0.0055	1.0000	1.0000	1.0000	1.0000	1.0000
Temperature (C)	187.0	800.0	800.0	800.0	800.0	1091
Pressure (kPa)	3300	1.154e+004	1.154e+004	1.154e+004	1.154e+004	3900
Molar Flow (kgmole/h)	187.2	2120	2429	5530	535.6	1.379e+004
Mass Flow (kg/h)	4.434e+004	5.796e+004	6.640e+004	1.115e+004	1080	1.737e+005
Liquid Volume Flow (m3/h)	50.77	52.51	60.16	159.6	15.46	405.5
Heat Flow (kJ/h)	-8.577e+007	-1.150e+008	-1.317e+008	1.273e+008	1.233e+007	-5.513e+008
Name	Steam_out_E-104	in_E-101	Steam+	HP_Steam	syngas-	H2_FT2-
Vapour Fraction	1.0000 *	1.0000	1.0000	1.0000	1.0000	1.0000
Temperature (C)	321.3	378.5	683.3	683.3	73.00	800.0
Pressure (kPa)	1.164e+004	3700	1.154e+004	1.154e+004	3700	1.154e+004
Molar Flow (kgmole/h)	8163	1.379e+004	7582	581.0	1.182e+004	385.0
Mass Flow (kg/h)	1.471e+005	1.737e+005	1.366e+005	1.047e+004	1.383e+005	776.2
Liquid Volume Flow (m3/h)	147.4	405.5	136.9	10.49	370.0	11.11
Heat Flow (kJ/h)	-1.935e+009	-8.793e+008	-1.662e+009	-1.273e+008	-5.355e+008	8.861e+006
Name	H2_FT3-	H2_FT2+	H2_FT3+	H2_FT2&3	H2_FT1	inlet_E-112
Vapour Fraction	1.0000	1.0000	1.0000	1.0000	1.0000	1.0000
Temperature (C)	800.0	800.0	800.0	800.0	800.0	98.14
Pressure (kPa)	1.154e+004	1.154e+004	1.154e+004	1.154e+004	1.154e+004	3500
Molar Flow (kgmole/h)	150.6	385.0	150.6	535.6	4.383e-004	4834
Mass Flow (kg/h)	303.6	776.1	303.6	1080	8.836e-004	6.302e+004
Liquid Volume Flow (m3/h)	4.346	20.62	8.066	15.46	1.265e-005	260.5
Heat Flow (kJ/h)	3.466e+006	8.881e+006	3.474e+006	1.233e+007	10.09	-2.568e+008
Name	inlet_E-114	Steam	Steam_out_E-105	inlet biomass_	hot_steam	purge+
Vapour Fraction	1.0000	1.0000	1.0000	0.0000	1.0000	1.0000
Temperature (C)	88.64	683.3 *	683.3	305.7	793.5	40.00
Pressure (kPa)	3300	1.154e+004 *	1.154e+004	4000 *	4000	3100
Molar Flow (kgmole/h)	2129	8163 *	8163	832.4	7582	98.19
Mass Flow (kg/h)	3.342e+004	1.471e+005	1.471e+005	8.333e+004	1.366e+005	1997
Liquid Volume Flow (m3/h)	116.0	147.4	147.4	117.9	136.9	3.944
Heat Flow (kJ/h)	-1.583e+008	-1.789e+009	-1.789e+009	-4.249e+008	-1.618e+009	-1.114e+007
Name	combustion_produ	10	air	H2_HTE	O2_HTE	LPsteam
Vapour Fraction	1.0000	1.0000	1.0000	1.0000	0.0000	1.0000
Temperature (C)	794.2	25.00 *	796.6	794.2	794.2 *	657.4
Pressure (kPa)	3000	3000 *	3000	4000	4000	4000 *
Molar Flow (kgmole/h)	2533	1.000 *	2430	1.061e+004	0.0000	7582
Mass Flow (kg/h)	6.938e+004	28.85	6.643e+004	1.366e+005	0.0000	1.366e+005
Liquid Volume Flow (m3/h)	64.47	3.335e-002	60.19	287.7	0.0000	136.9
Heat Flow (kJ/h)	-1.920e+008	-232.4	-1.317e+008	-1.090e+008	-0.0000	-1.662e+009

Workbook: Case (Main) (continued)

Material Streams (continued)

Fluid Pkg: All

Name		purge++	cooled_comb_prod	Excess_O2_	water_tot	Water+	
Vapour Fraction		1.0000	0.6411	1.0000	0.0001	0.0003	
Temperature	(C)	40.00 *	50.00 *	800.0 *	49.43	67.34	
Pressure	(kPa)	3100 *	3000	1.154e+004 *	3100	3700	
Molar Flow	(kgmole/h)	145.0 *	2533	2429 *	5751	1964	
Mass Flow	(kg/h)	2949	6.938e+004	6.640e+004	1.036e+005	3.539e+004	
Liquid Volume Flow	(m3/h)	5.825	64.47	60.16	103.8	35.48	
Heat Flow	(kJ/h)	-1.646e+007	-2.977e+008	-1.317e+008	-1.633e+009	-5.551e+008	

* Specified by user.

C.2 Composition workbook from Hysys

The composition workbook from Hysys with compositions of each stream. It is split in two parts as there are two different fluid basis used for the streams.

Workbook: Case (Main)

Compositions

Fluid Pkg: Basis-1

Name	inlet biomass	inlet vap GBR_	inlet liq GBR	inlet vap GBR	vap2	liq2
Master Comp Mole Frac (Hydrogen)	0.0000 *	0.6961	0.0000	0.6622	0.3018	0.3018
Master Comp Mole Frac (CO)	0.0000 *	0.0000	0.0000	0.0000	0.4172	0.4172
Master Comp Mole Frac (CO2)	0.0000 *	0.0000	0.0000	0.0000	0.0888	0.0888
Master Comp Mole Frac (H2O)	0.0000 *	0.0000	0.0000	0.0487	0.1892	0.1892
Master Comp Mole Frac (Methane)	0.0000 *	0.0000	0.0000	0.0000	0.0002	0.0002
Master Comp Mole Frac (H2S)	0.0000 *	0.0000	0.0000	0.0000	0.0003	0.0003
Master Comp Mole Frac (dry biomas	1.0000 *	0.0000	0.0000	0.0000	0.0000	0.0000
Master Comp Mole Frac (Ammonia)	0.0000 *	0.0000	0.0000	0.0000	0.0000	0.0000
Master Comp Mole Frac (Nitrogen)	0.0000 *	0.0014	0.0000	0.0013	0.0025	0.0025
Name	H2O+	intlet ERV	vap out ERV	out_GBR	liq out ERV	Dry syngas
Master Comp Mole Frac (Hydrogen)	0.0000 *	0.5819	0.5449	0.3018	0.5449	0.6354
Master Comp Mole Frac (CO)	0.0000 *	0.2499	0.2868	0.4172	0.2868	0.3345
Master Comp Mole Frac (CO2)	0.0000 *	0.0532	0.0162	0.0888	0.0162	0.0189
Master Comp Mole Frac (H2O)	1.0000 *	0.1133	0.1502	0.1892	0.1502	0.0091
Master Comp Mole Frac (Methane)	0.0000 *	0.0001	0.0001	0.0002	0.0001	0.0001
Master Comp Mole Frac (H2S)	0.0000 *	0.0002	0.0002	0.0003	0.0002	0.0002
Master Comp Mole Frac (dry biomas	0.0000 *	0.0000	0.0000	0.0000	0.0000	0.0000
Master Comp Mole Frac (Ammonia)	0.0000 *	0.0000	0.0000	0.0000	0.0000	0.0000
Master Comp Mole Frac (Nitrogen)	0.0000 *	0.0015	0.0015	0.0025	0.0015	0.0018
Name	Water-	in_E-105	in dryer	Sulfur	Clean_syngas	recycle_gasifier3
Master Comp Mole Frac (Hydrogen)	0.0001	0.5449	0.5449	0.0000	0.6356	0.4028
Master Comp Mole Frac (CO)	0.0000	0.2868	0.2868	0.0000	0.3345	0.2418
Master Comp Mole Frac (CO2)	0.0001	0.0162	0.0162	0.0000	0.0189	0.1997
Master Comp Mole Frac (H2O)	0.9997	0.1502	0.1502	0.0000	0.0091	0.0030
Master Comp Mole Frac (Methane)	0.0000	0.0001	0.0001	0.0000	0.0001	0.0865
Master Comp Mole Frac (H2S)	0.0000	0.0002	0.0002	0.9642	0.0000	0.0000
Master Comp Mole Frac (dry biomas	0.0000	0.0000	0.0000	0.0000	0.0000	0.0000
Master Comp Mole Frac (Ammonia)	0.0000	0.0000	0.0000	0.0270	0.0000	0.0000
Master Comp Mole Frac (Nitrogen)	0.0000	0.0015	0.0015	0.0000	0.0018	0.0180
Name	Water_in_E-104	Out_H2_HTE	Out_O2_HTE	MIX	Out_O2_HTE_	Excess_O2
Master Comp Mole Frac (Hydrogen)	0.0000 *	1.0000	0.0000	0.5714	0.0000	0.0000
Master Comp Mole Frac (CO)	0.0000 *	0.0000	0.0000	0.0000	0.0000	0.0000
Master Comp Mole Frac (CO2)	0.0000 *	0.0000	0.0000	0.0000	0.0000	0.0000
Master Comp Mole Frac (H2O)	1.0000 *	0.0000	0.3333	0.1429	0.3333	0.3333
Master Comp Mole Frac (Methane)	0.0000 *	0.0000	0.0000	0.0000	0.0000	0.0000
Master Comp Mole Frac (H2S)	0.0000 *	0.0000	0.0000	0.0000	0.0000	0.0000
Master Comp Mole Frac (dry biomas	0.0000 *	0.0000	0.0000	0.0000	0.0000	0.0000
Master Comp Mole Frac (Ammonia)	0.0000 *	0.0000	0.0000	0.0000	0.0000	0.0000
Master Comp Mole Frac (Nitrogen)	0.0000 *	0.0000	0.0000	0.0000	0.0000	0.0000
Name	H2_SOEC_HTE	H2_HTE_FT1	out_ERV-100	Steam_out_E-104	in_E-101	Steam+
Master Comp Mole Frac (Hydrogen)	1.0000	1.0000	0.5449	0.0000	0.5449	0.0000
Master Comp Mole Frac (CO)	0.0000	0.0000	0.2868	0.0000	0.2868	0.0000
Master Comp Mole Frac (CO2)	0.0000	0.0000	0.0162	0.0000	0.0162	0.0000
Master Comp Mole Frac (H2O)	0.0000	0.0000	0.1502	1.0000	0.1502	1.0000
Master Comp Mole Frac (Methane)	0.0000	0.0000	0.0001	0.0000	0.0001	0.0000
Master Comp Mole Frac (H2S)	0.0000	0.0000	0.0002	0.0000	0.0002	0.0000
Master Comp Mole Frac (dry biomas	0.0000	0.0000	0.0000	0.0000	0.0000	0.0000
Master Comp Mole Frac (Ammonia)	0.0000	0.0000	0.0000	0.0000	0.0000	0.0000
Master Comp Mole Frac (Nitrogen)	0.0000	0.0000	0.0015	0.0000	0.0015	0.0000

Workbook: Case (Main) (continued)

Compositions (continued)

Fluid Pkg: Basis-1

Name	HP_Steam	syngas-	H2_FT2-	H2_FT3-	H2_FT2&3	H2_FT1
Master Comp Mole Frac (Hydrogen)	0.0000	0.6356	1.0000	1.0000	1.0000	1.0000
Master Comp Mole Frac (CO)	0.0000	0.3345	0.0000	0.0000	0.0000	0.0000
Master Comp Mole Frac (CO2)	0.0000	0.0189	0.0000	0.0000	0.0000	0.0000
Master Comp Mole Frac (H2O)	1.0000	0.0091	0.0000	0.0000	0.0000	0.0000
Master Comp Mole Frac (Methane)	0.0000	0.0001	0.0000	0.0000	0.0000	0.0000
Master Comp Mole Frac (H2S)	0.0000	0.0000	0.0000	0.0000	0.0000	0.0000
Master Comp Mole Frac (dry biomas	0.0000	0.0000	0.0000	0.0000	0.0000	0.0000
Master Comp Mole Frac (Ammonia)	0.0000	0.0000	0.0000	0.0000	0.0000	0.0000
Master Comp Mole Frac (Nitrogen)	0.0000	0.0018	0.0000	0.0000	0.0000	0.0000
Name	Steam	Steam_out_E-105	inlet biomass_	hot_steam	purge+	combustion_produ
Master Comp Mole Frac (Hydrogen)	0.0000 *	0.0000	0.0000	0.0000	0.4028	0.0000
Master Comp Mole Frac (CO)	0.0000 *	0.0000	0.0000	0.0000	0.2418	0.0000
Master Comp Mole Frac (CO2)	0.0000 *	0.0000	0.0000	0.0000	0.1997	0.0383
Master Comp Mole Frac (H2O)	1.0000 *	1.0000	0.0000	1.0000	0.0030	0.3620
Master Comp Mole Frac (Methane)	0.0000 *	0.0000	0.0000	0.0000	0.0865	0.0000
Master Comp Mole Frac (H2S)	0.0000 *	0.0000	0.0000	0.0000	0.0000	0.0000
Master Comp Mole Frac (dry biomas	0.0000 *	0.0000	1.0000	0.0000	0.0000	0.0000
Master Comp Mole Frac (Ammonia)	0.0000 *	0.0000	0.0000	0.0000	0.0000	0.0000
Master Comp Mole Frac (Nitrogen)	0.0000 *	0.0000	0.0000	0.0000	0.0180	0.0013
Name	10	air	H2_HTE	O2_HTE	LPsteam	purge++
Master Comp Mole Frac (Hydrogen)	0.0000 *	0.0000	0.5714	0.5714	0.0000	0.4028 *
Master Comp Mole Frac (CO)	0.0000 *	0.0000	0.0000	0.0000	0.0000	0.2418 *
Master Comp Mole Frac (CO2)	0.0000 *	0.0000	0.0000	0.0000	0.0000	0.1997 *
Master Comp Mole Frac (H2O)	0.0000 *	0.3332	0.1429	0.1428	1.0000	0.0030 *
Master Comp Mole Frac (Methane)	0.0000 *	0.0000	0.0000	0.0000	0.0000	0.0865 *
Master Comp Mole Frac (H2S)	0.0000 *	0.0000	0.0000	0.0000	0.0000	-0.0000 *
Master Comp Mole Frac (dry biomas	0.0000 *	0.0000	0.0000	0.0000	0.0000	-0.0000 *
Master Comp Mole Frac (Ammonia)	0.0000 *	0.0000	0.0000	0.0000	0.0000	-0.0000 *
Master Comp Mole Frac (Nitrogen)	0.7900 *	0.0003	0.0000	0.0000	0.0000	0.0180 *
Name	cooled_comb_prod	Excess_O2_				
Master Comp Mole Frac (Hydrogen)	0.0000	0.0000 *				
Master Comp Mole Frac (CO)	0.0000	0.0000 *				
Master Comp Mole Frac (CO2)	0.0383	0.0000 *				
Master Comp Mole Frac (H2O)	0.3620	0.3333 *				
Master Comp Mole Frac (Methane)	0.0000	0.0000 *				
Master Comp Mole Frac (H2S)	0.0000	0.0000 *				
Master Comp Mole Frac (dry biomas	0.0000	0.0000 *				
Master Comp Mole Frac (Ammonia)	0.0000	0.0000 *				
Master Comp Mole Frac (Nitrogen)	0.0013	0.0000 *				

Workbook: Case (Main)

Compositions

Fluid Pkg: Basis-2

Name	out_FT3_cooled	LightHC_FT3	out_WaterFT3	tail gas	heavyHC_FT1	out_FT1_
Master Comp Mole Frac (CO)	0.1698	0.0125	0.0000	0.2338	0.0145	0.2217
Master Comp Mole Frac (H2)	0.2813	0.0078	0.0000	0.3875	0.0158	0.3657
Master Comp Mole Frac (h2o)	0.2671	0.0296	1.0000	0.0030	0.2446	0.3575
Master Comp Mole Frac (METHA-01	0.0622	0.0121	0.0000	0.0855	0.0009	0.0083
Master Comp Mole Frac (Paraf1*)	0.0032	0.2661	0.0000	0.0009	0.0094	0.0026
Master Comp Mole Frac (Paraf2*)	0.0019	0.2045	0.0000	0.0000	0.1318	0.0023
Master Comp Mole Frac (Paraf3*)	0.0000	0.0044	0.0000	0.0000	0.5647	0.0000
Master Comp Mole Frac (Olef1*)	0.0020	0.1394	0.0000	0.0009	0.0030	0.0011
Master Comp Mole Frac (Olef2*)	0.0002	0.0192	0.0000	0.0000	0.0059	0.0002
Master Comp Mole Frac (Olef3*)	0.0000	0.0001	0.0000	0.0000	0.0010	0.0000
Master Comp Mole Frac (Nitrogen)	0.0149	0.0011	0.0000	0.0206	0.0002	0.0030
Master Comp Mole Frac (Carbo-01)	0.1579	0.1046	0.0000	0.2162	0.0055	0.0320
Master Comp Mole Frac (ETHAN-01	0.0042	0.0038	0.0000	0.0057	0.0001	0.0006
Master Comp Mole Frac (PROPY-01	0.0072	0.0171	0.0000	0.0097	0.0003	0.0010
Master Comp Mole Frac (PROPA-01	0.0039	0.0104	0.0000	0.0052	0.0002	0.0005
Master Comp Mole Frac (1-BUT-01)	0.0049	0.0330	0.0000	0.0063	0.0004	0.0007
Master Comp Mole Frac (N-BUT-01)	0.0034	0.0260	0.0000	0.0044	0.0003	0.0005
Master Comp Mole Frac (N-PEN-01	0.0026	0.0511	0.0000	0.0029	0.0005	0.0005
Master Comp Mole Frac (1-pen-01)	0.0030	0.0509	0.0000	0.0034	0.0005	0.0005
Master Comp Mole Frac (Ethylene)	0.0102	0.0064	0.0000	0.0139	0.0003	0.0013

Name	out_FT1	tail gas recycle	purge-	inlet FT1	syngas+	recycle_gasifier
Master Comp Mole Frac (CO)	0.2192	0.2405 *	0.2405	0.3345	0.3345	0.2405
Master Comp Mole Frac (H2)	0.3614	0.4007 *	0.4007	0.6356	0.6356	0.4007
Master Comp Mole Frac (h2o)	0.3561	0.0030 *	0.0030	0.0091	0.0091	0.0030
Master Comp Mole Frac (METHA-01	0.0082	0.0861 *	0.0861	0.0001	0.0001	0.0861
Master Comp Mole Frac (Paraf1*)	0.0027	0.0009 *	0.0009	0.0000	0.0000	0.0009
Master Comp Mole Frac (Paraf2*)	0.0039	0.0000 *	0.0000	0.0000	0.0000	0.0000
Master Comp Mole Frac (Paraf3*)	0.0069	0.0000 *	0.0000	0.0000	0.0000	0.0000
Master Comp Mole Frac (Olef1*)	0.0011	0.0009 *	0.0009	0.0000	0.0000	0.0009
Master Comp Mole Frac (Olef2*)	0.0003	0.0000 *	0.0000	0.0000	0.0000	0.0000
Master Comp Mole Frac (Olef3*)	0.0000	0.0000 *	0.0000	0.0000	0.0000	0.0000
Master Comp Mole Frac (Nitrogen)	0.0030	0.0179 *	0.0179	0.0018	0.0018	0.0179
Master Comp Mole Frac (Carbo-01)	0.0317	0.1987 *	0.1987	0.0189	0.0189	0.1987
Master Comp Mole Frac (ETHAN-01	0.0006	0.0058 *	0.0058	0.0000	0.0000	0.0058
Master Comp Mole Frac (PROPY-01	0.0010	0.0096 *	0.0096	0.0000	0.0000	0.0096
Master Comp Mole Frac (PROPA-01	0.0005	0.0053 *	0.0053	0.0000	0.0000	0.0053
Master Comp Mole Frac (1-BUT-01)	0.0007	0.0062 *	0.0062	0.0000	0.0000	0.0062
Master Comp Mole Frac (N-BUT-01)	0.0005	0.0044 *	0.0044	0.0000	0.0000	0.0044
Master Comp Mole Frac (N-PEN-01	0.0005	0.0030 *	0.0030	0.0000	0.0000	0.0030
Master Comp Mole Frac (1-pen-01)	0.0005	0.0034 *	0.0034	0.0000	0.0000	0.0034
Master Comp Mole Frac (Ethylene)	0.0013	0.0137 *	0.0137	0.0000	0.0000	0.0137

Workbook: Case (Main) (continued)

Compositions (continued)

Fluid Pkg: Basis-2

Name	recycle_gasifier2	recycle gas	products	Out_WaterFT1	unconverted_FT1	out_FT1_cooled
Master Comp Mole Frac (CO)	0.2405	0.2405	0.0154	0.0000	0.3473	0.2217
Master Comp Mole Frac (H2)	0.4007	0.4007	0.0134	0.0000	0.5730	0.3657
Master Comp Mole Frac (h2o)	0.0030	0.0030	0.1518	1.0000	0.0025	0.3575
Master Comp Mole Frac (METHA-01	0.0861	0.0861	0.0031	0.0000	0.0130	0.0083
Master Comp Mole Frac (Paraf1*)	0.0009	0.0009	0.1308	0.0000	0.0008	0.0026
Master Comp Mole Frac (Paraf2*)	0.0000	0.0000	0.1960	0.0000	0.0000	0.0023
Master Comp Mole Frac (Paraf3*)	0.0000	0.0000	0.3569	0.0000	0.0000	0.0000
Master Comp Mole Frac (Olef1*)	0.0009	0.0009	0.0531	0.0000	0.0006	0.0011
Master Comp Mole Frac (Olef2*)	0.0000	0.0000	0.0145	0.0000	0.0000	0.0002
Master Comp Mole Frac (Olef3*)	0.0000	0.0000	0.0007	0.0000	0.0000	0.0000
Master Comp Mole Frac (Nitrogen)	0.0179	0.0179	0.0004	0.0000	0.0047	0.0030
Master Comp Mole Frac (Carbo-01)	0.1987	0.1987	0.0250	0.0000	0.0499	0.0320
Master Comp Mole Frac (ETHAN-01	0.0058	0.0058	0.0008	0.0000	0.0009	0.0006
Master Comp Mole Frac (PROPY-01	0.0096	0.0096	0.0032	0.0000	0.0015	0.0010
Master Comp Mole Frac (PROPA-01	0.0053	0.0053	0.0020	0.0000	0.0008	0.0005
Master Comp Mole Frac (1-BUT-01)	0.0062	0.0062	0.0061	0.0000	0.0010	0.0007
Master Comp Mole Frac (N-BUT-01)	0.0044	0.0044	0.0049	0.0000	0.0007	0.0005
Master Comp Mole Frac (N-PEN-01	0.0030	0.0030	0.0106	0.0000	0.0006	0.0005
Master Comp Mole Frac (1-pen-01)	0.0034	0.0034	0.0101	0.0000	0.0007	0.0005
Master Comp Mole Frac (Ethylene)	0.0137	0.0137	0.0013	0.0000	0.0021	0.0013

Name	LightHC_FT1	HC_FT1	inlet_FT2	out_FT2	out_FT2_	heavyHC_FT2
Master Comp Mole Frac (CO)	0.0205	0.0165	0.3196	0.2034	0.2054	0.0128
Master Comp Mole Frac (H2)	0.0123	0.0147	0.6070	0.3355	0.3390	0.0140
Master Comp Mole Frac (h2o)	0.0301	0.1731	0.0023	0.3196	0.3209	0.2091
Master Comp Mole Frac (METHA-01	0.0021	0.0013	0.0119	0.0266	0.0268	0.0029
Master Comp Mole Frac (Paraf1*)	0.3324	0.1170	0.0008	0.0037	0.0036	0.0125
Master Comp Mole Frac (Paraf2*)	0.3683	0.2106	0.0000	0.0035	0.0022	0.1239
Master Comp Mole Frac (Paraf3*)	0.0058	0.3785	0.0000	0.0065	0.0000	0.5930
Master Comp Mole Frac (Olef1*)	0.1186	0.0415	0.0005	0.0019	0.0019	0.0049
Master Comp Mole Frac (Olef2*)	0.0341	0.0153	0.0000	0.0003	0.0002	0.0056
Master Comp Mole Frac (Olef3*)	0.0002	0.0007	0.0000	0.0000	0.0000	0.0010
Master Comp Mole Frac (Nitrogen)	0.0003	0.0002	0.0043	0.0070	0.0071	0.0005
Master Comp Mole Frac (Carbo-01)	0.0287	0.0132	0.0459	0.0745	0.0752	0.0124
Master Comp Mole Frac (ETHAN-01	0.0007	0.0003	0.0008	0.0018	0.0018	0.0004
Master Comp Mole Frac (PROPY-01	0.0032	0.0013	0.0014	0.0031	0.0031	0.0010
Master Comp Mole Frac (PROPA-01	0.0020	0.0008	0.0008	0.0017	0.0017	0.0006
Master Comp Mole Frac (1-BUT-01)	0.0068	0.0025	0.0010	0.0022	0.0022	0.0012
Master Comp Mole Frac (N-BUT-01)	0.0056	0.0021	0.0007	0.0016	0.0016	0.0009
Master Comp Mole Frac (N-PEN-01	0.0143	0.0051	0.0006	0.0014	0.0014	0.0013
Master Comp Mole Frac (1-pen-01)	0.0130	0.0046	0.0006	0.0015	0.0015	0.0013
Master Comp Mole Frac (Ethylene)	0.0011	0.0005	0.0019	0.0043	0.0044	0.0008

Workbook: Case (Main) (continued)

Compositions (continued)

Fluid Pkg: Basis-2

Name	out_FT2_cooled	out_WaterFT2	unconverted_FT2	LightHC_FT2	inlet_FT3	out_FT3
Master Comp Mole Frac (CO)	0.2054	0.0000	0.3053	0.0171	0.2837	0.1685
Master Comp Mole Frac (H2)	0.3390	0.0000	0.5040	0.0104	0.5391	0.2790
Master Comp Mole Frac (h2o)	0.3209	1.0000	0.0027	0.0301	0.0025	0.2662
Master Comp Mole Frac (METHA-0	0.0268	0.0000	0.0398	0.0060	0.0370	0.0617
Master Comp Mole Frac (Paraf1*)	0.0036	0.0000	0.0010	0.3333	0.0009	0.0033
Master Comp Mole Frac (Paraf2*)	0.0022	0.0000	0.0000	0.2506	0.0000	0.0028
Master Comp Mole Frac (Paraf3*)	0.0000	0.0000	0.0000	0.0043	0.0000	0.0055
Master Comp Mole Frac (Olef1*)	0.0019	0.0000	0.0008	0.1489	0.0008	0.0020
Master Comp Mole Frac (Olef2*)	0.0002	0.0000	0.0000	0.0233	0.0000	0.0002
Master Comp Mole Frac (Olef3*)	0.0000	0.0000	0.0000	0.0001	0.0000	0.0000
Master Comp Mole Frac (Nitrogen)	0.0071	0.0000	0.0105	0.0006	0.0098	0.0148
Master Comp Mole Frac (Carbo-01)	0.0752	0.0000	0.1111	0.0589	0.1032	0.1568
Master Comp Mole Frac (ETHAN-01	0.0018	0.0000	0.0027	0.0019	0.0025	0.0042
Master Comp Mole Frac (PROPY-0	0.0031	0.0000	0.0046	0.0089	0.0042	0.0072
Master Comp Mole Frac (PROPA-0	0.0017	0.0000	0.0025	0.0055	0.0023	0.0039
Master Comp Mole Frac (1-BUT-01)	0.0022	0.0000	0.0031	0.0182	0.0028	0.0049
Master Comp Mole Frac (N-BUT-01)	0.0016	0.0000	0.0022	0.0147	0.0020	0.0034
Master Comp Mole Frac (N-PEN-01	0.0014	0.0000	0.0016	0.0328	0.0015	0.0026
Master Comp Mole Frac (1-pen-01)	0.0015	0.0000	0.0018	0.0312	0.0017	0.0030
Master Comp Mole Frac (Ethylene)	0.0044	0.0000	0.0064	0.0032	0.0060	0.0101

Name	heavyHC_FT3	out_FT3_	HC_FT1&2	H2_FT2+	H2_FT3+	inlet_E-112
Master Comp Mole Frac (CO)	0.0101	0.1698	0.0160	0.0000	0.0000	0.3196
Master Comp Mole Frac (H2)	0.0110	0.2813	0.0139	1.0000	1.0000	0.6070
Master Comp Mole Frac (h2o)	0.1650	0.2671	0.1596	0.0000	0.0000	0.0023
Master Comp Mole Frac (METHA-0	0.0063	0.0622	0.0022	0.0000	0.0000	0.0119
Master Comp Mole Frac (Paraf1*)	0.0107	0.0032	0.1289	0.0000	0.0000	0.0008
Master Comp Mole Frac (Paraf2*)	0.1047	0.0019	0.2012	0.0000	0.0000	0.0000
Master Comp Mole Frac (Paraf3*)	0.6404	0.0000	0.3638	0.0000	0.0000	0.0000
Master Comp Mole Frac (Olef1*)	0.0050	0.0020	0.0500	0.0000	0.0000	0.0005
Master Comp Mole Frac (Olef2*)	0.0048	0.0002	0.0147	0.0000	0.0000	0.0000
Master Comp Mole Frac (Olef3*)	0.0011	0.0000	0.0007	0.0000	0.0000	0.0000
Master Comp Mole Frac (Nitrogen)	0.0009	0.0149	0.0003	0.0000	0.0000	0.0043
Master Comp Mole Frac (Carbo-01)	0.0247	0.1579	0.0194	0.0000	0.0000	0.0459
Master Comp Mole Frac (ETHAN-01	0.0008	0.0042	0.0005	0.0000	0.0000	0.0008
Master Comp Mole Frac (PROPY-0	0.0023	0.0072	0.0023	0.0000	0.0000	0.0014
Master Comp Mole Frac (PROPA-0	0.0013	0.0039	0.0014	0.0000	0.0000	0.0008
Master Comp Mole Frac (1-BUT-01)	0.0025	0.0049	0.0045	0.0000	0.0000	0.0010
Master Comp Mole Frac (N-BUT-01)	0.0019	0.0034	0.0036	0.0000	0.0000	0.0007
Master Comp Mole Frac (N-PEN-01	0.0024	0.0026	0.0083	0.0000	0.0000	0.0006
Master Comp Mole Frac (1-pen-01)	0.0025	0.0030	0.0077	0.0000	0.0000	0.0006
Master Comp Mole Frac (Ethylene)	0.0017	0.0102	0.0010	0.0000	0.0000	0.0019

Workbook: Case (Main) (continued)

Compositions (continued)

Fluid Pkg: Basis-2

Name	inlet_E-114	water_tot	Water+			
Master Comp Mole Frac (CO)	0.2837	0.0000	0.0000			
Master Comp Mole Frac (H2)	0.5391	0.0000	0.0001			
Master Comp Mole Frac (h2o)	0.0025	0.9999	0.9997			
Master Comp Mole Frac (METHA-0	0.0370	0.0000	0.0000			
Master Comp Mole Frac (Paraf1*)	0.0009	0.0000	0.0000			
Master Comp Mole Frac (Paraf2*)	0.0000	0.0000	0.0000			
Master Comp Mole Frac (Paraf3*)	0.0000	0.0000	0.0000			
Master Comp Mole Frac (Olef1*)	0.0008	0.0000	0.0000			
Master Comp Mole Frac (Olef2*)	0.0000	0.0000	0.0000			
Master Comp Mole Frac (Olef3*)	0.0000	0.0000	0.0000			
Master Comp Mole Frac (Nitrogen)	0.0098	0.0000	0.0000			
Master Comp Mole Frac (Carbo-01)	0.1032	0.0001	0.0001			
Master Comp Mole Frac (ETHAN-01	0.0025	0.0000	0.0000			
Master Comp Mole Frac (PROPY-0	0.0042	0.0000	0.0000			
Master Comp Mole Frac (PROPA-0	0.0023	0.0000	0.0000			
Master Comp Mole Frac (1-BUT-01)	0.0028	0.0000	0.0000			
Master Comp Mole Frac (N-BUT-01)	0.0020	0.0000	0.0000			
Master Comp Mole Frac (N-PEN-01)	0.0015	0.0000	0.0000			
Master Comp Mole Frac (1-pen-01)	0.0017	0.0000	0.0000			
Master Comp Mole Frac (Ethylene)	0.0060	0.0000	0.0000			

* Specified by user.